AD-A033 555 DAVID W TAYLOR NAVAL SHIP RESEARCH AND DEVELOPMENT CE--ETC F/G 20/4
EXPERIMENTAL EVALUATION OF THE EFFECT OF ROTATION ON THE AERODY--ETC(U)
SEP 76 P S MONTANA

UNCLASSIFIED DTNSRDC/ASED-364 NL

1 OF 1

AD A033555

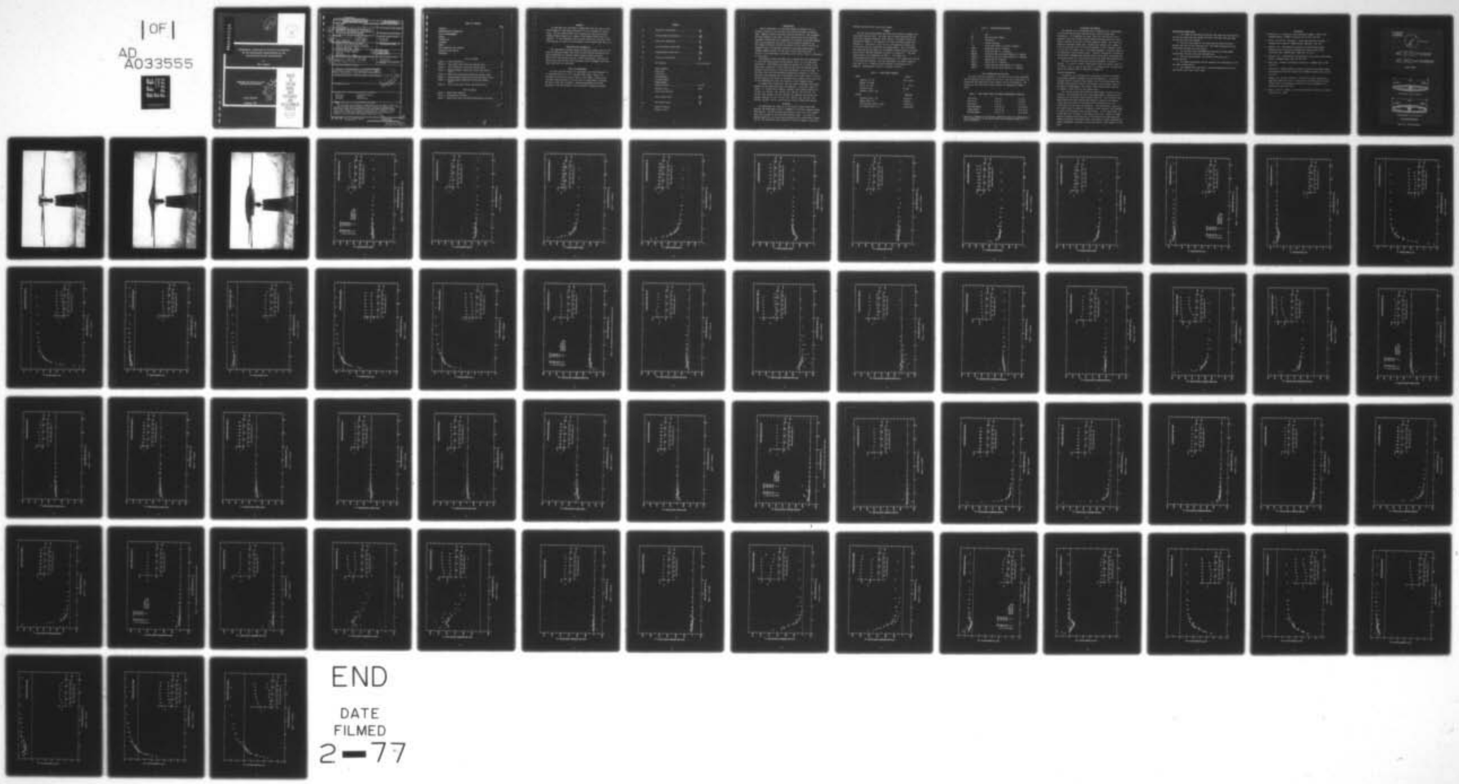

END

DATE FILMED

2-77

DEPARTMENT OF THE NAVY
DTNSRDC

EXPERIMENTAL EVALUATION OF THE EFFECT OF ROTATION ON THE AERODYNAMIC CHARACTERISTICS OF TWO HELICOPTER ROTOR HUB FAIRING SHAPES

by

Peter S. Montana

APPROVED FOR PUBLIC RELEASE:
DISTRIBUTION UNLIMITED

Report ASED-364

September 1976

DAVID W. TAYLOR NAVAL SHIP RESEARCH AND DEVELOPMENT CENTER

BETHESDA
MARYLAND
20084

UNCLASSIFIED

SECURITY CLASSIFICATION OF THIS PAGE (When Data Entered)

REPORT DOCUMENTATION PAGE		READ INSTRUCTIONS BEFORE COMPLETING FORM
1. REPORT NUMBER ASED-364	2. GOVT ACCESSION NO.	3. RECIPIENT'S CATALOG NUMBER
4. TITLE (and Subtitle) EXPERIMENTAL EVALUATION OF THE EFFECT OF ROTATION ON THE AERODYNAMIC CHARACTERISTICS OF TWO ROTOR HUB FAIRING SHAPES		5. TYPE OF REPORT & PERIOD COVERED
		6. PERFORMING ORG. REPORT NUMBER
7. AUTHOR(s) Peter S. Montana 12 71p.		8. CONTRACT OR GRANT NUMBER(s) F41.421.201 1-1619-105
9. PERFORMING ORGANIZATION NAME AND ADDRESS David W. Taylor Naval Ship R&D Center Aviation and Surface Effects Department Bethesda, Maryland 20084		10. PROGRAM ELEMENT, PROJECT, TASK AREA & WORK UNIT NUMBERS
11. CONTROLLING OFFICE NAME AND ADDRESS Naval Air Systems Command AIR-320D Washington, D.C. 20361		12. REPORT DATE Sep 76
		13. NUMBER OF PAGES
14. MONITORING AGENCY NAME & ADDRESS(if different from Controlling Office) DTNSRDC/ASED-364		15. SECURITY CLASS. (of this report) Unclassified
		15a. DECLASSIFICATION/DOWNGRADING SCHEDULE

16. DISTRIBUTION STATEMENT (of this Report)

Approved for Public Release: Distribution Unlimited

16 F41421 17 WFH1421201

17. DISTRIBUTION STATEMENT (of the abstract entered in Block 20, if different from Report)

18. SUPPLEMENTARY NOTES

19. KEY WORDS (Continue on reverse side if necessary and identify by block number)

Helicopter	Aerodynamic Forces
Rotor Hub	Rotation
Fairings	Advance Ratio

20. ABSTRACT (Continue on reverse side if necessary and identify by block number)

An experiment was performed to demonstrate that the drag of rotor hub fairings for high speed helicopters is not a function of advance ratio. Two hub fairing shapes were evaluated both with and without simulated blade shanks over a range of hub advance ratios from 0.5 to infinity. It was determined that the drag coefficient (and most other coefficients) is constant for hub advance ratios greater than about 3.0.

DD FORM 1 JAN 73 1473 EDITION OF 1 NOV 65 IS OBSOLETE S/N 0102-014-6601

UNCLASSIFIED

SECURITY CLASSIFICATION OF THIS PAGE (When Data Entered)

LB

387695

TABLE OF CONTENTS

LIST OF FIGURES

LIFT OF TABLES

A

ABSTRACT

An experiment was performed to demonstrate that the drag of rotor hub fairings for high speed helicopters is not a function of advance ratio. Two hub fairing shapes were evaluated both with and without simulated blade shanks over a range of hub advance ratios from 0.5 to infinity. It was determined that the drag coefficient (and most other coefficients) is constant for hub advance ratios greater than about 3.0.

ADMINISTRATIVE INFORMATION

The experimental program reported herein was funded jointly by the Naval Air Systems Command (AIR-320D) and the National Aeronautics and Space Administration (Langley Research Center) under task area WF41.421.201 and purchase request L-97786 respectively. The David W. Taylor Naval Ship Research and Development Center (DTNSRDC) work units were 1-1619-105 and 1-1619-108.

UNITS OF MEASUREMENT

All data recorded during this experiment were either measured in or converted directly to U.S. customary (US) units. Hence, U.S. customary units are the primary units in this report. Metric units are given either adjacent to the US units in parentheses or opposite US units in the case of graphs. Angular measurement is the only exception. The unit degrees is not converted to radians on graphs.

SYMBOLS

C_D	Drag Force Coefficient	$\frac{D}{qs}$
$C_{\ell'}$	Rolling Moment Coefficient	$\frac{L'}{qsd}$
C_L	Lift Force Coefficient	$\frac{L}{qs}$
C_M	Pitching Moment Coefficient	$\frac{M}{qsd}$
C_N	Yawing Moment Coefficient	$\frac{N}{qsd}$
C_Y	Side Force Coefficient	$\frac{Y}{qs}$
d	Hub Diameter	2.5 ft (0.76 m)
d'	Rotor Diameter	
D	Drag Force	
L	Lift Force	
L'	Rolling Moment	
M	Pitching Moment	
N	Yawing Moment	
q	Dynamic Pressure	$1/2\ \rho V^2$
s	Reference Area	$\pi d^2/4$
V	Free Stream Velocity	
μ	Rotor Advance Ratio	$\frac{2V}{\Omega d'}$
μ_H	Hub Advance Ratio	$\frac{2V}{\Omega d}$
Ω	Angular Velocity	
ρ	Density of Air	

INTRODUCTION

Future improvements in helicopter flight performance will be directly related to the reduction of helicopter fuselage aerodynamic drag. Numerous publications have shown the validity of this statement. The Navy program in this area, titled the Helicopter Drag Technology Program,[1] is funded under the cognizance of the Naval Air Systems Command with the participation of the U.S. Army Air Mobility Research and Development Laboratory (Eustis Directorate) in the area of interactive graphics[2] and of the National Aeronautics and Space Administration (Langley Research Center) in the area of rotor hub-pylon drag[3]. A portion of the experimental evaluations of the latter effort is documented in this report.

The purpose of this experiment was to demonstrate the independence of rotor hub fairing drag from hub advance ratio, μ_H, for high speed helicopters. This premise was stated in reference 4, a report on the wind tunnel evaluation of three non-rotating rotor hub fairings which included a brief survey of literature pertaining to rotor hub drag. Of the three rotor hub fairing shapes evaluated in reference 4, two were selected to be evaluated over a hub advance ratio range from 0.5 to 12.0. The hub advance ratio range can encompass rotor advance ratios from 0.025 to 2.40 depending the rotor hub diameter to rotor diameter ratio.

The models were tested both with and without simulated rotor blade shanks over the following ranges of parameters: rotor shaft angle of attack, -5. (0.0873) and 0 degrees (radians); wind tunnel velocity, 50. (15.24), 75. (22.86), 100. (30.48), 125. (38.10), 150. (45.72), 175. (53.34), 200. (60.96), and 225. (68.58) feet (meters) per second; and angular velocity, 0, 143. (14.97), 286. (29.95), 501. (52.46), 716. (74.98), and 875. (91.63) revolutions per minute (radians per second).

APPARATUS

The experiment was conducted in the David W. Taylor Naval Ship Research and Development Center's (DTNSRDC) 8- by 10-Foot Subsonic North Wind Tunnel[5]. The hub fairings were mounted on the rotor drive system[6] which was fastened to the wind tunnel balance frame. The output of sensors mounted in the rotor drive system and of the wind tunnel balance, and air flow information were digitally recorded on magnetic tape with a

Beckman high speed data acquisition system.

MODELS

The two hub fairing models were both thirty inches in diameter and twenty-five percent thick. One model was an oblate ellipsoid and the other had a reflexed curvature cross section. The models, which are described in Figure 1, are identical to those statically evaluated in reference 4. There were a total of four configurations tested; each fairing was tested by itself and with blade shanks. The four shanks were simulated by the blades of the DTNSRDC reverse blowing circulation control rotor (RB-CCR) described in detail in reference 7. The blade characteristics are summarized in Table 1. The blade root characteristics given are for the intersection of the blades with the hub of the rotor drive system. For this experiment, the blade collective angle was set at -2 degrees (0.0349 radians), and blowing was not employed. Configuration notation is defined in Table 2.

Table 1 - BLADE SHANK GEOMETRY

BLADE	RB-CCR
Diameter, ft (m)	6.67 (2.03)
Number of Blades	4
Chord, in. (cm)	5 (12.7)
Solidity Ratio	0.1592
Geometric Twist, deg.	0
AIRFOIL	**ROOT/TIP**
Thickness Ratio, t/C	0.20/0.15
Camber Ratio, δ/C	0.05/0.0
Trailing Edge Radius, R_{TE}/C	0.052/0.022
Slot Height Ratio, h/c	0.002/0.002

Table 2 - CONFIGURATION NOTATION

H	Hub
HB	Hub with Blade Shanks
E	Elliptical
R	Reflex Curvature
( )	Rotor Shaft Angle of Attack in Degrees
EH(0)	Elliptical Hub at 0 Degrees
EH(-5)	Elliptical Hub at -5 Degrees
EHB(0)	Elliptical Hub with Blade Shanks at 0 Degrees
EHB(-5)	Elliptical Hub with Blade Shanks at -5 Degrees
RH(0)	Reflex Hub at 0 Degrees
RH(-5)	Reflex Hub at -5 Degrees
RHB(0)	Reflex Hub with Blade Shanks at 0 Degrees
RHB(-5)	Reflex Hub with Blade Shanks at -5 Degrees

DATA CORRECTIONS AND ACCURACY

The only corrections applied to the data* were for solid blockage[8] and for hydraulic hose pressure forces due to the rotor drive motor. No corrections were applied for rotor support tare or interference. The accuracy of the wind tunnel balance system is summarized in Table 3 below.

Table 3 - WIND TUNNEL FORCE AND MOMENT MEASUREMENT ACCURACIES

Lift Force	0.25 lb.	(1.1 N)
Drag Force	0.05 lb.	(0.22 N)
Side Force	0.25 lb.	(1.1 N)
Pitching Moment	0.10 lb ft.	(0.14 N·m)
Yawing Moment	0.10 lb ft.	(0.14 N·m)
Rolling Moment	0.10 lb ft.	(0.14 N·m)

*The data presented is in wind axes coefficient form with reference area of 4.91 square feet (0.456 square meter) and reference length of 2.5 feet (0.76 meter).

DISCUSSION AND RESULTS

The purpose of this experiment was to demonstrate the independence of rotor hub fairing drag from hub advance ratio for high speed helicopters. To accomplish this goal, four rotor hub fairing configurations (two with simulated blade shanks) were evaluated over a wide range of advance ratios for two shaft angles of attack. The variety of wind and rotational speeds used yielded rotor advance ratio ranges of 0.025 to 0.60 and 0.10 to 2.4 for hub diameter to rotor diameter ratios of 0.05 and 0.20 respectively. The ranges represent a complete survey of the spectrum of rotor advance ratios. (Current conventional helicopters operate with a maximum rotor advance ratio of 0.40 which translates into hub advance ratios of 8.0 and 2.0 for small and large hubs respectively.)

The data recorded during this test are presented in Figures 2 through 7 as force or moment coefficients versus hub advance ratio in the order of C_D, C_L, C_M, C_Y, C_N, and $C_{\ell'}$. In addition lift to drag ratio versus hub advance ratio is presented in Figure 8.

GENERAL OBSERVATIONS

In general, as hub advance ratio increases, the force and moment coefficients approach constants for each configuration. For the hub fairings without simulated blade shanks, all of the coefficients have reached their constant values for hub advance ratios greater than 3.0. The drag, pitching moment, and lateral coefficients become constants at somewhat lower values of hub advance ratio.

For the hub fairing with simulated blade shanks, the data is not as dramatic. The drag and side force, and yawing moment coefficients are constants for hub advance ratios greater than 4.0. The relatively thin blade shanks contribute significant amounts of thrust at low advance ratios and this results in the delay in the stabilization of the coefficients of the shank configurations. Two coefficients, C_M and $C_{\ell'}$, at a shaft angle of attack of -5 degrees (-0.087 radians), are functions of both rotor rotational speed and wind speed. In all other cases, all coefficients are functions of hub advance ratio only. There is a small amount of scatter in the data due to the excitation of some rotor and support structural vibrational modes. The effect of these vibrations is usually negligible, although an occasional spurious point appears in the data.

QUANTITATIVE OBSERVATIONS

1. The reflex hub had about 30 percent less drag than the elliptical hub and the reflex hub with shanks had about 20 percent less drag than the elliptical hub with shanks.

2. The lift curve slope of the reflex hub was about 40 percent greater than that of the elliptical hub. The shank configurations had essentially the same lift curve slope.

3. The elliptical hub configurations had lower pitching moment coefficients than the reflex hub configurations.

4. Without shanks mounted, the lateral coefficients were essentially zero.

5. The shank aerodynamics usually dominated the aerodynamics of the hub shank configurations.

6. The stopped rotor data gives a very good approximation of the high advance ratio data in all cases.

REFERENCES

1. Montana, P.S., "Helicopter Drag Technology Program - Fiscal 1973 Progress Report," DTNSRDC Technical Note AL-310, Sep 1973.

2. Kelly, B.M. and M.B. Marquardt, "Interactive Helicopter Design: A Geometry User's Manual," DTNSRDC Report CMD-28-74, Sep 1974.

3. Montana, P.S., "Experimental Evaluation of Analytically Shaped Helicopter Rotor Hub-Pylon Configurations Using the Hub Pylon Evaluation Rig," DTNSRDC Report ASED 355, Jul 1976.

4. Montana, P.S., "Experimental Investigation of Three Rotor Hub Fairing Shapes," DTNSRDC Report ASED 333, May 1975.

5. Kidd, M.A., "Subsonic Wind Tunnel Facilities," DTNSRDC Report 3782, Jan 1972.

6. Stone, M.B., "Higher Harmonic Circulation Control Rotor Model, Model Instrumentation and Data Acquisition," DTNSRDC Technical Note AL-288, Apr 1973.

7. Reader, K.R. and J.B. Wilkerson, "Circulation Control Applied To A High Speed Helicopter Rotor," presented at the 32nd Annual National V/STOL Forum of the American Helicopter Society, Washington, D.C., Preprint No. 1003, May 1976.

8. Pope, A. and J.J. Harper, "Low Speed Wind Tunnel Testing," John Wiley and Sons, Inc., 1966.

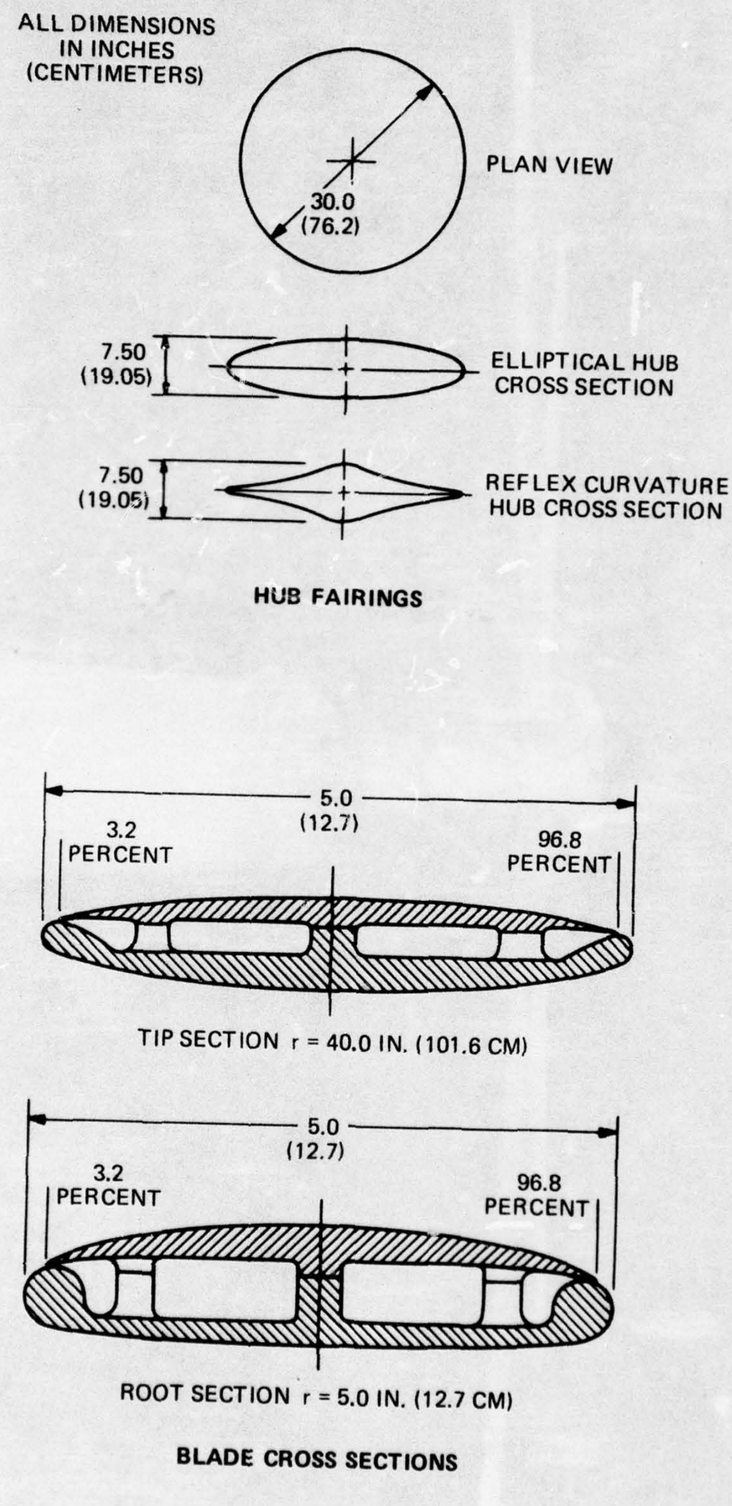

Figure 1(a) – Model Description

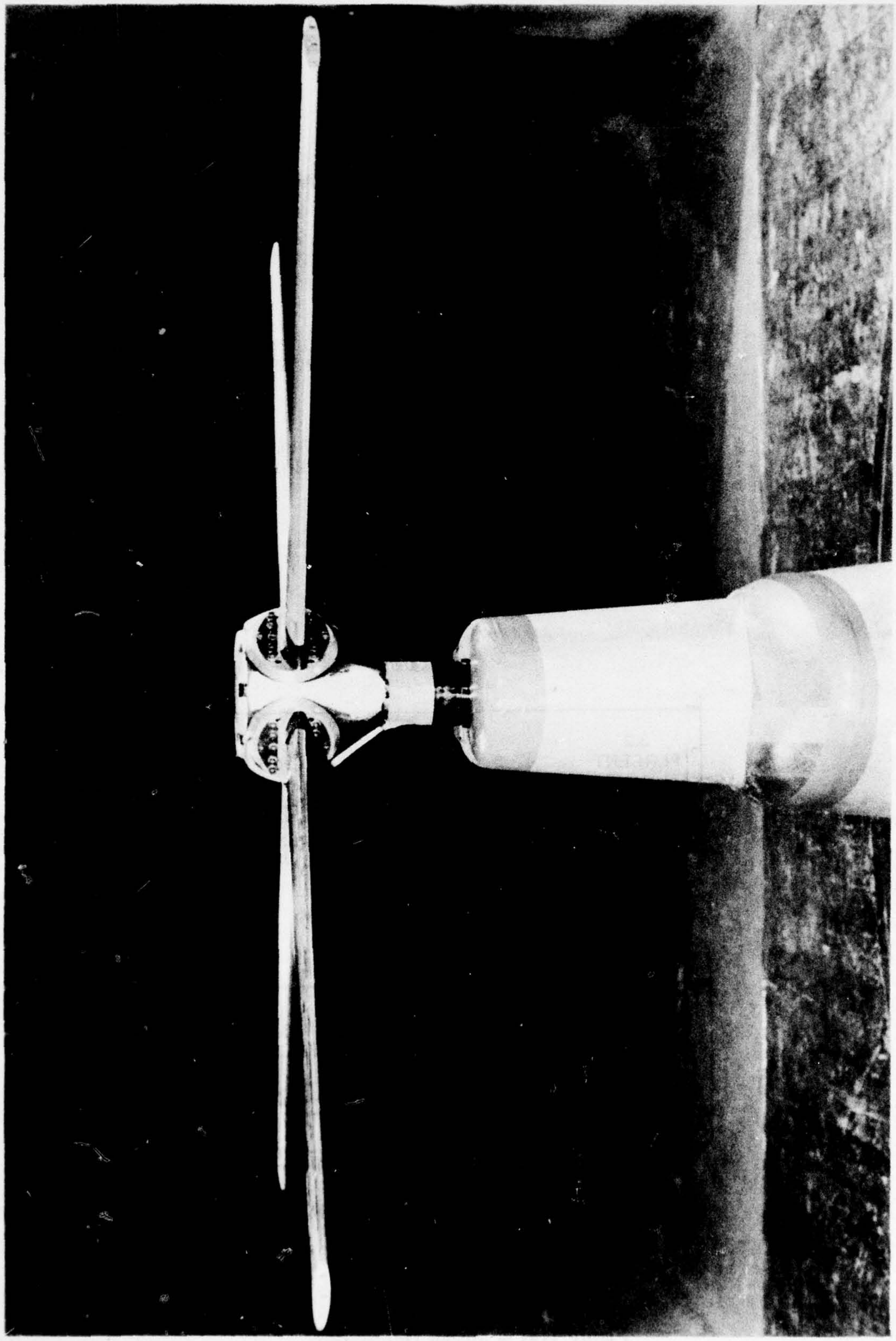

Figure 1(b) – Wind Tunnel Photographs – RB-CCR and Support System

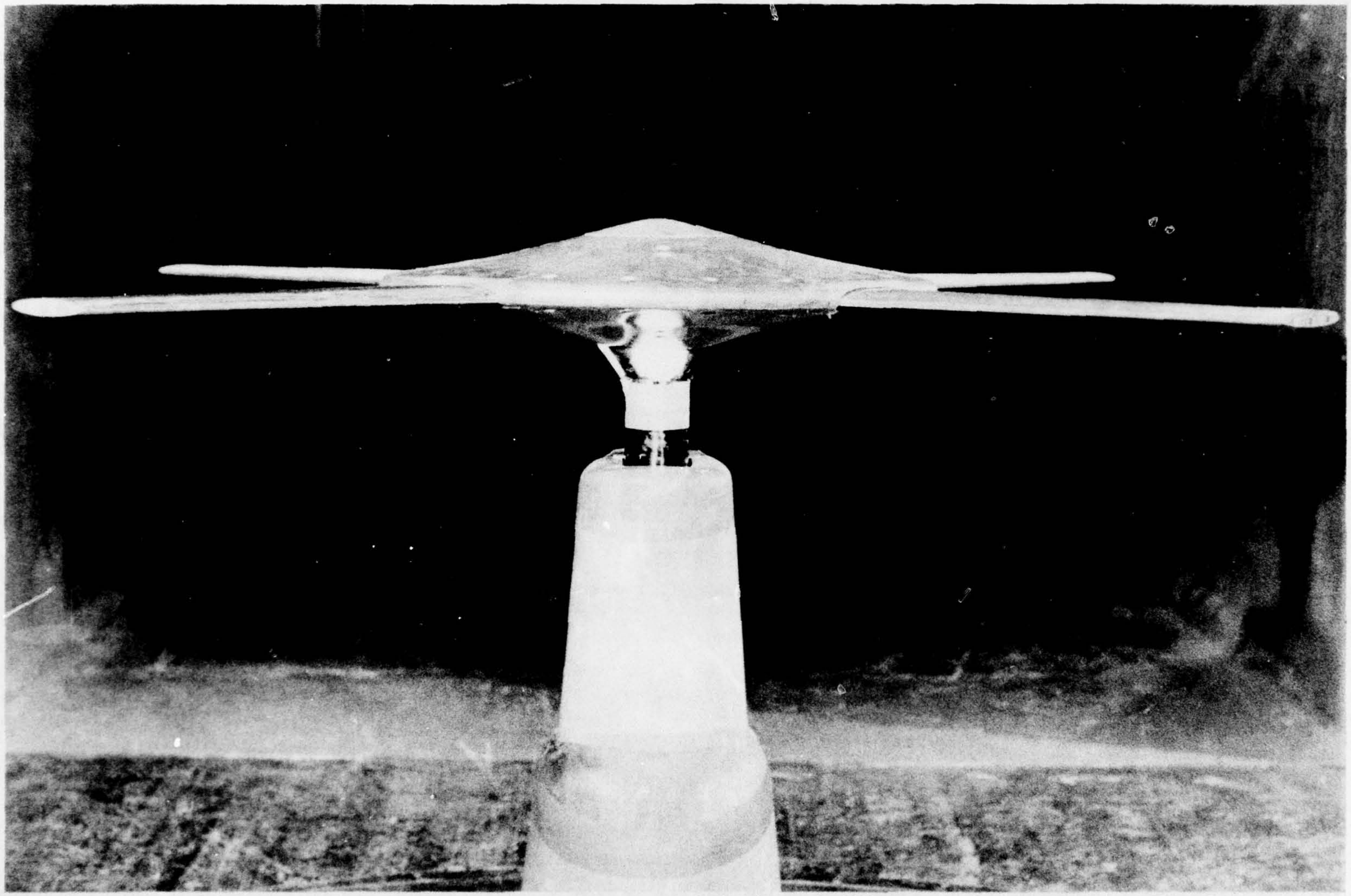

Figure 1(b) – Wind Tunnel Photographs – Reflex Hub Fairing

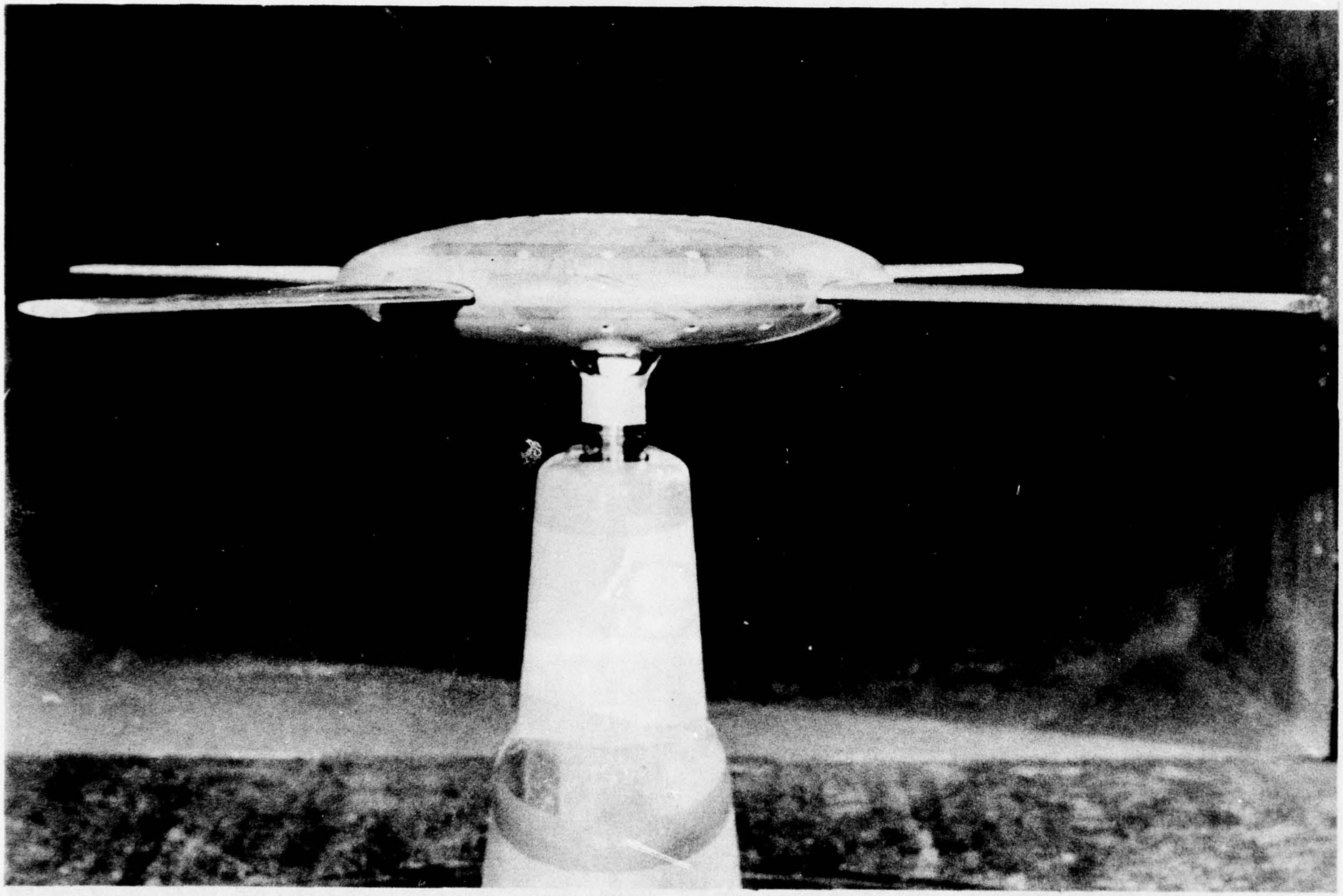

Figure 1(b) – Wind Tunnel Photographs – Elliptical Hub Fairing

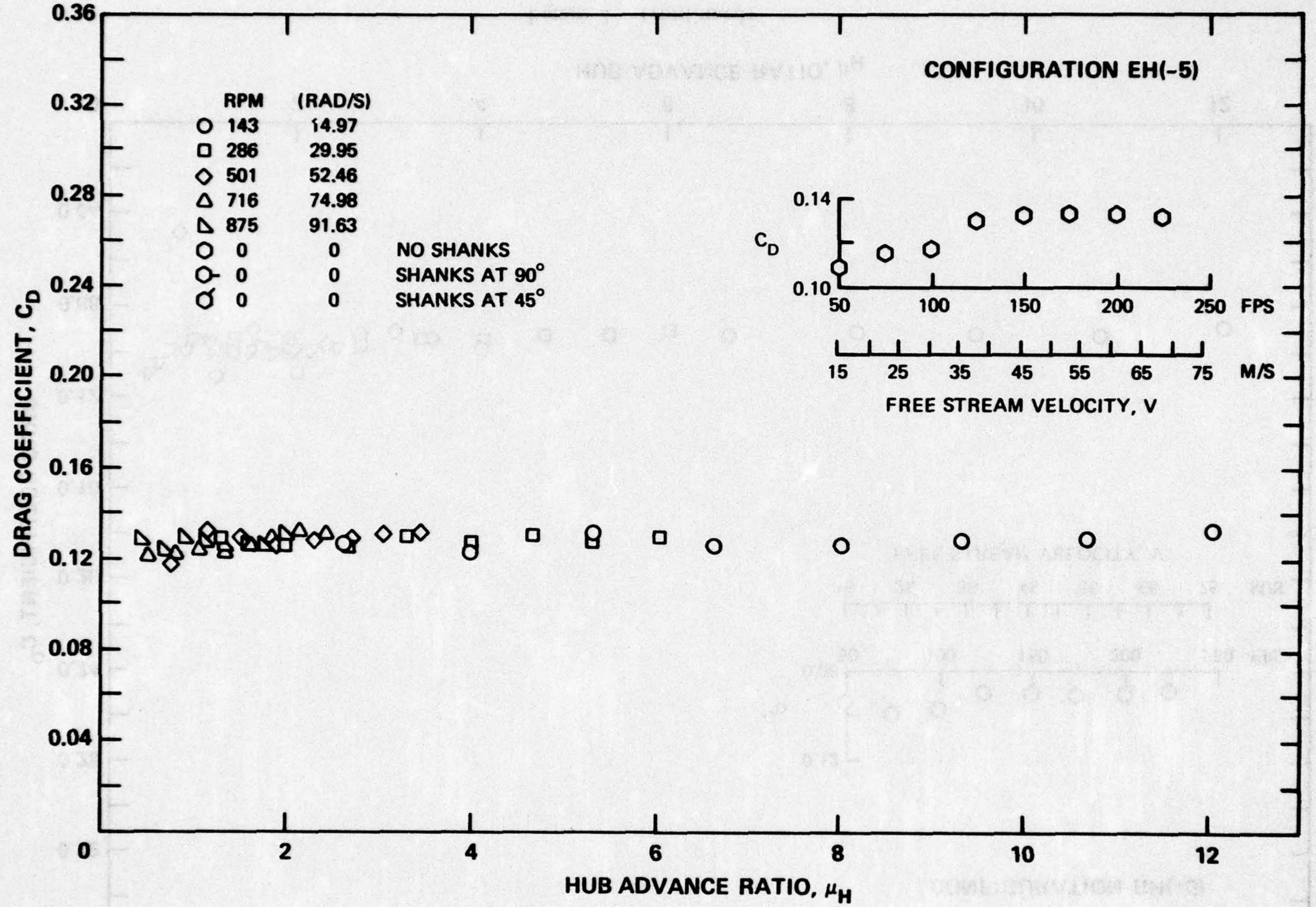

Figure 2 – Drag Coefficient Versus Hub Advance Ratio

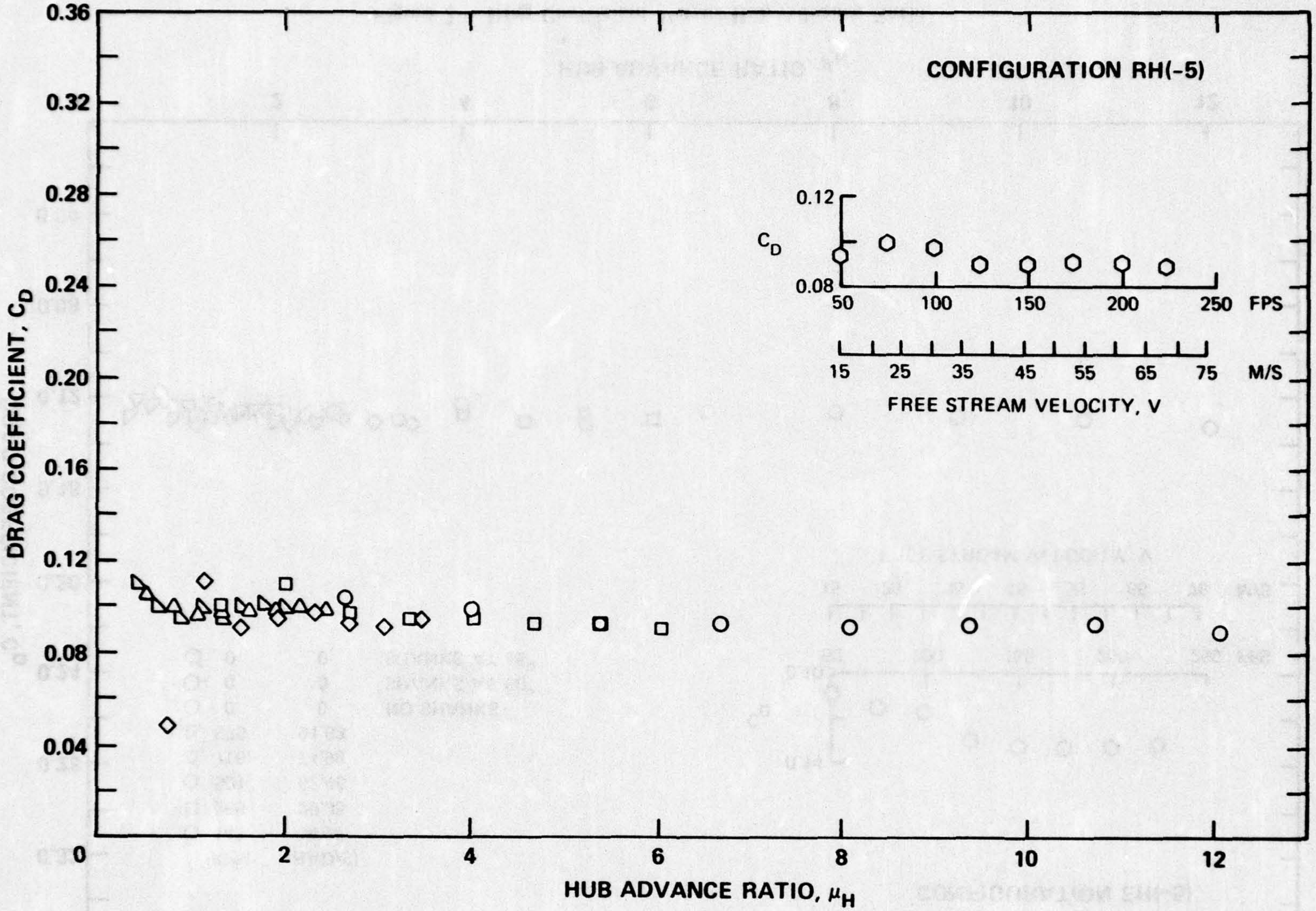

Figure 2 – (continued)

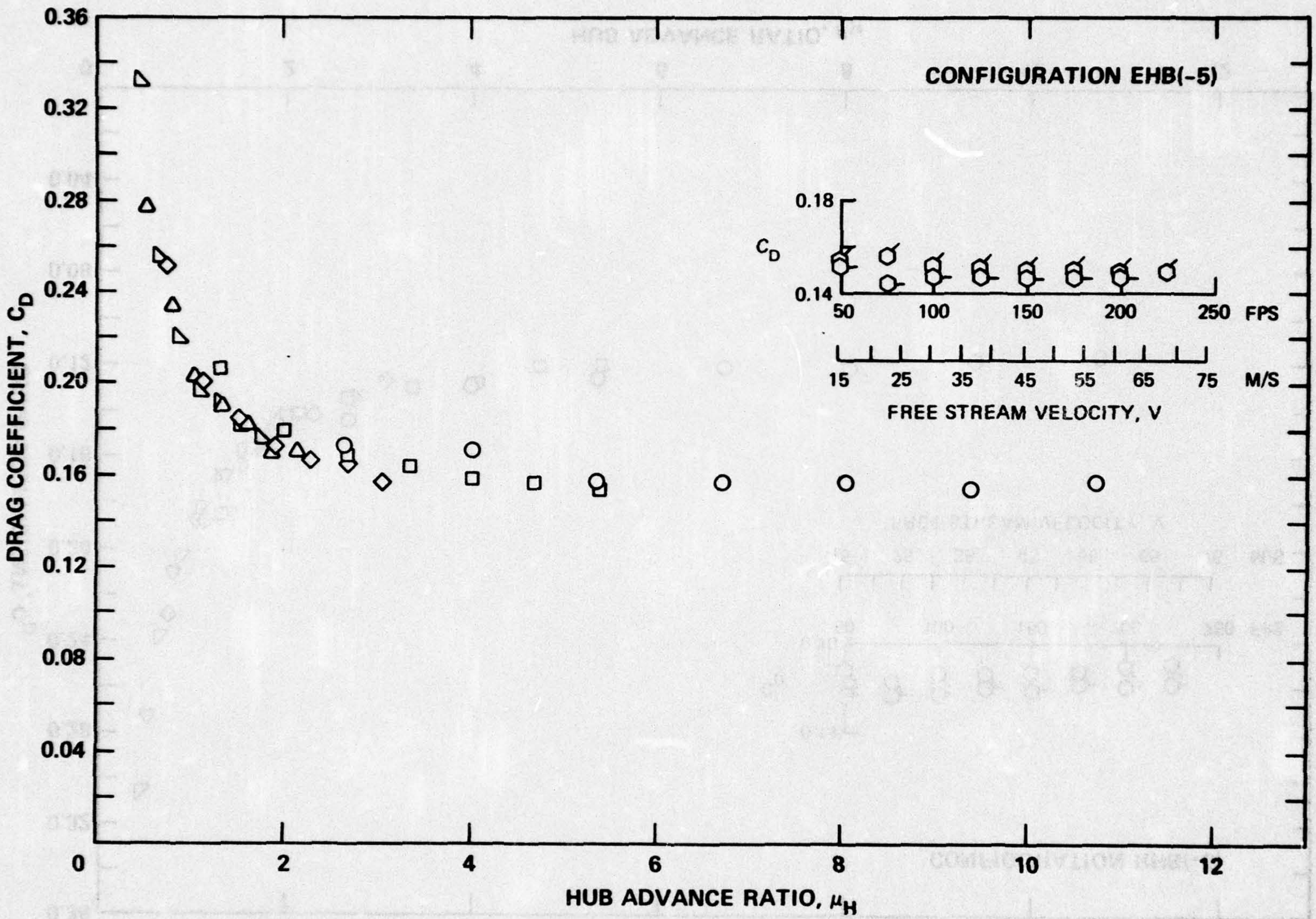

Figure 2 – (continued)

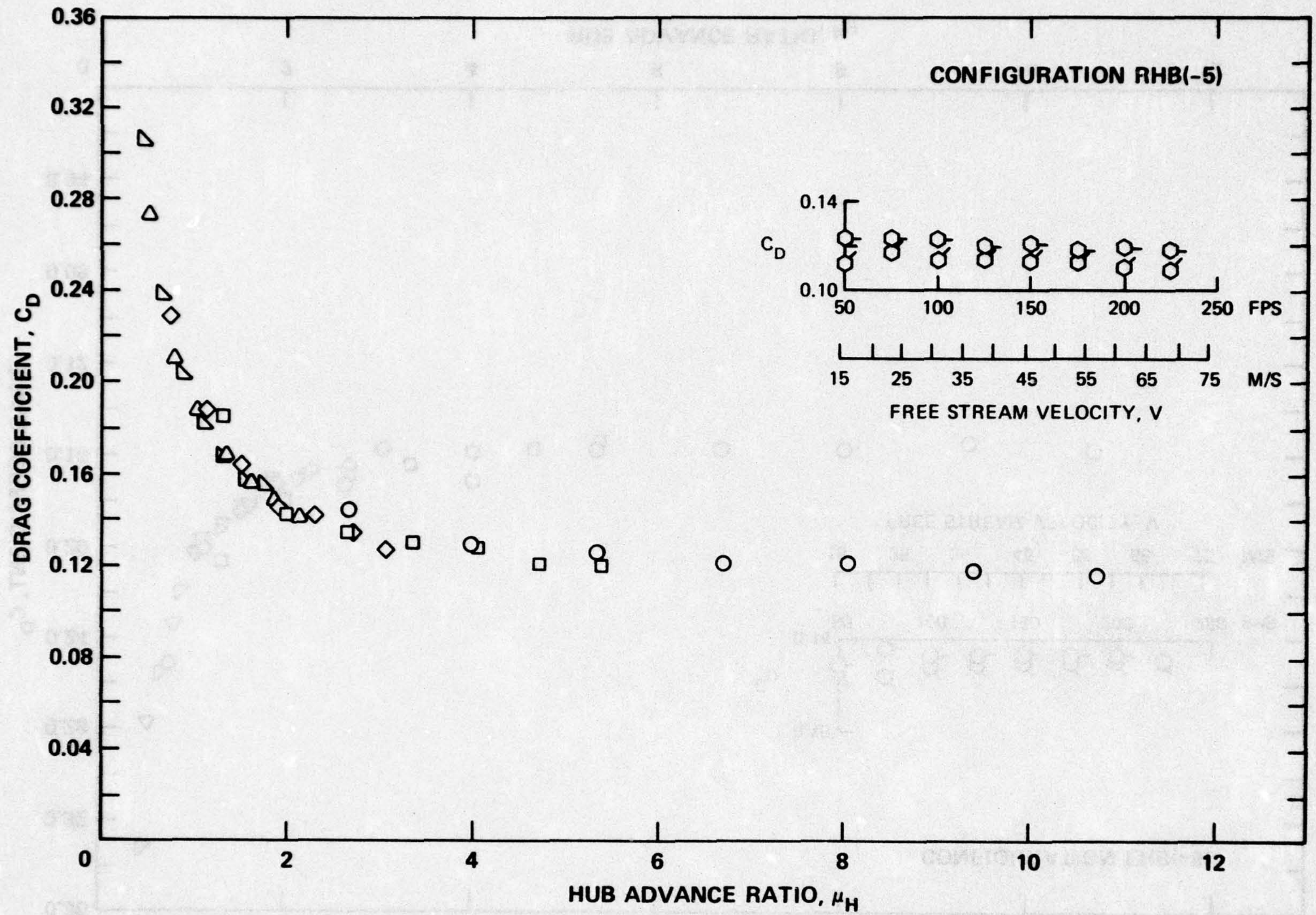

Figure 2 – (continued)

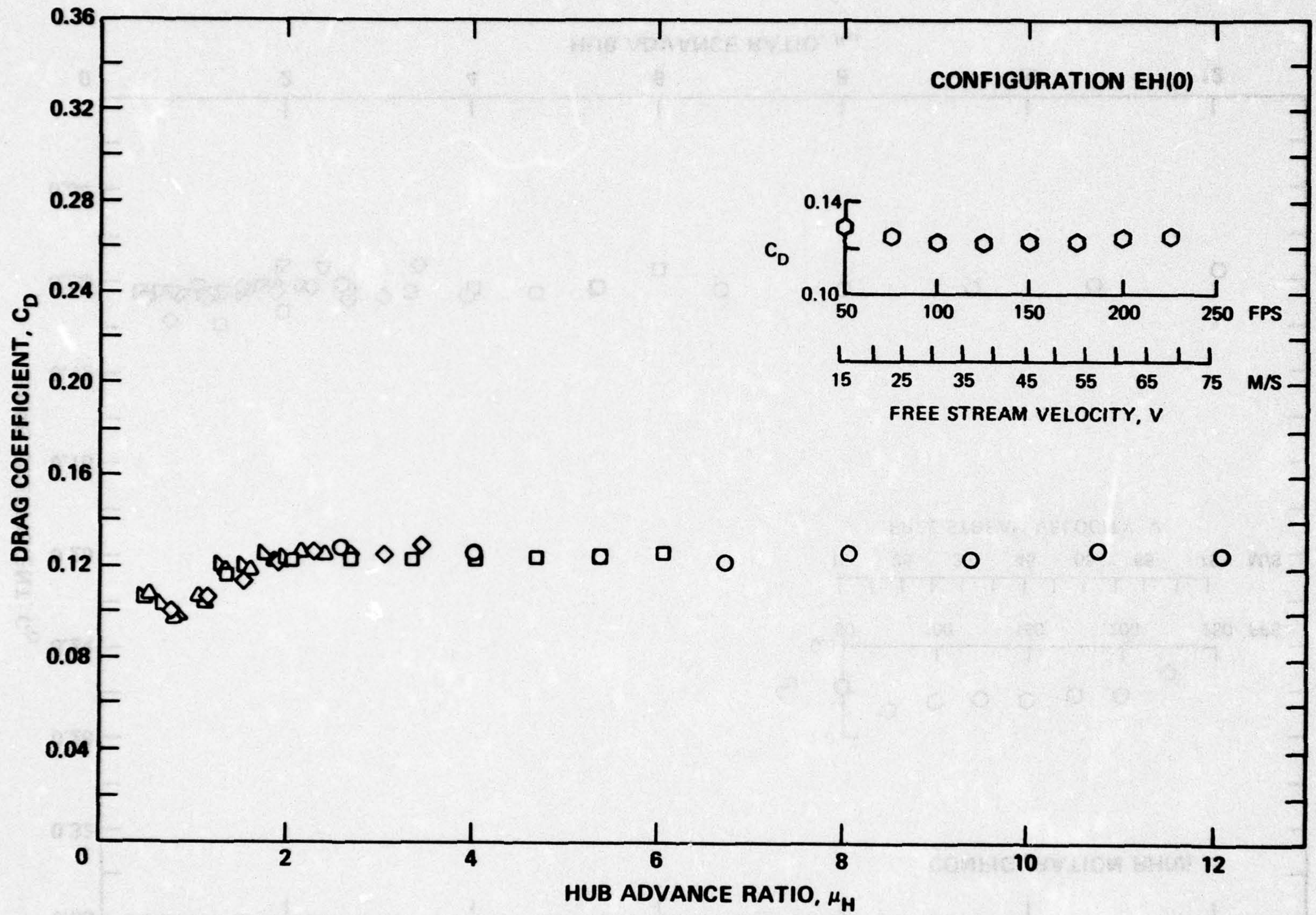

Figure 2 – (continued)

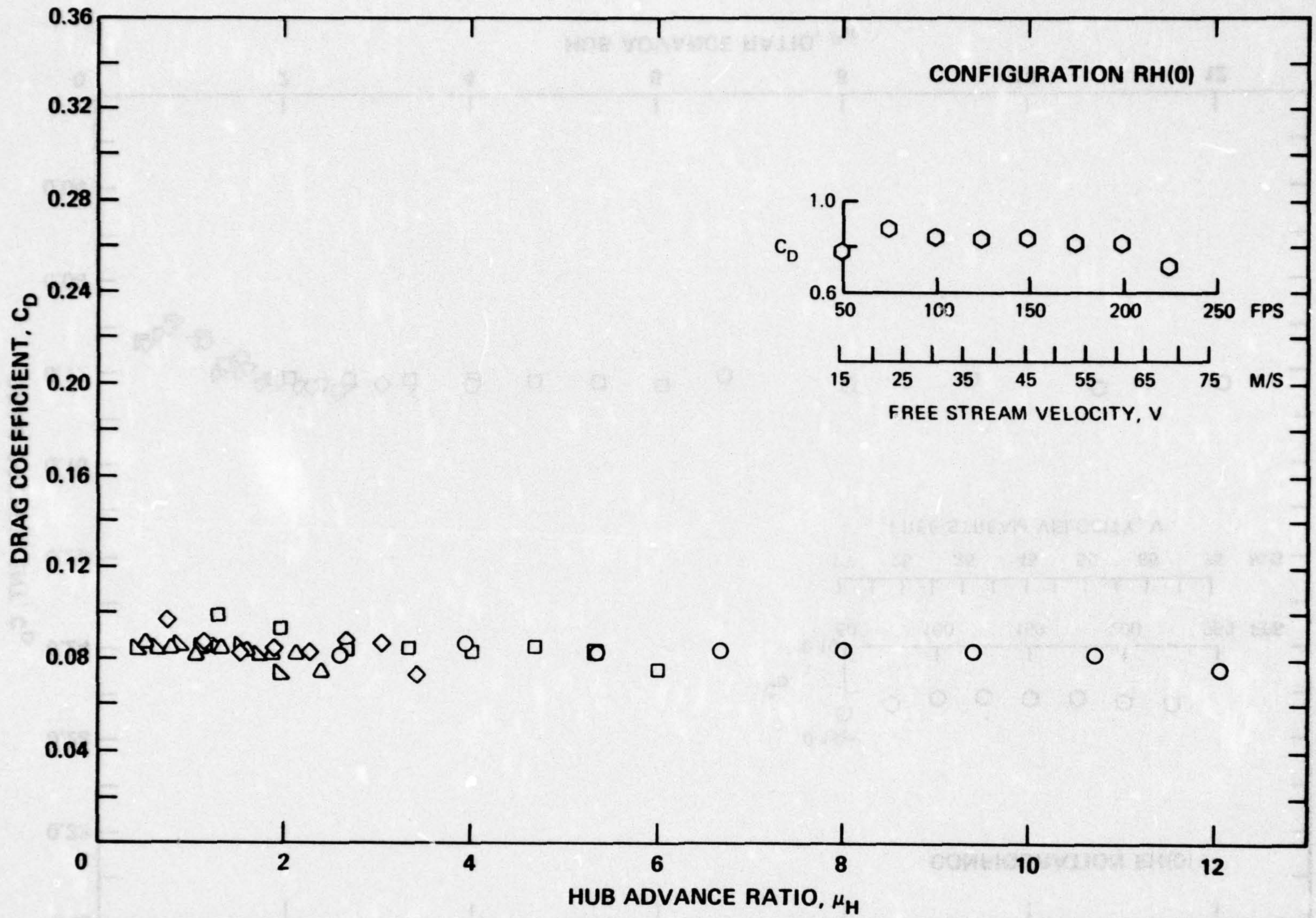

Figure 2 – (continued)

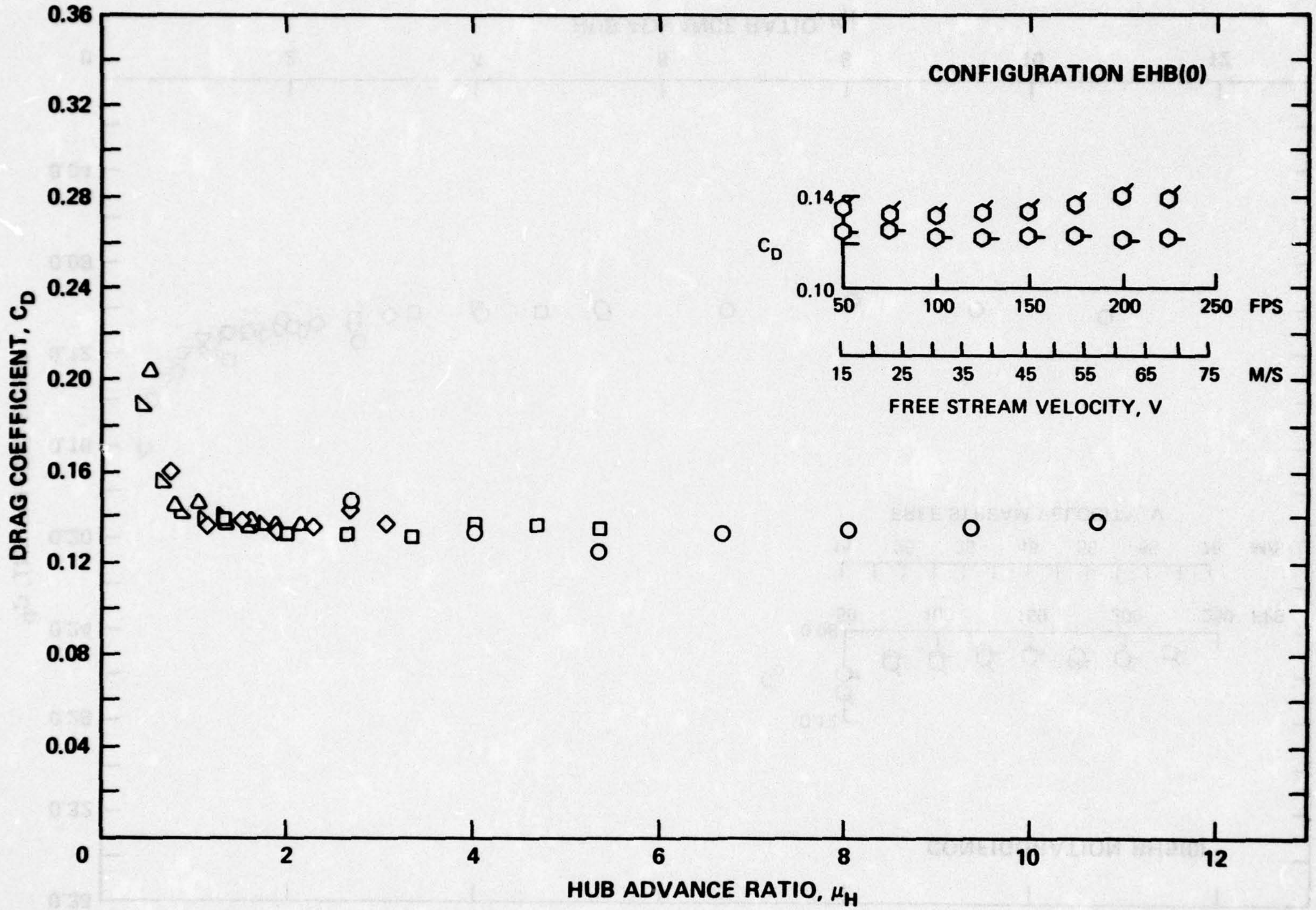

Figure 2 – (continued)

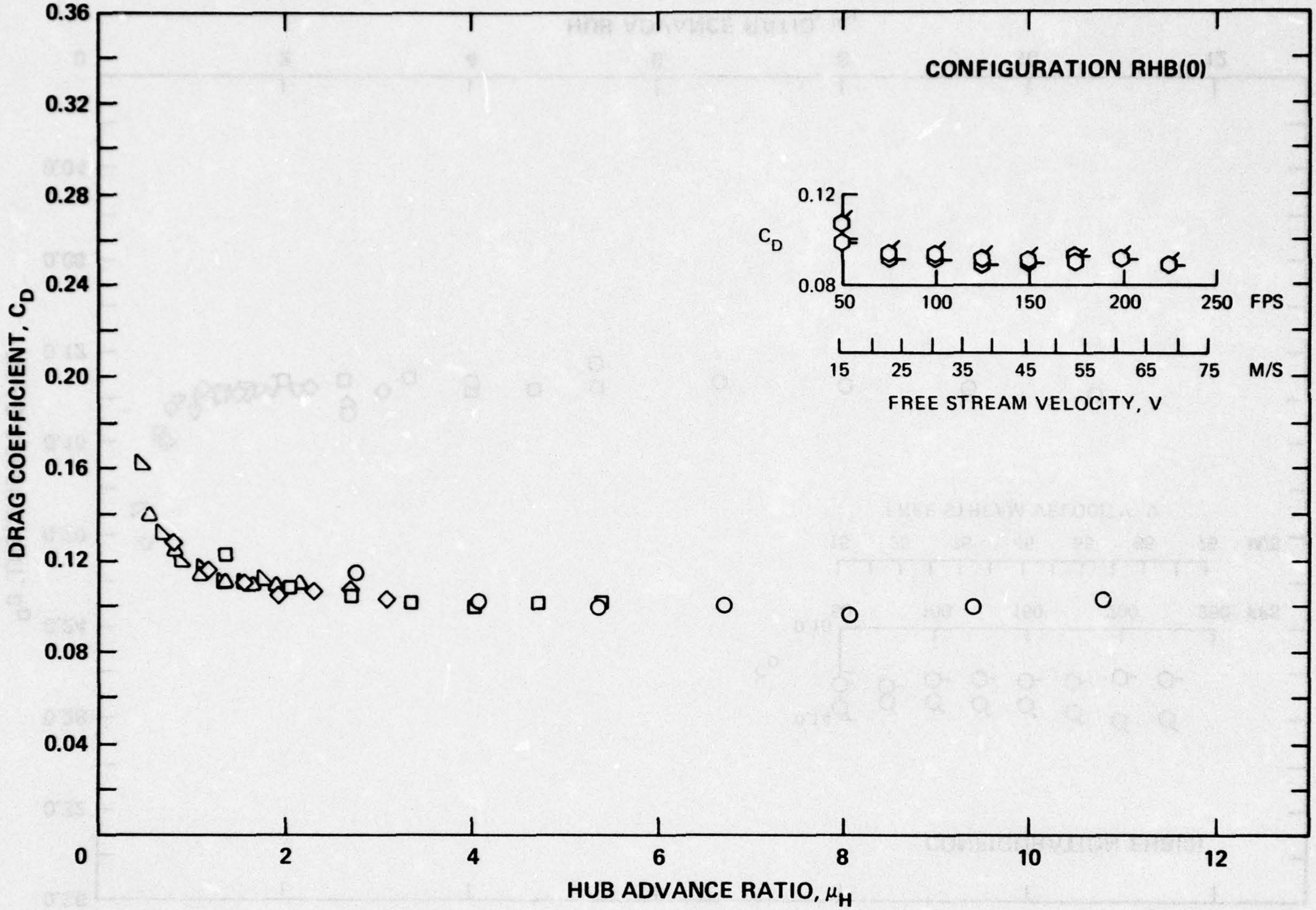

Figure 2 – (concluded)

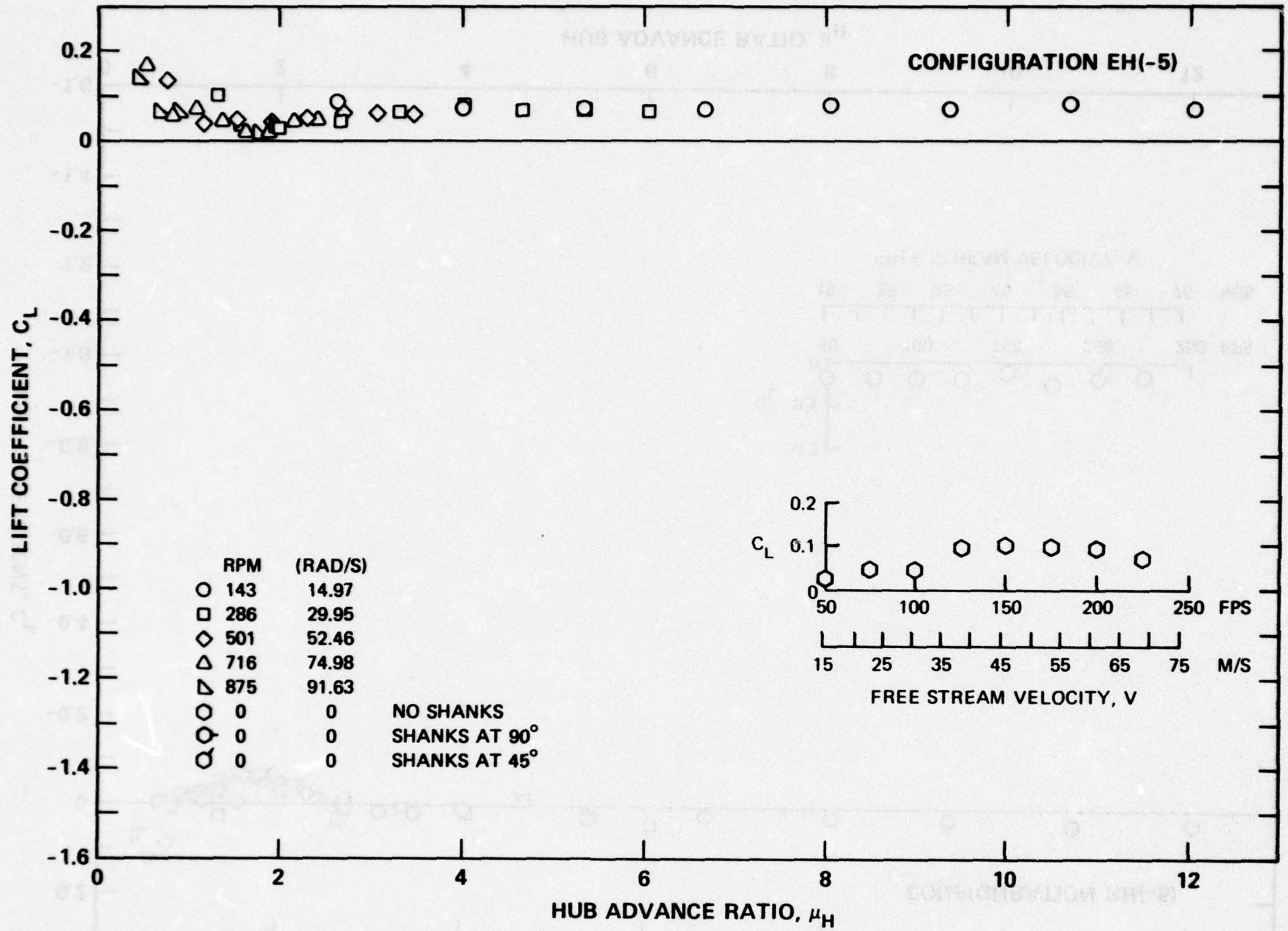

Figure 3 – Lift Coefficient Versus Hub Advance Ratio

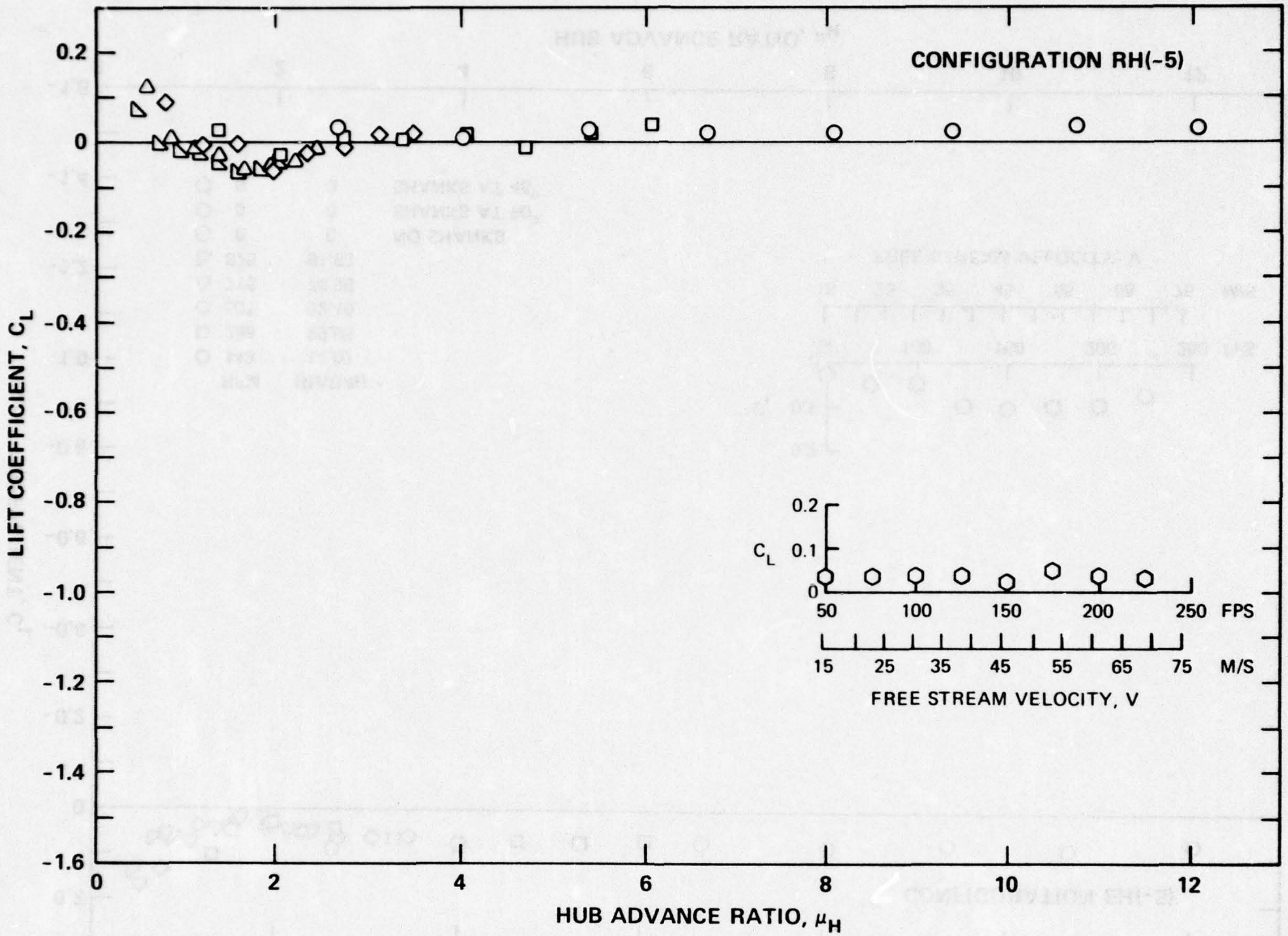

Figure 3 – (continued)

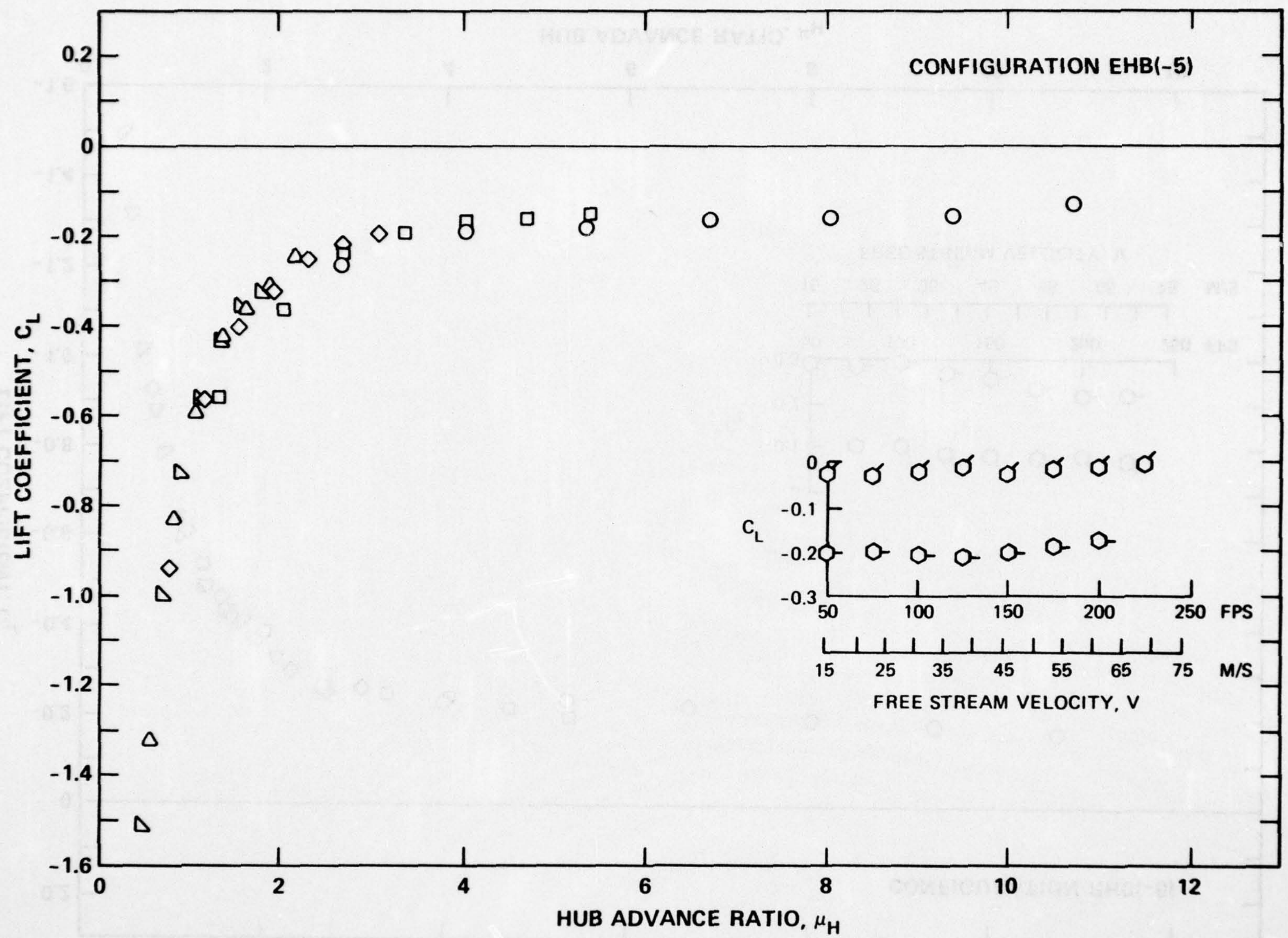

Figure 3 – (continued)

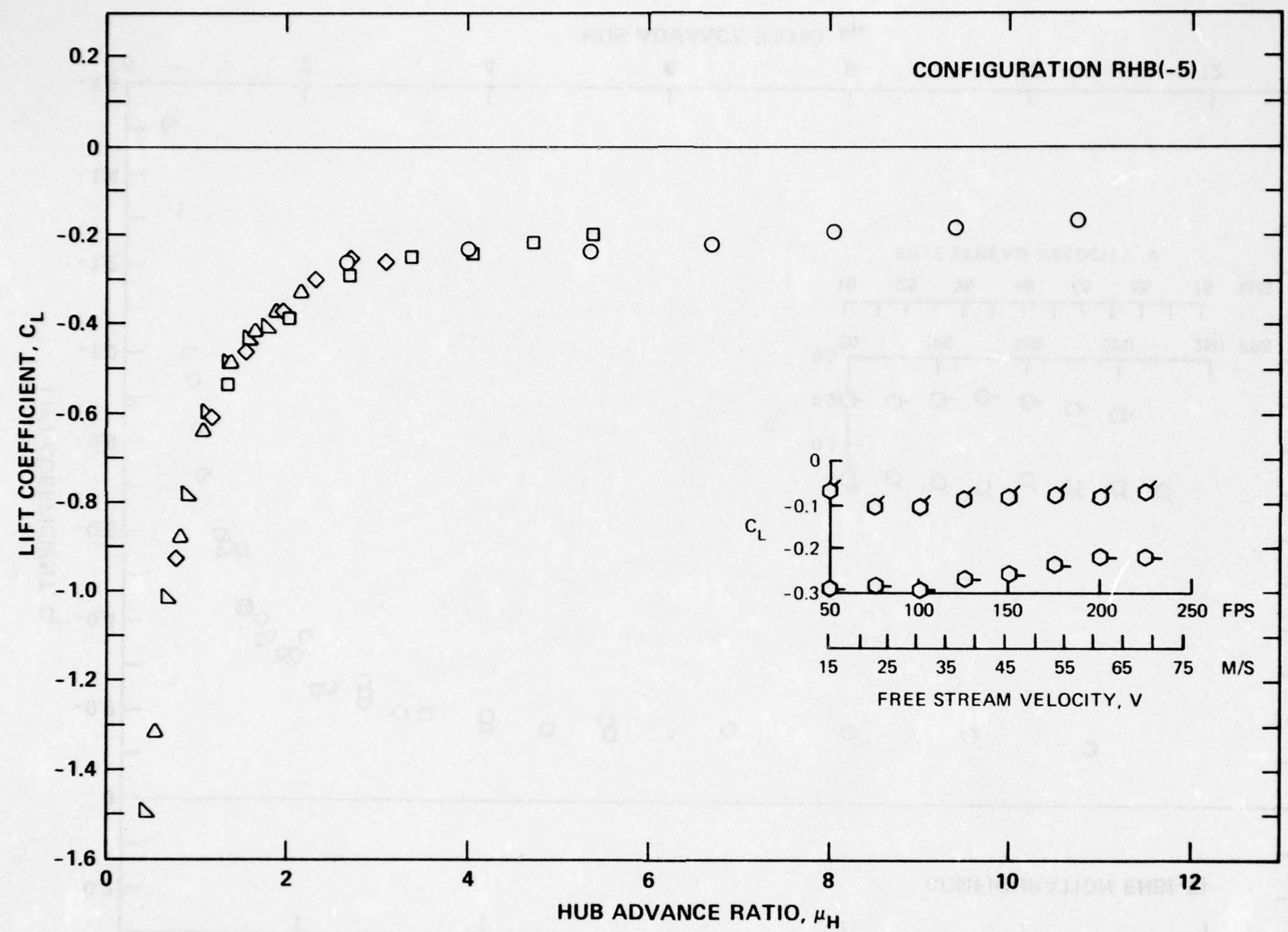

Figure 3 – (continued)

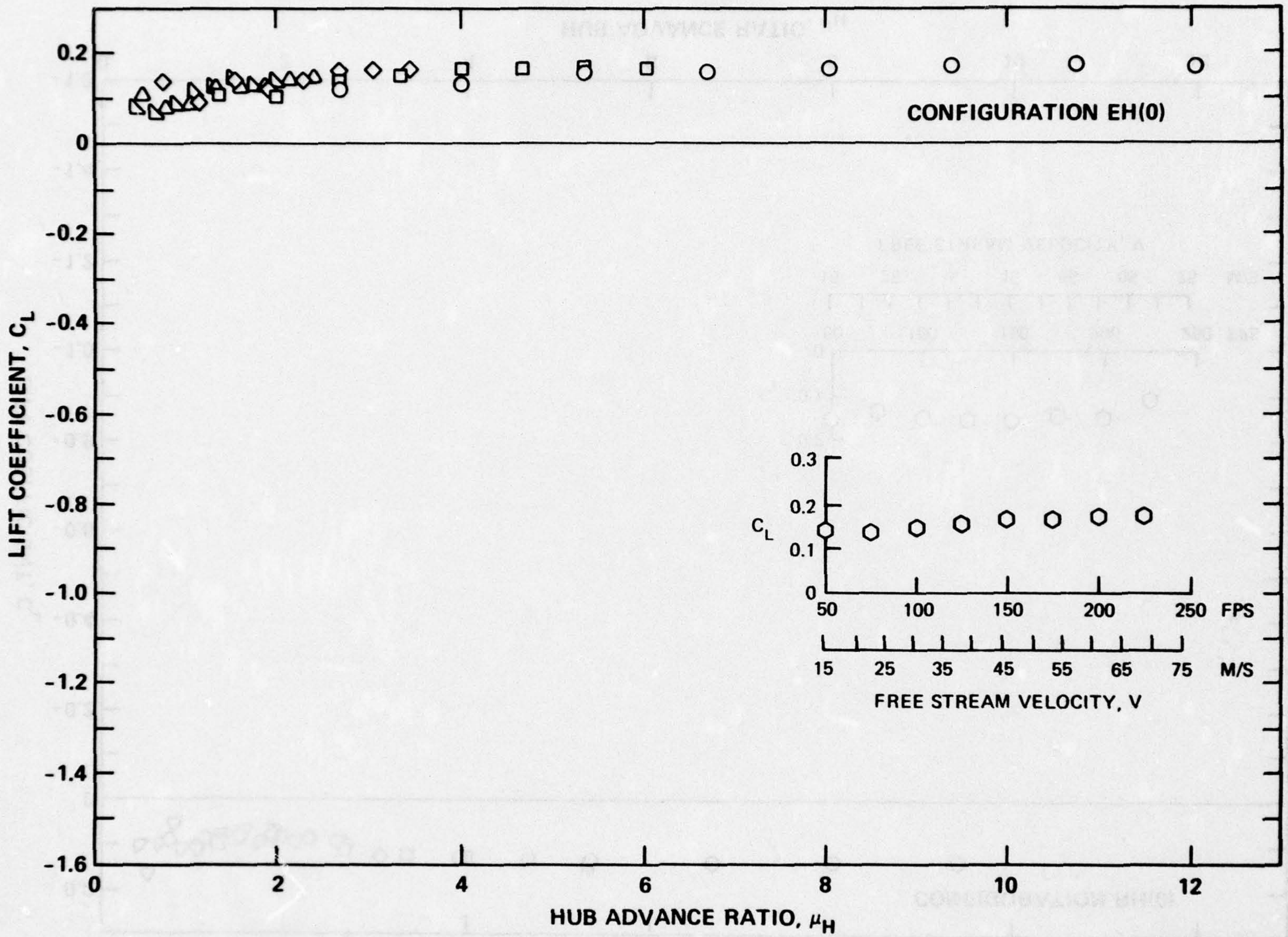

Figure 3 – (continued)

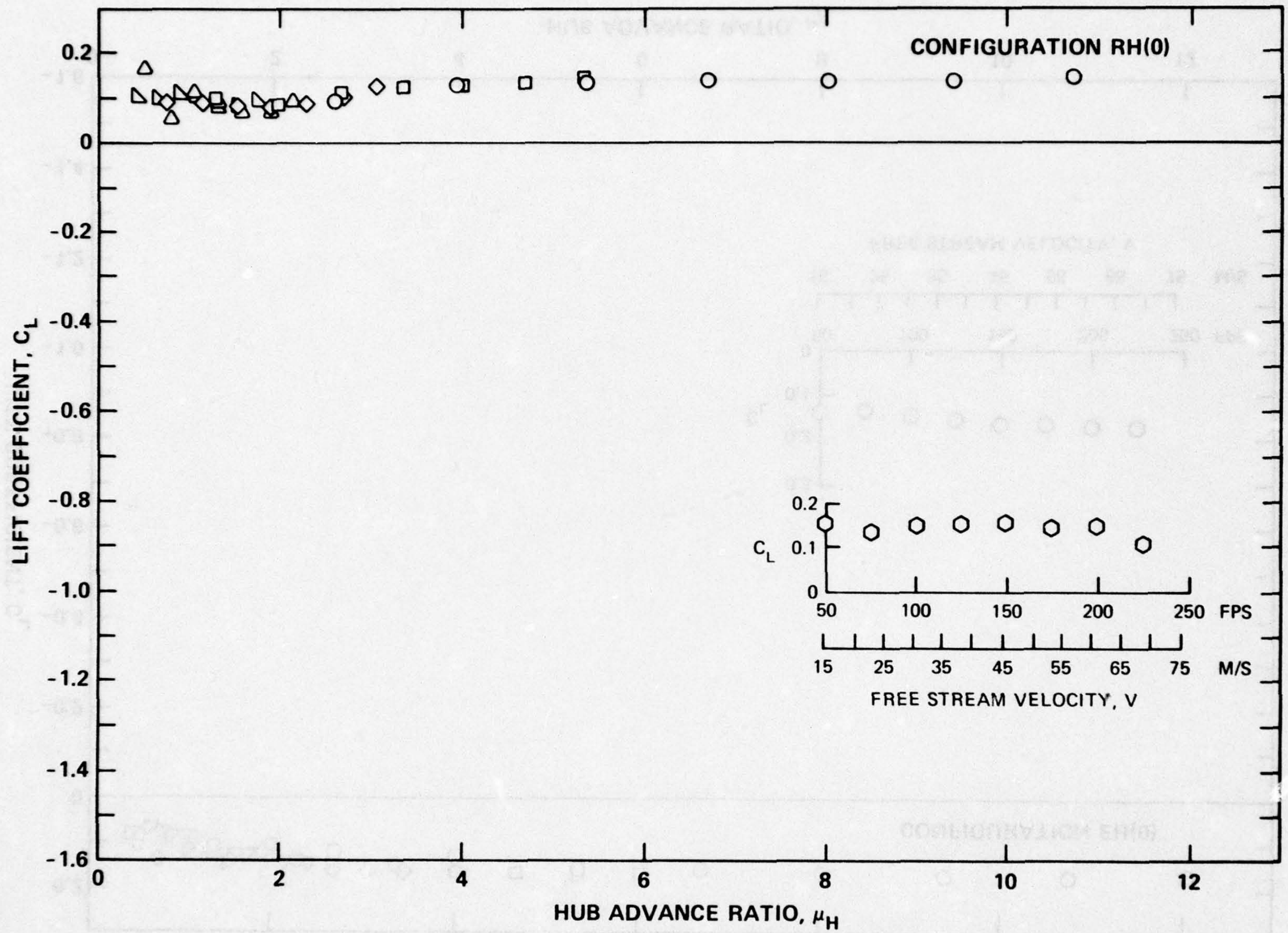

Figure 3 – (continued)

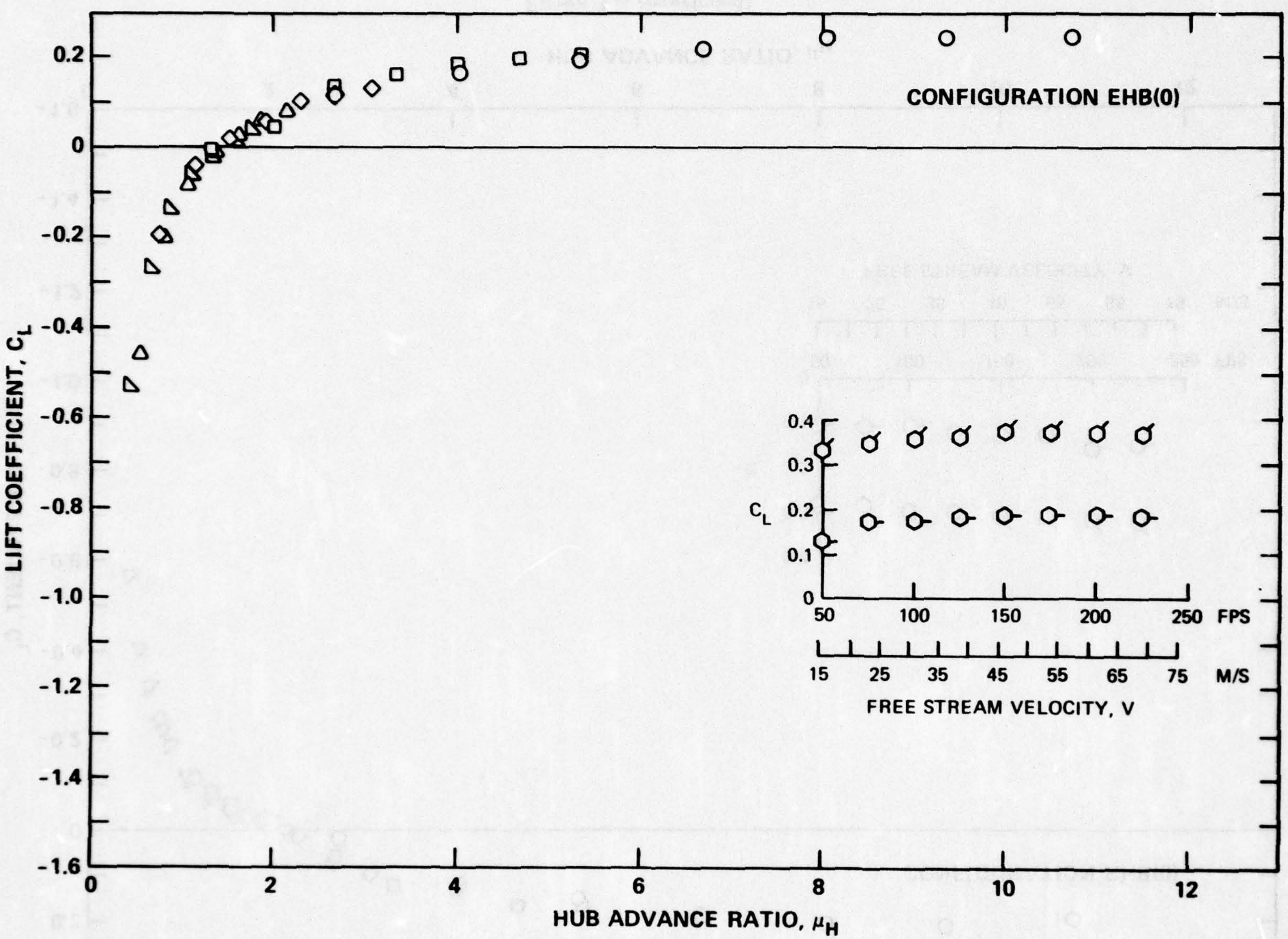

Figure 3 – (continued)

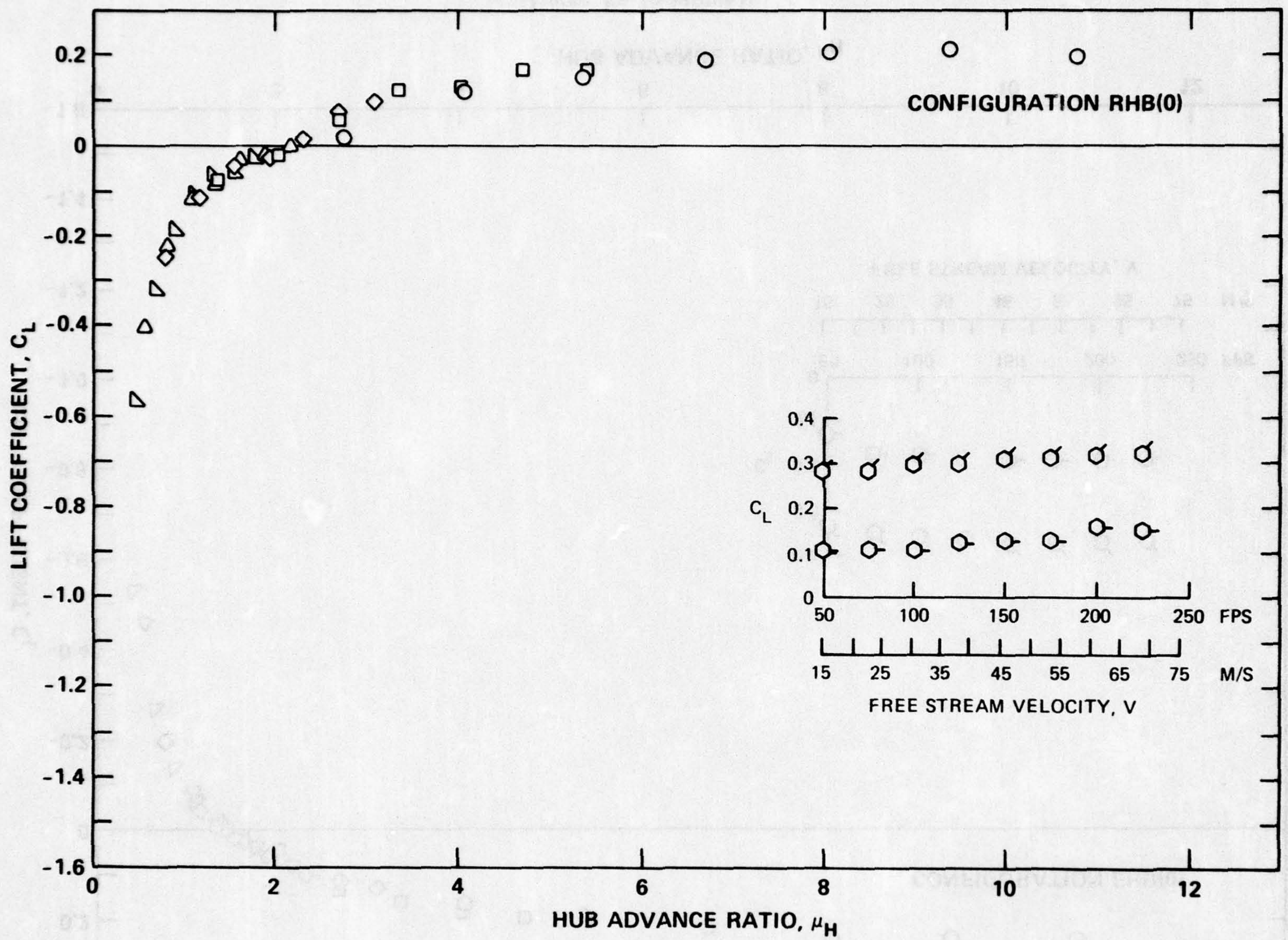

Figure 3 – (concluded)

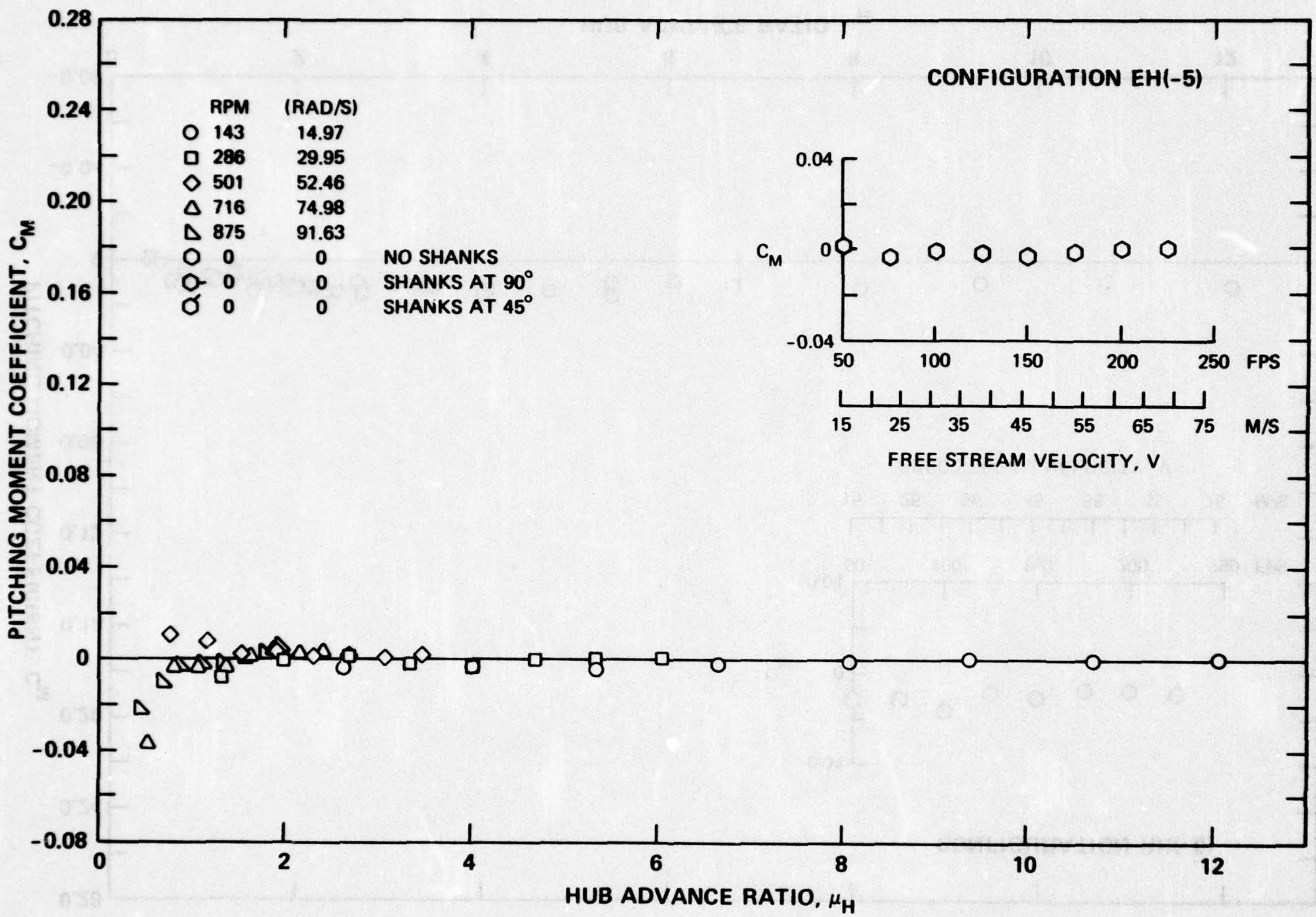

Figure 4 – Pitching Moment Coefficient Versus Hub Advance Ratio

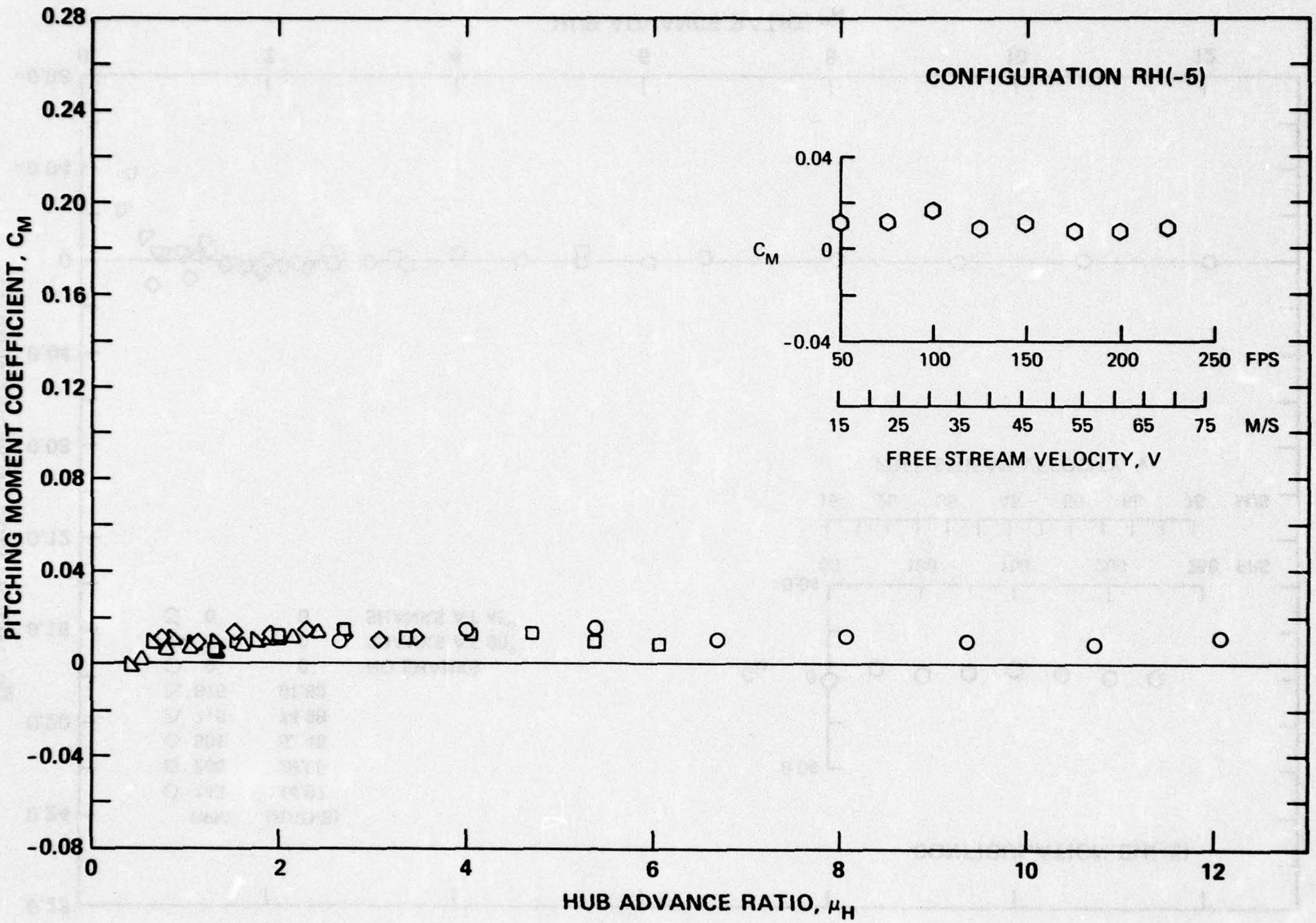

Figure 4 – (continued)

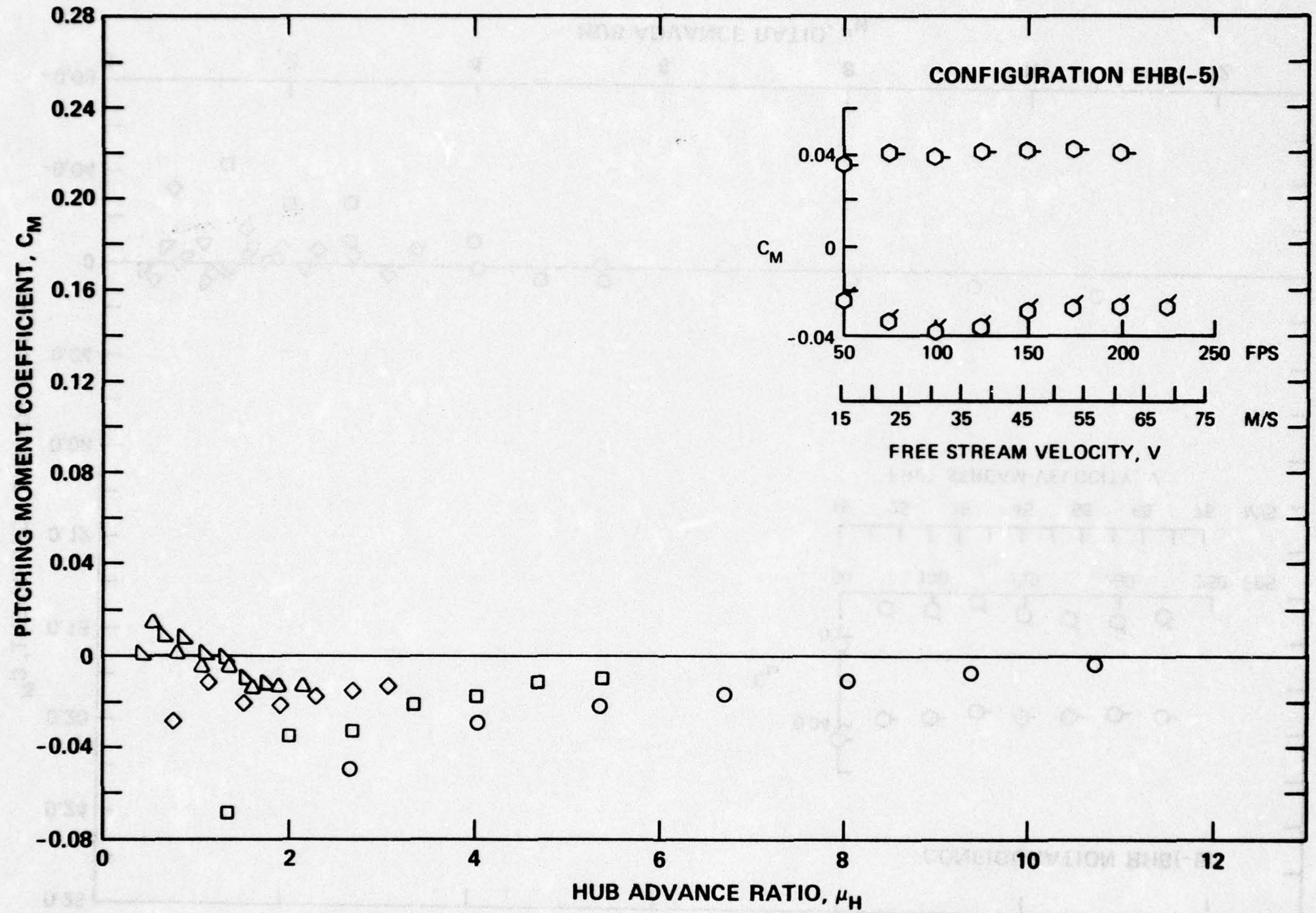

Figure 4 – (continued)

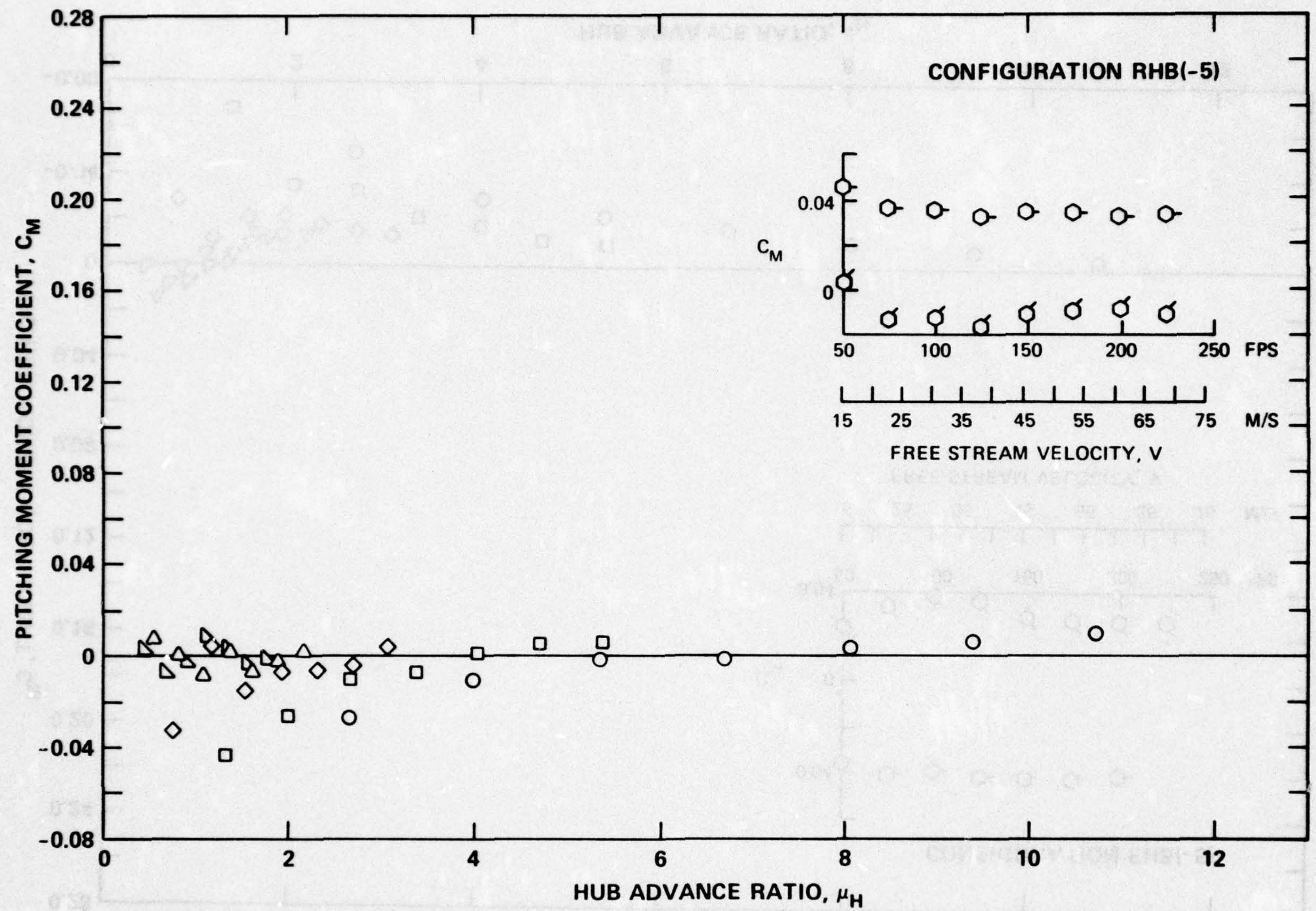

Figure 4 – (continued)

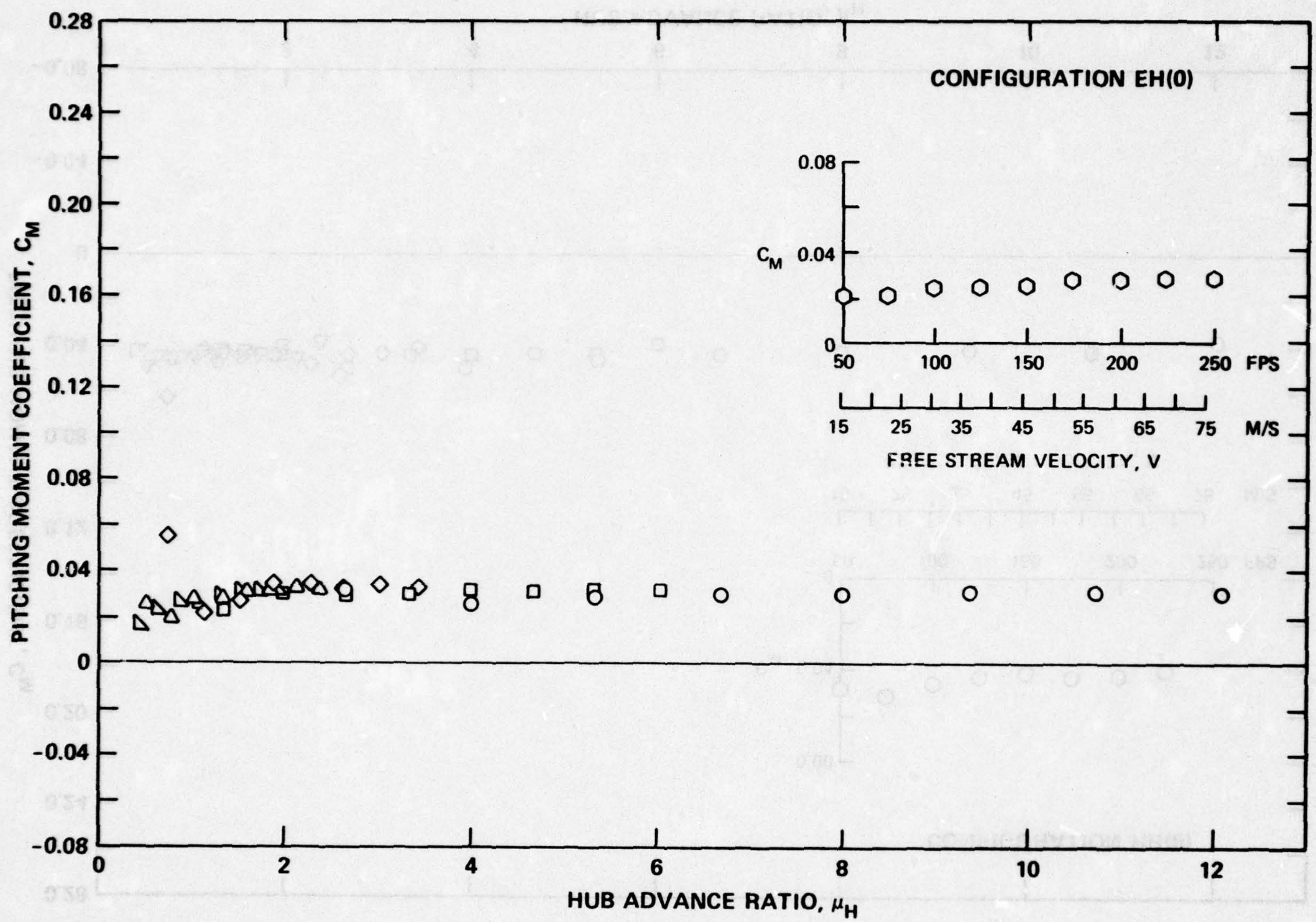

Figure 4 – (continued)

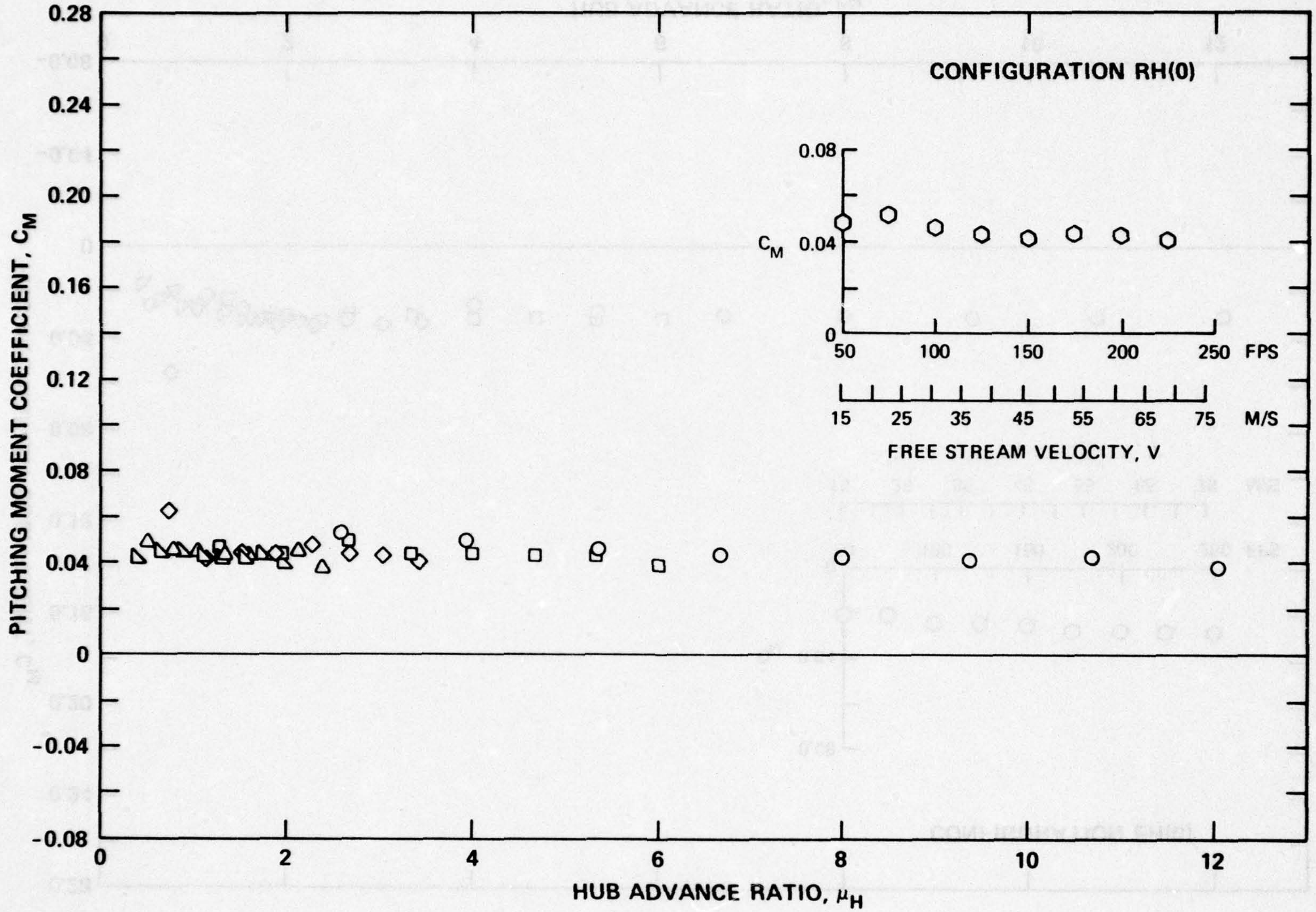

Figure 4 – (continued)

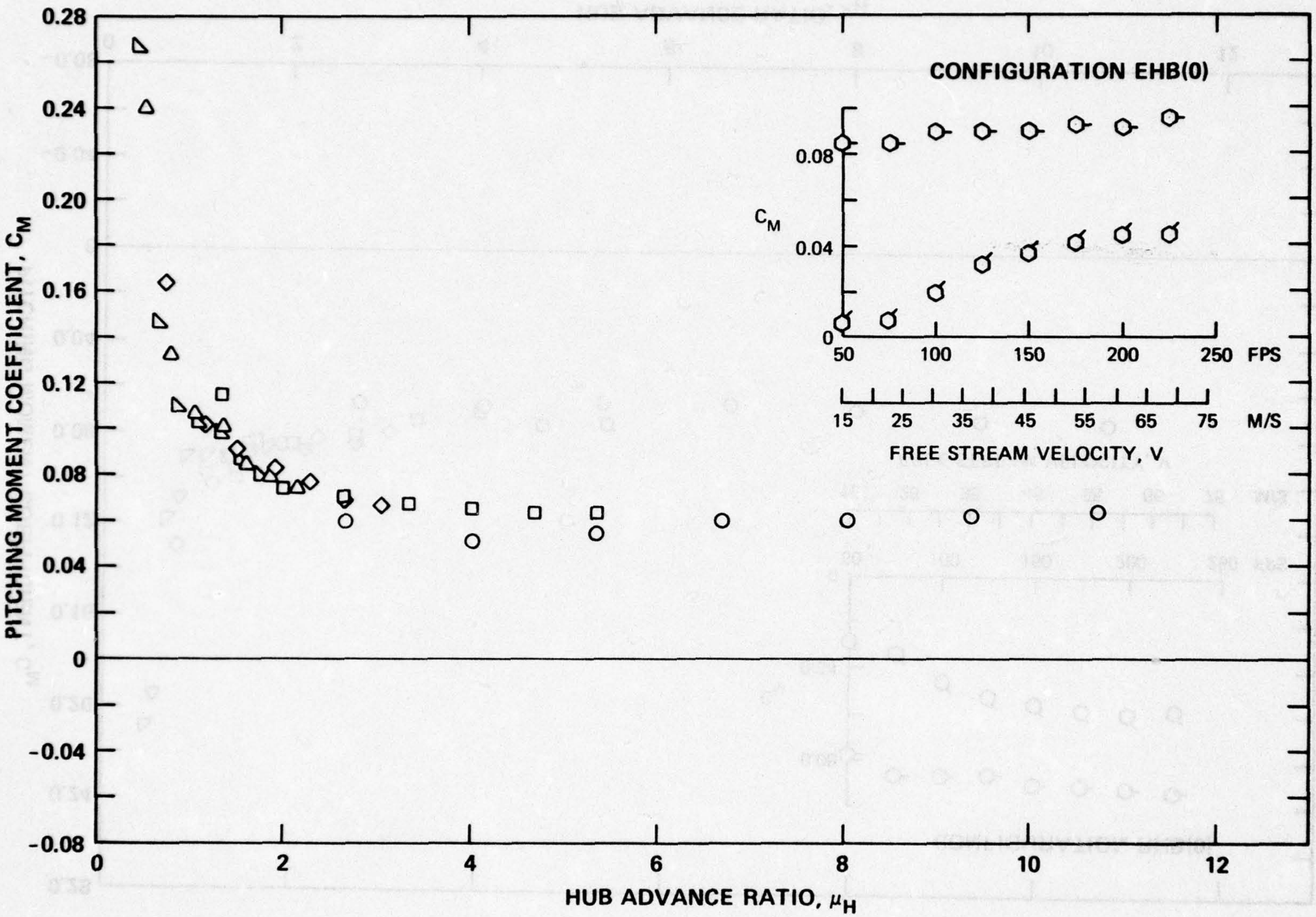

Figure 4 – (continued)

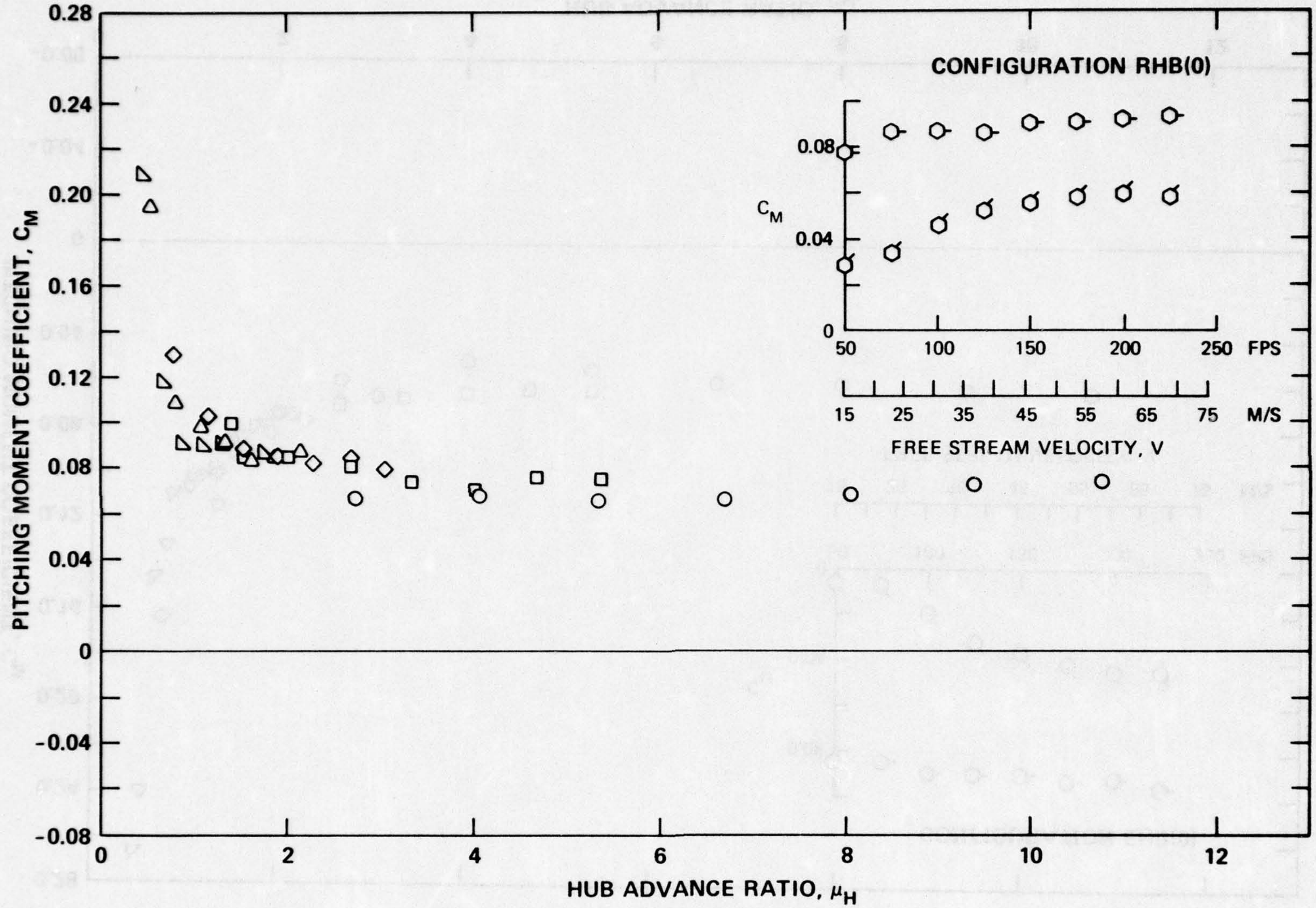

Figure 4 – (concluded)

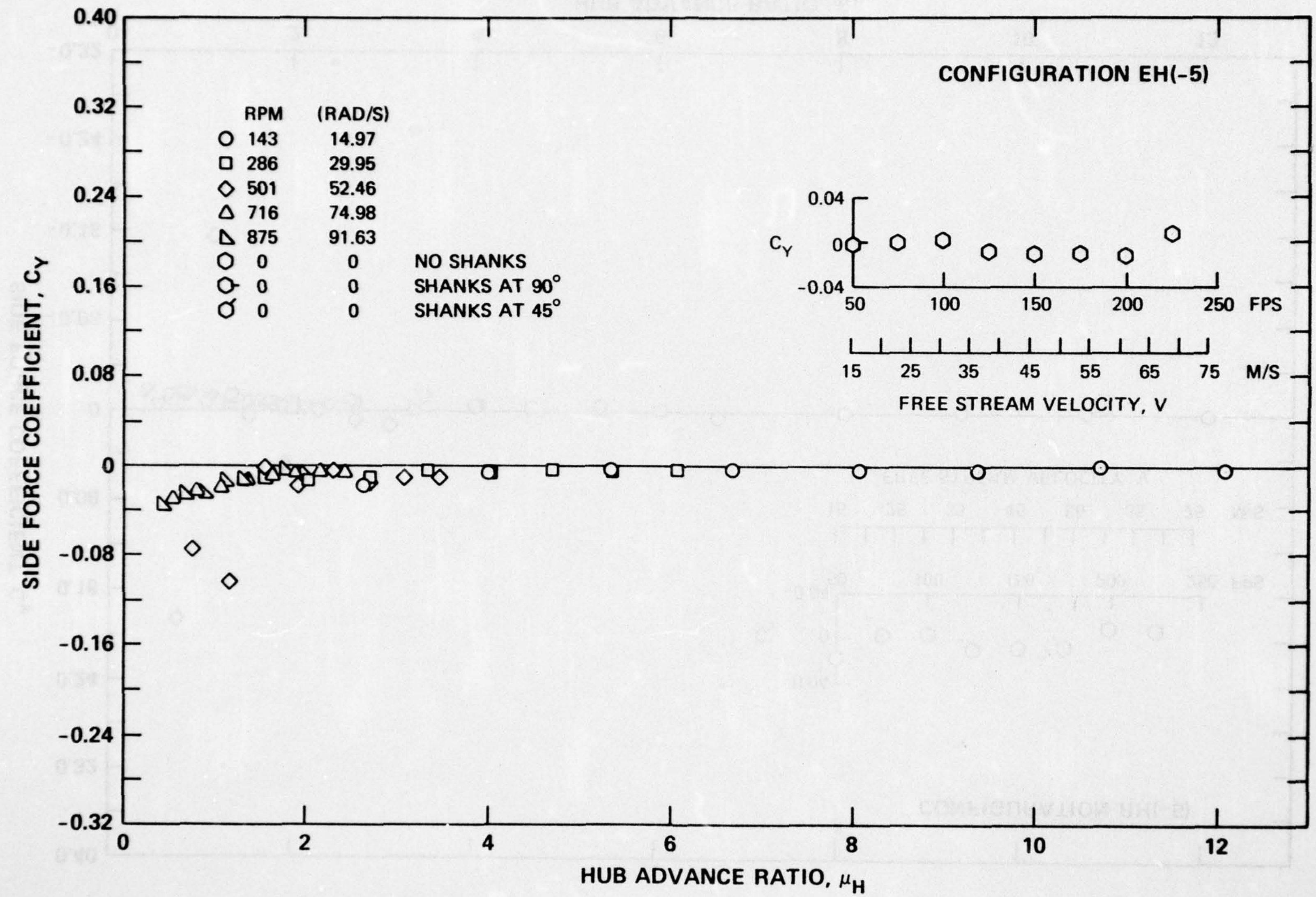

Figure 5 – Side Force Coefficient Versus Hub Advance

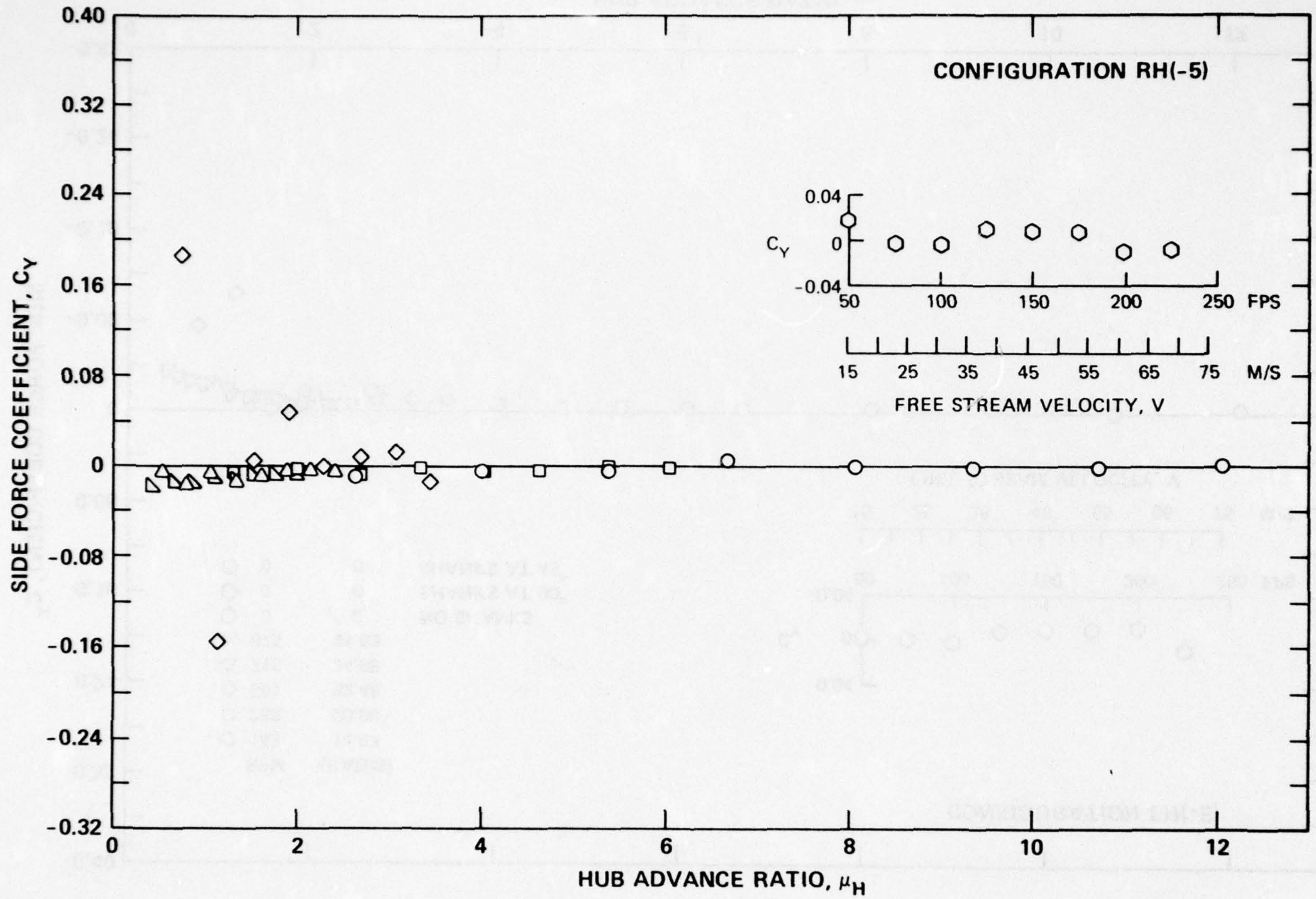

Figure 5 – (continued)

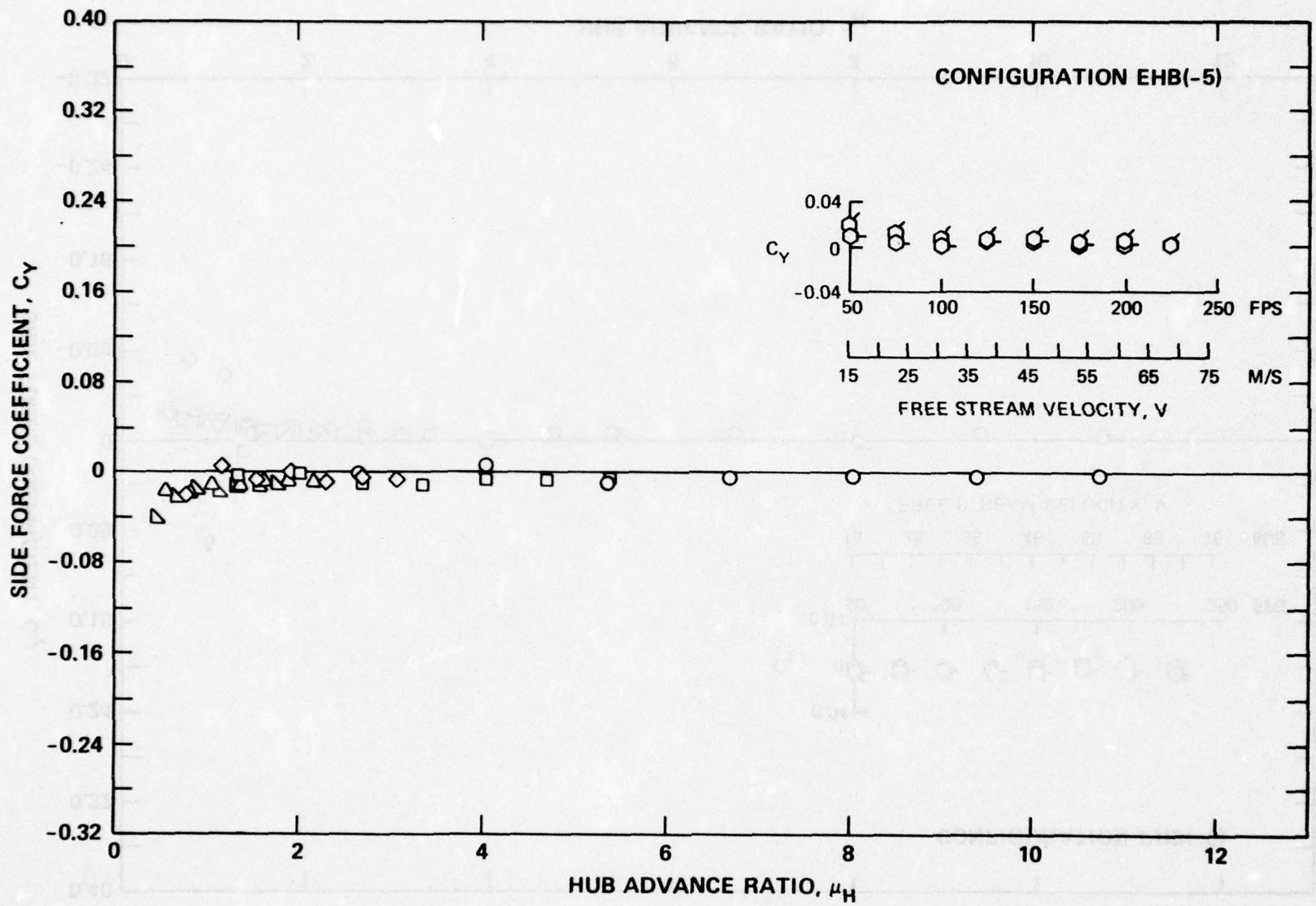

Figure 5 – (continued)

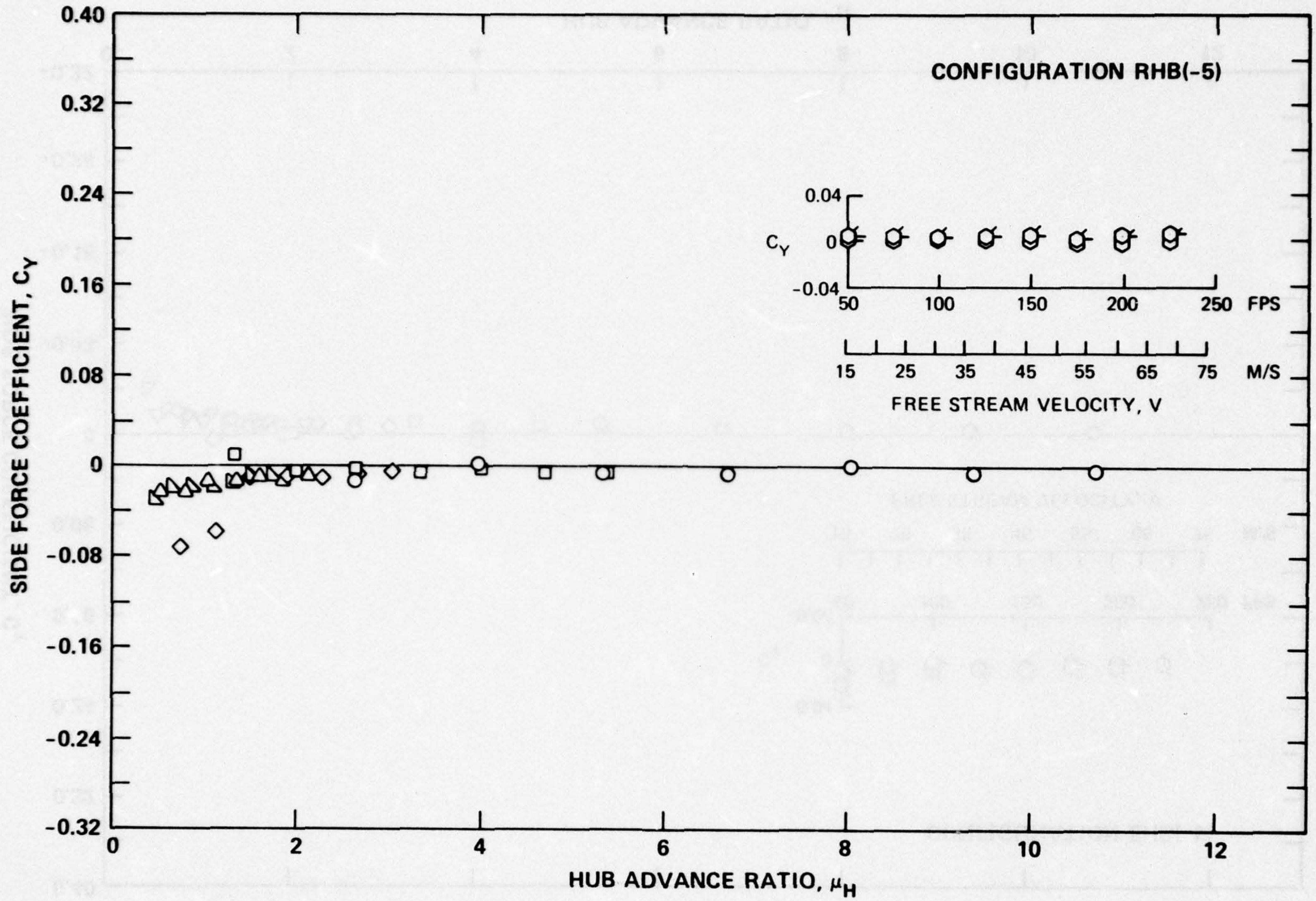

Figure 5 – (continued)

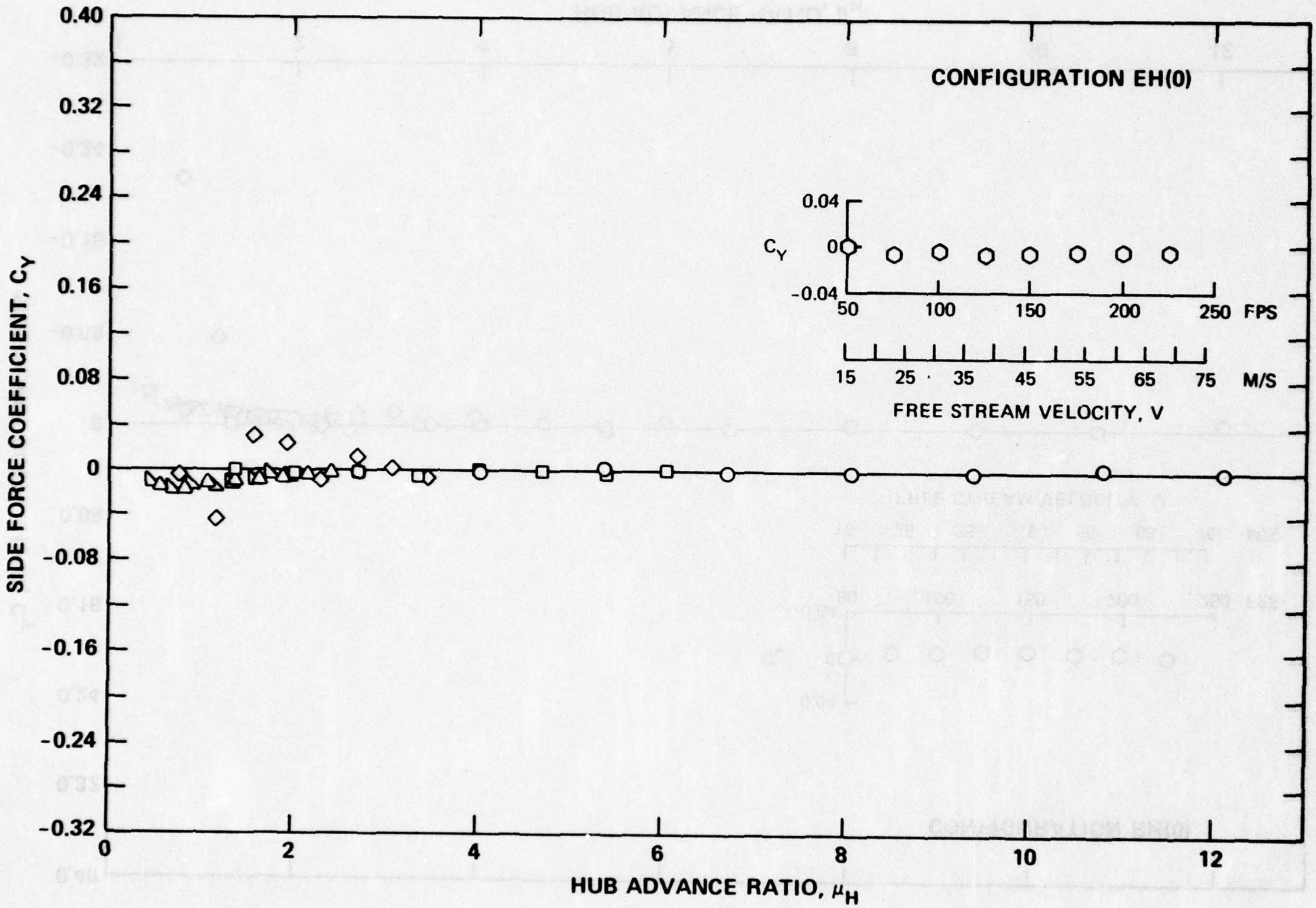

Figure 5 – (continued)

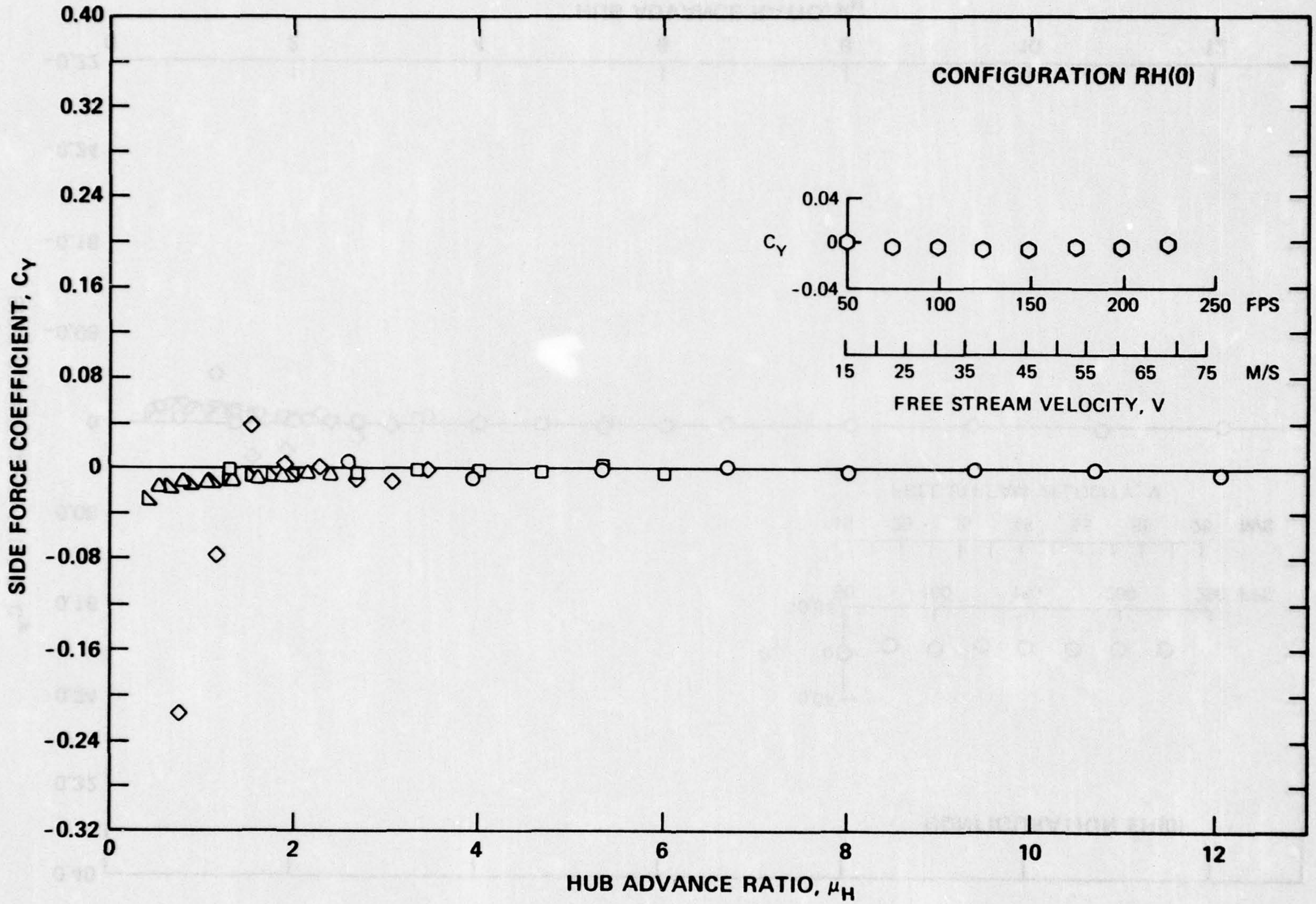

Figure 5 – (continued)

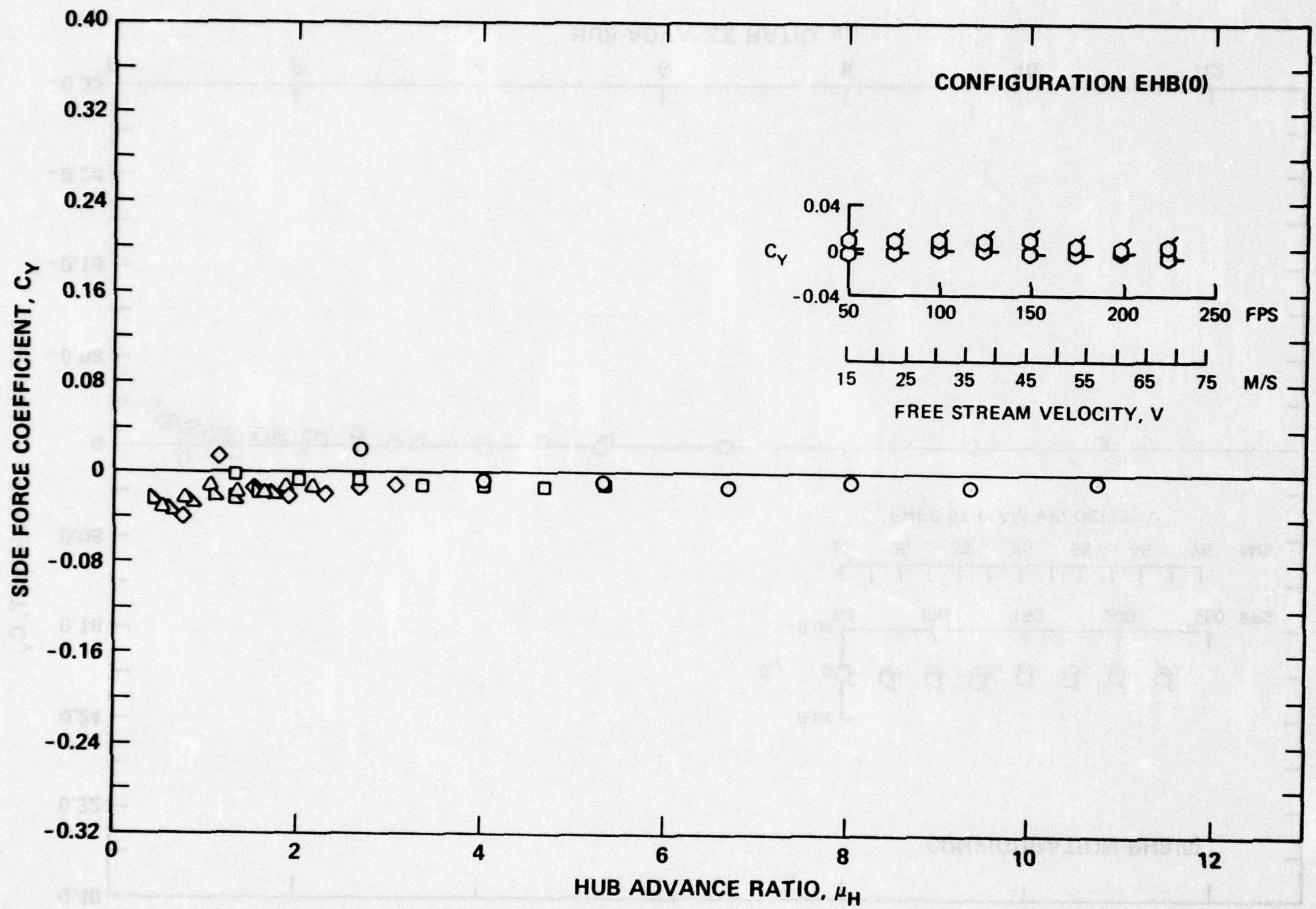

Figure 5 – (continued)

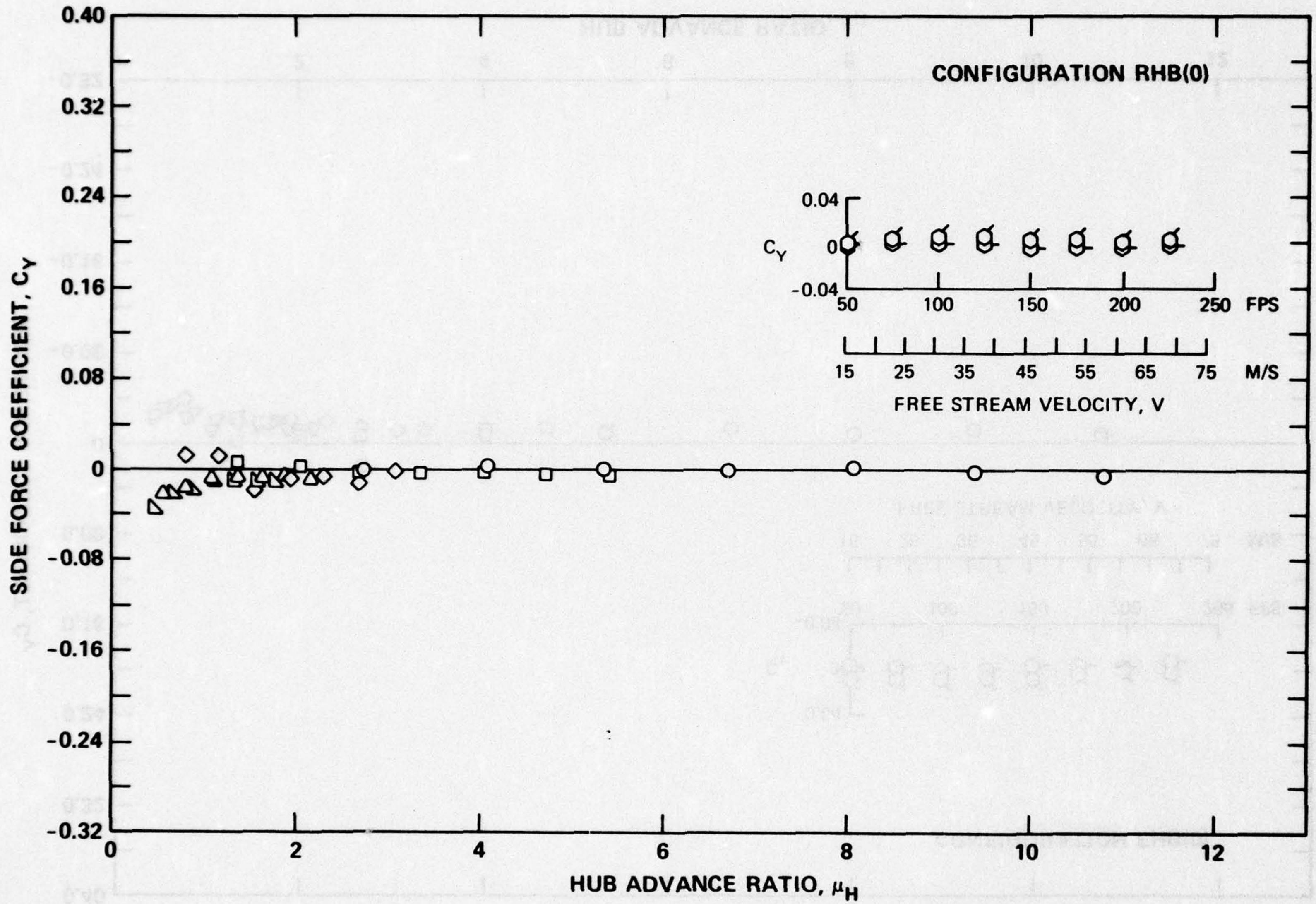

Figure 5 – (concluded)

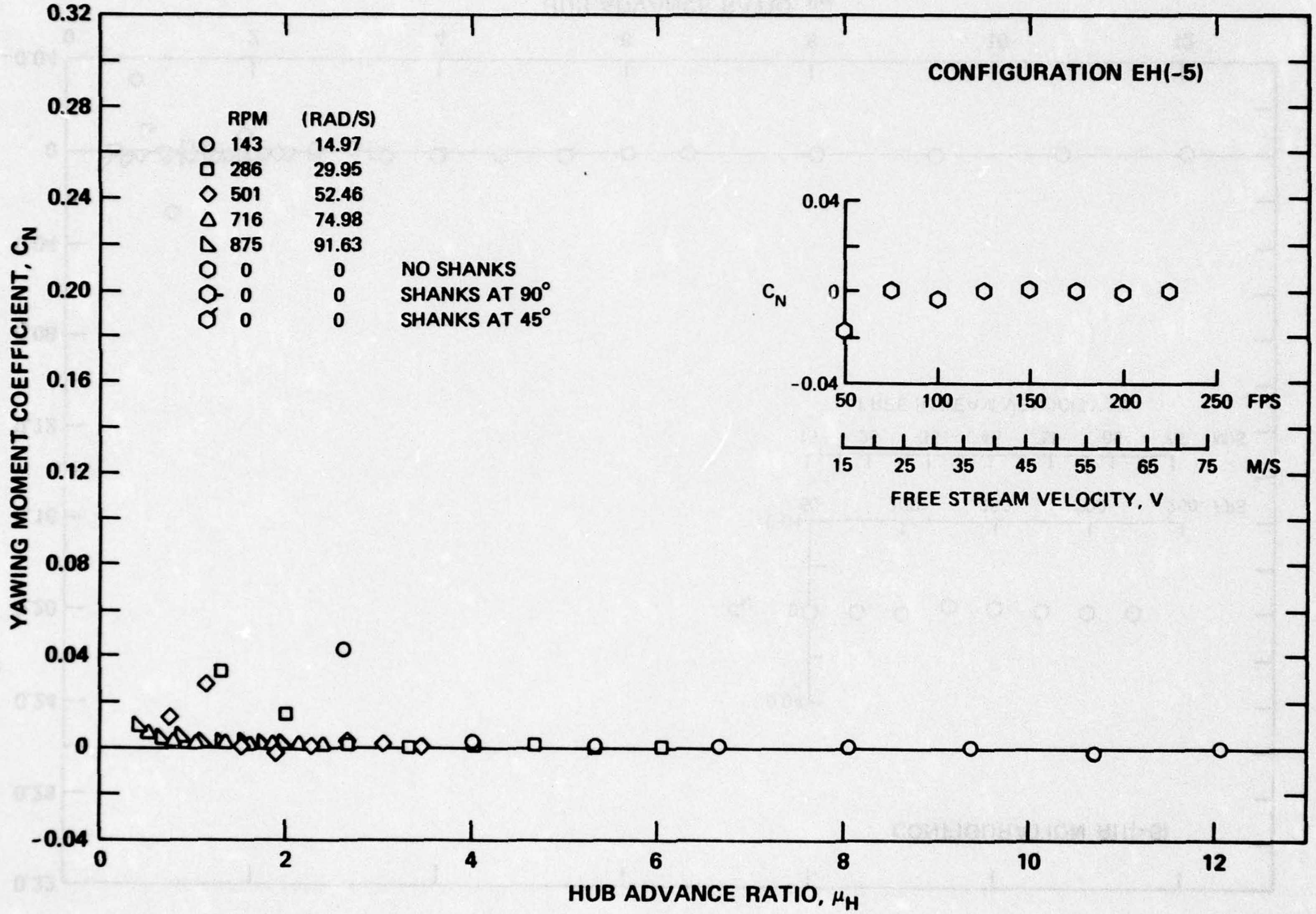

Figure 6 – Yawing Moment Coefficient Versus Hub Advance Ratio

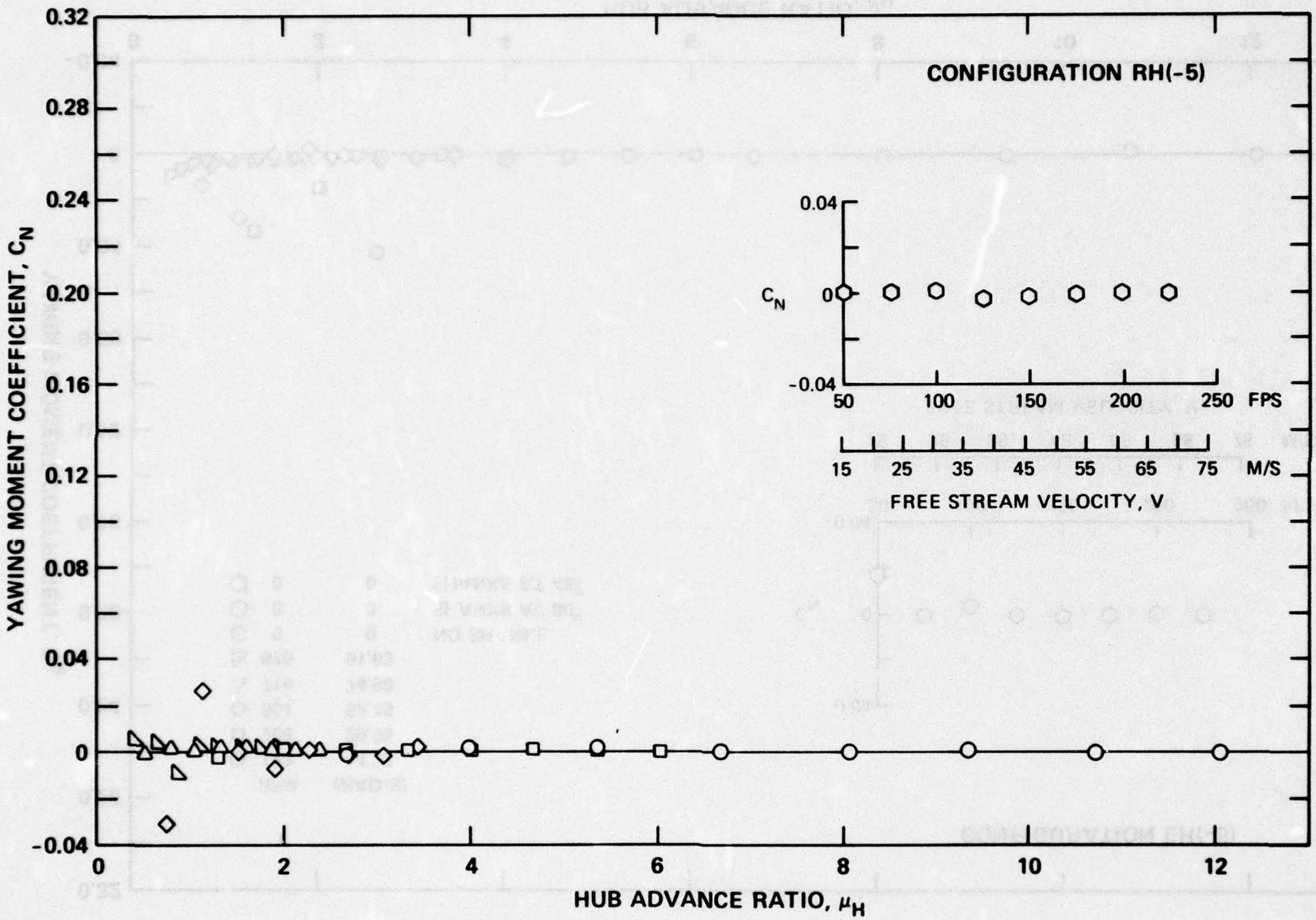

Figure 6 – (continued)

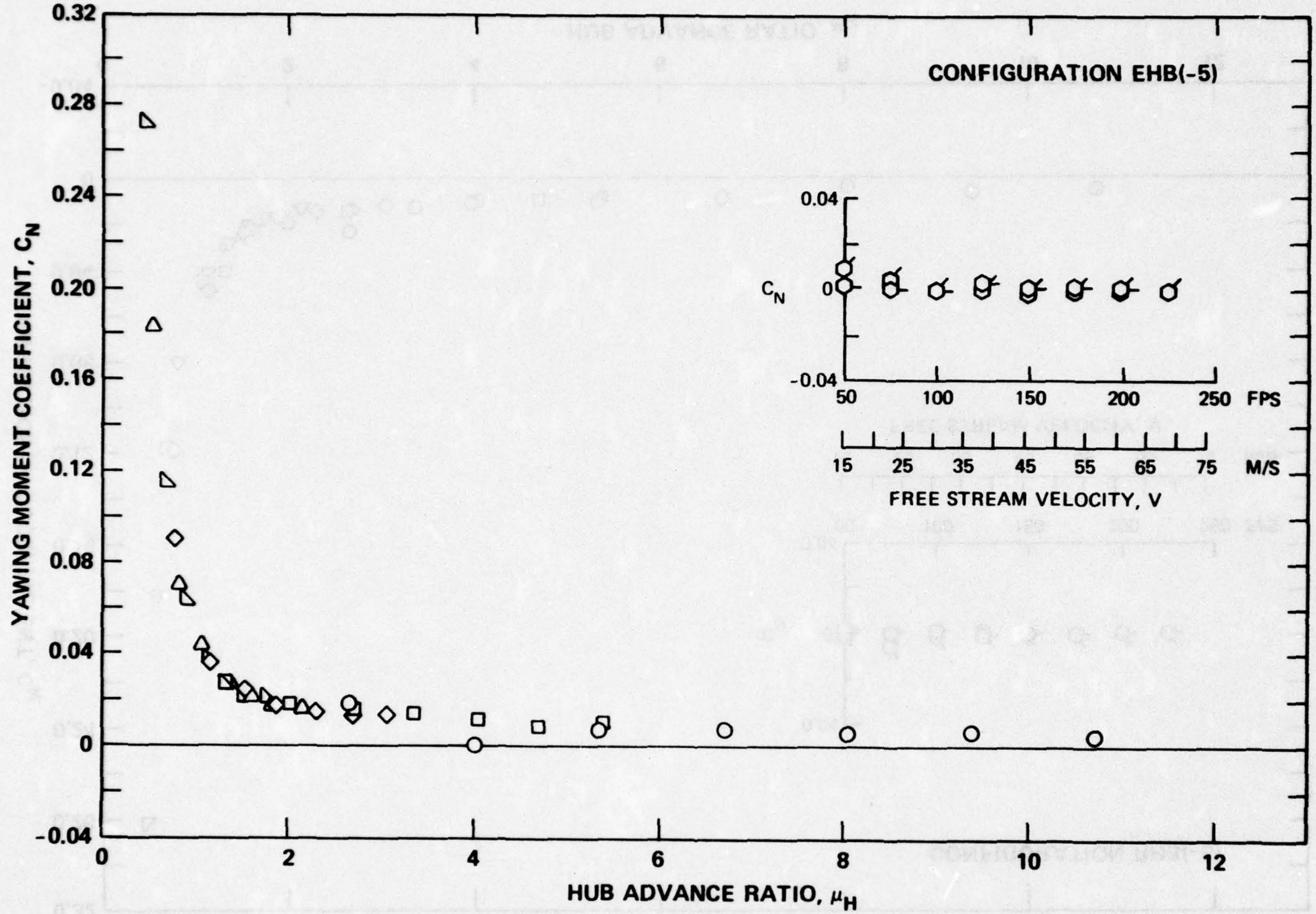

Figure 6 – (continued)

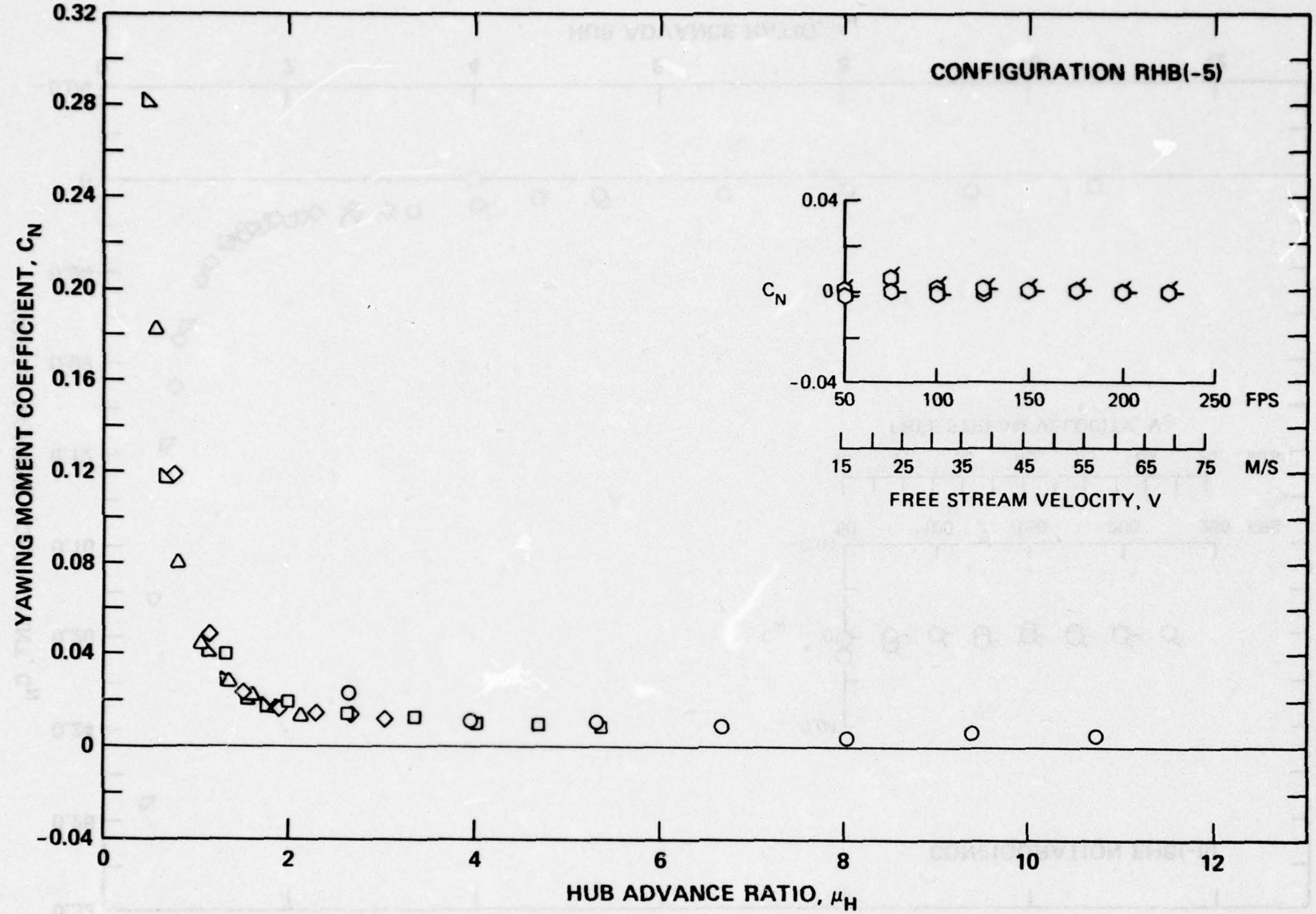

Figure 6 – (continued)

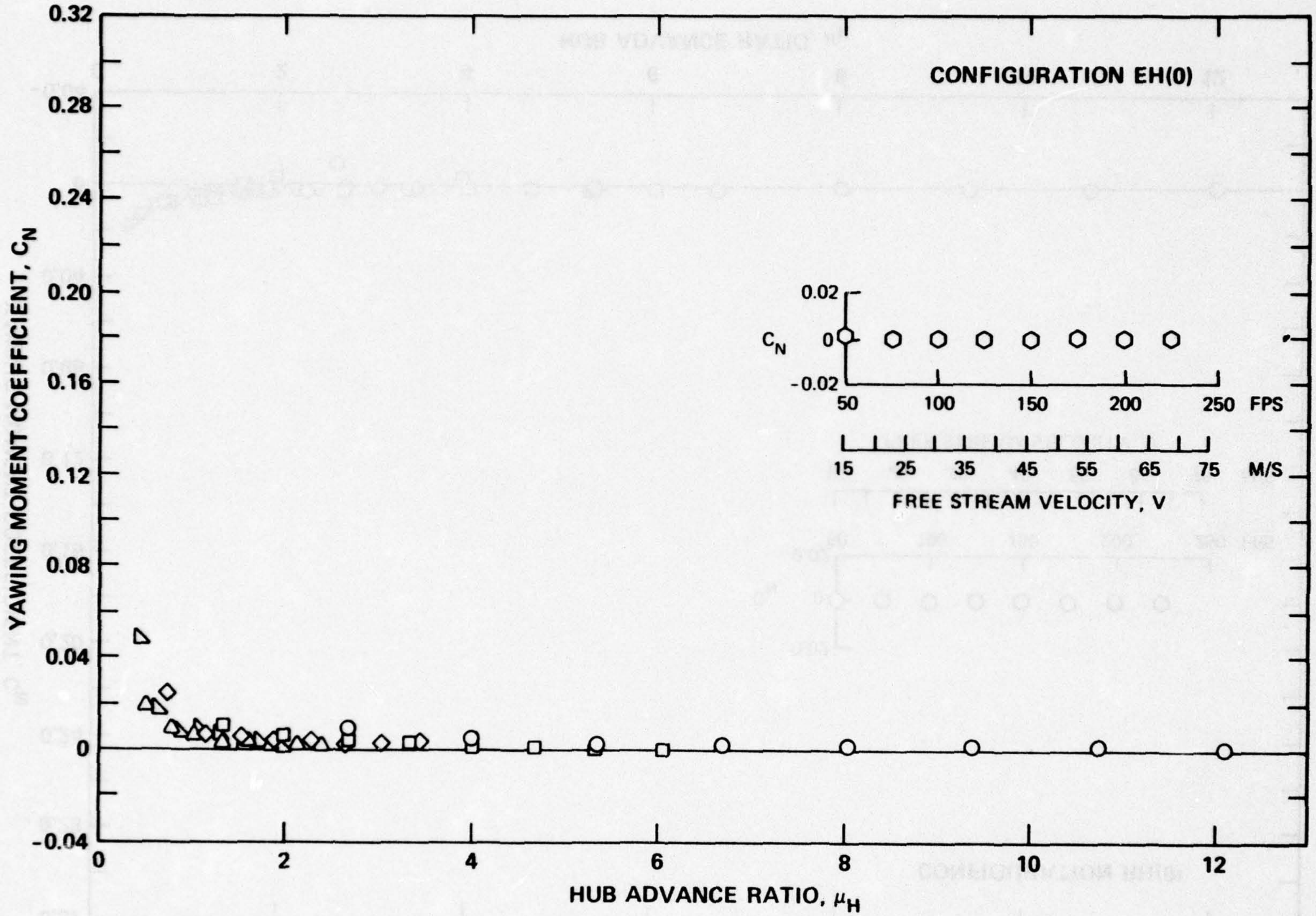

Figure 6 – (continued)

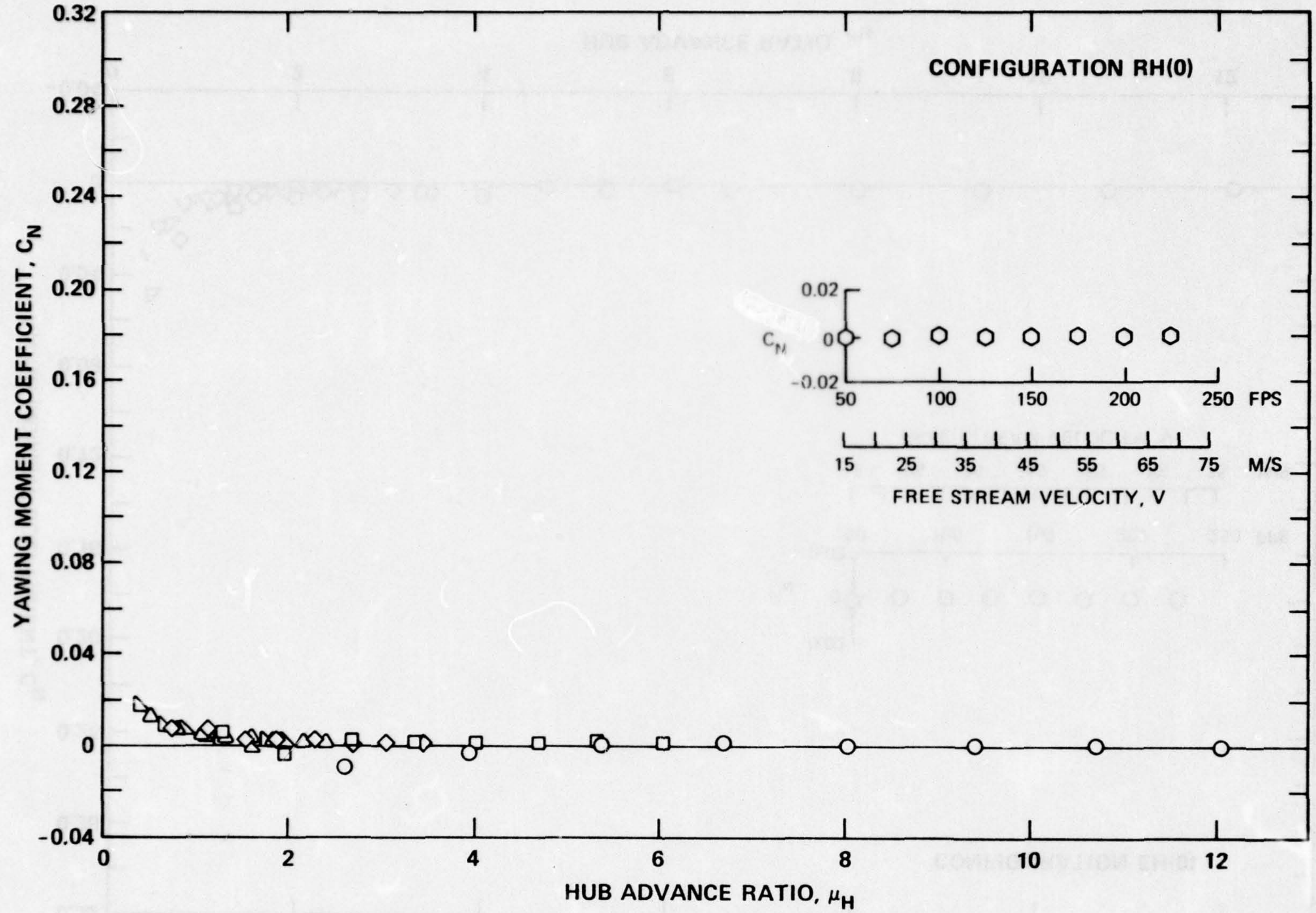

Figure 6 – (continued)

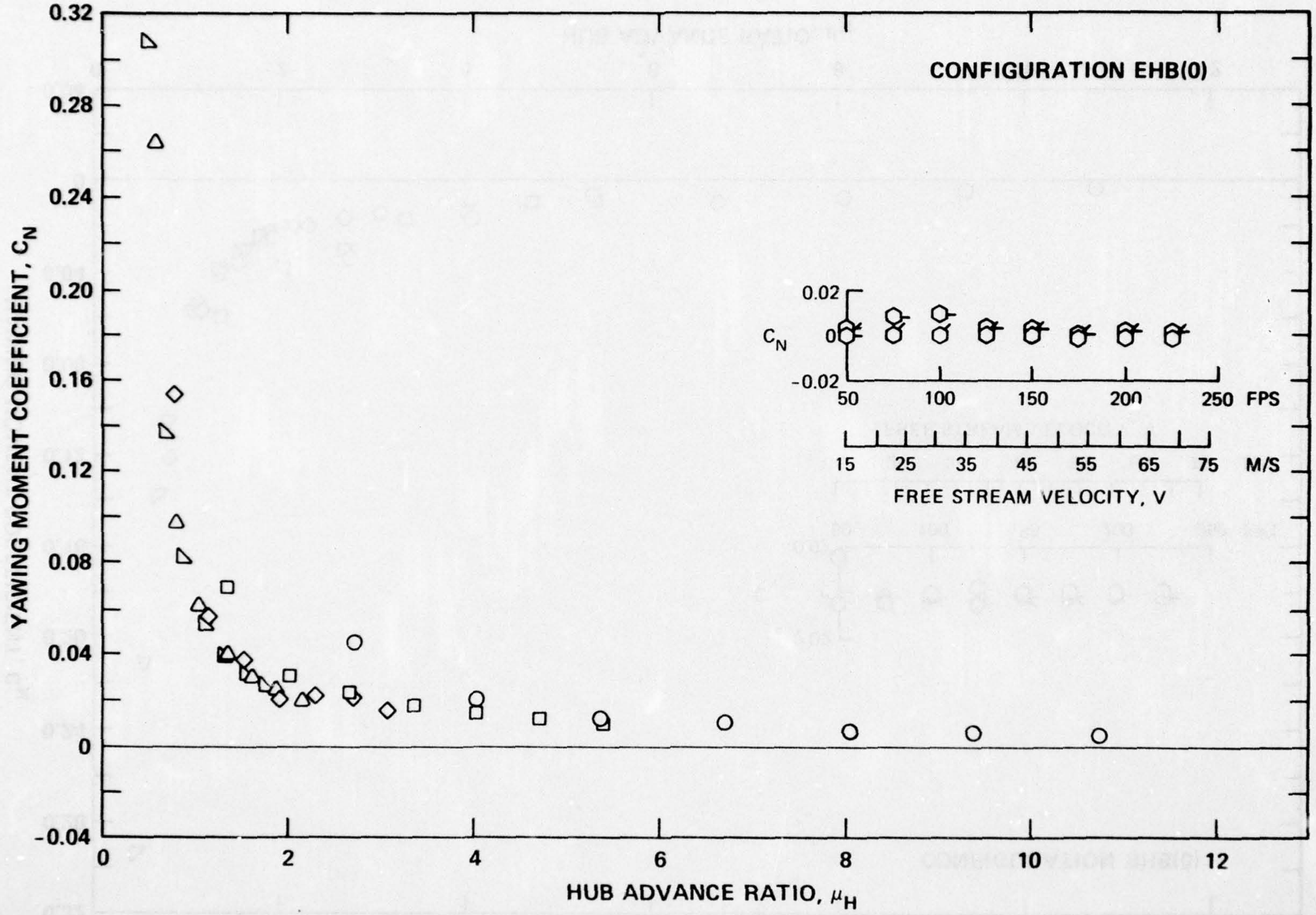

Figure 6 – (continued)

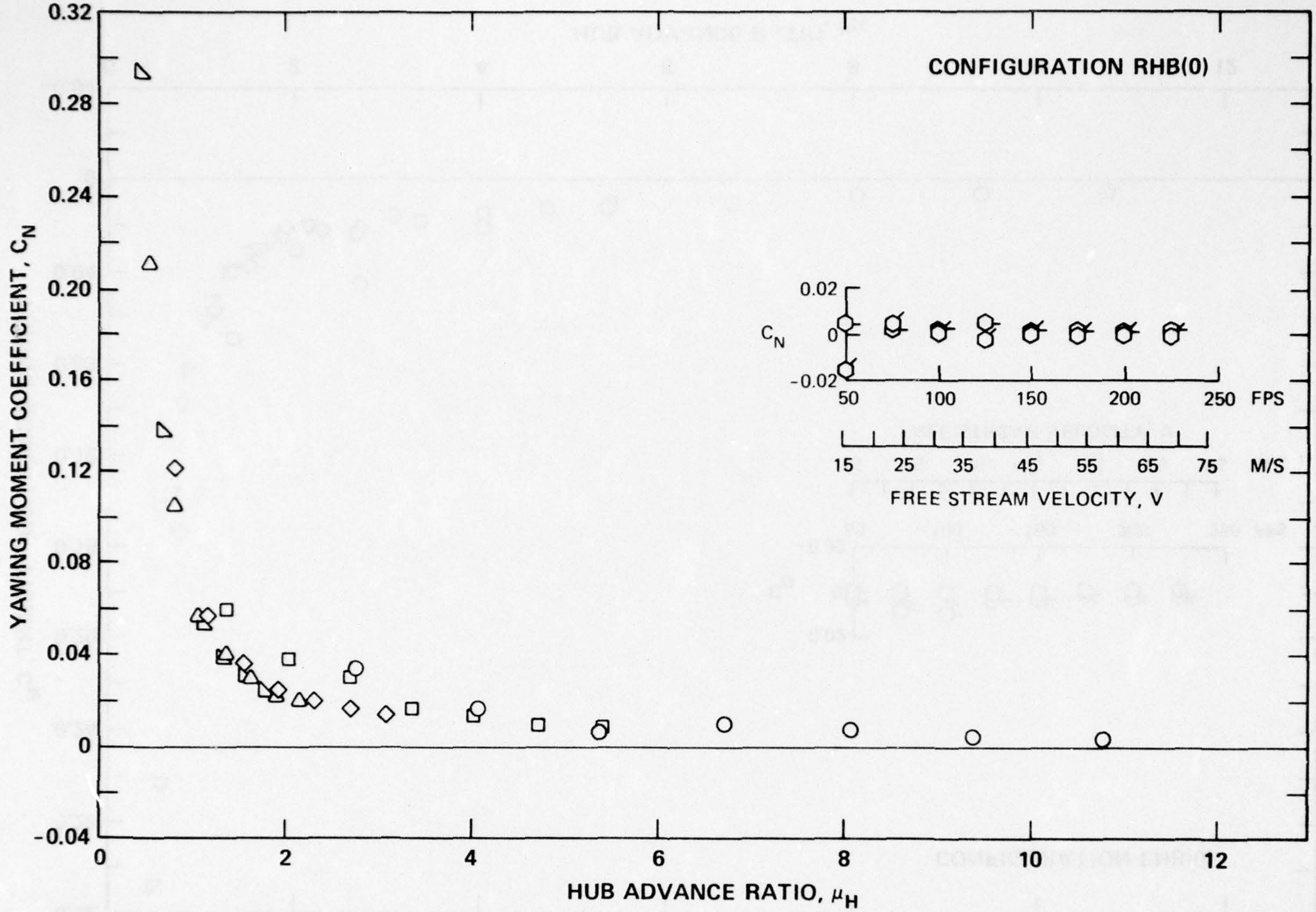

Figure 6 – (concluded)

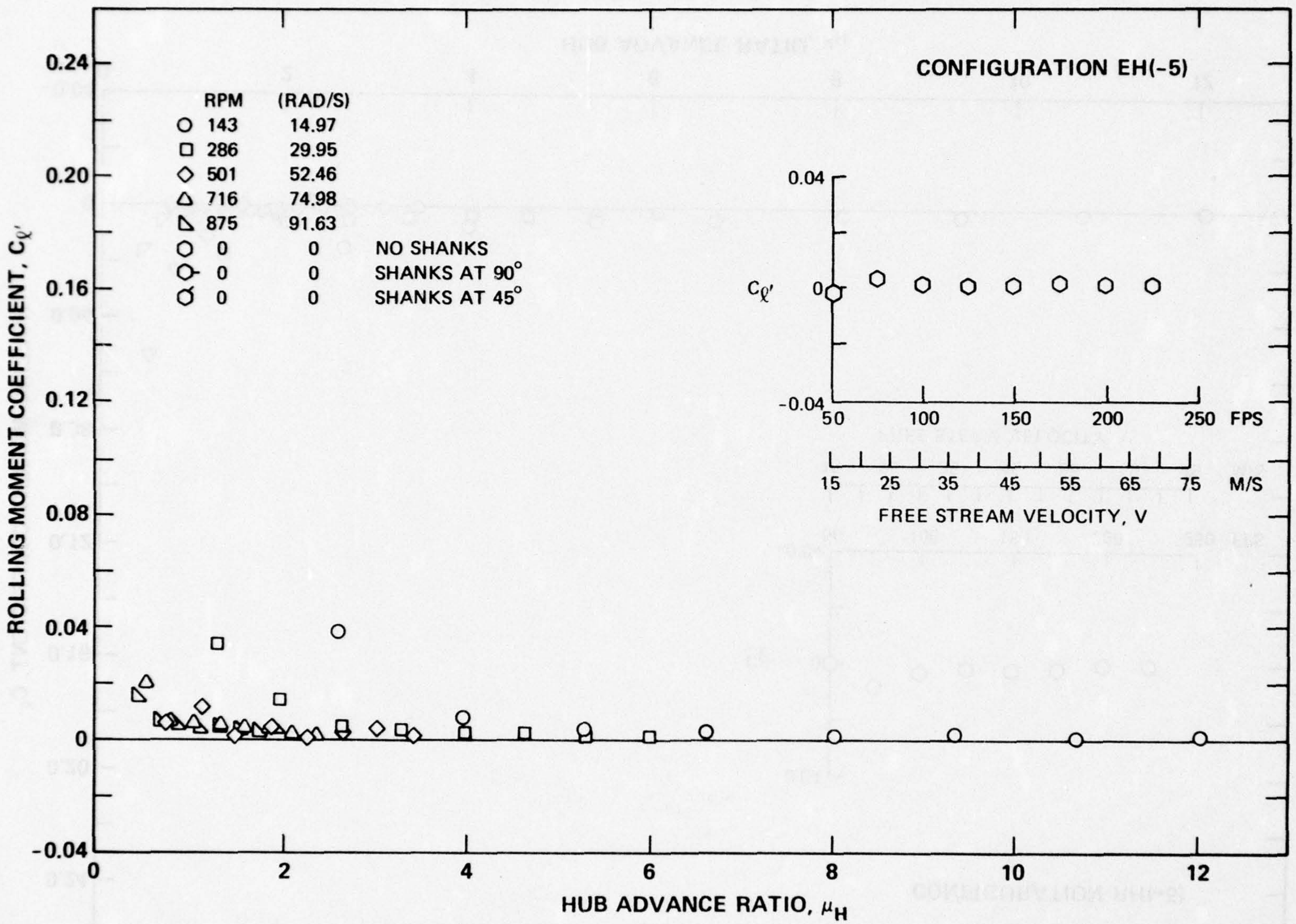

Figure 7 – Rolling Moment Coefficient Versus Hub Advance Ratio

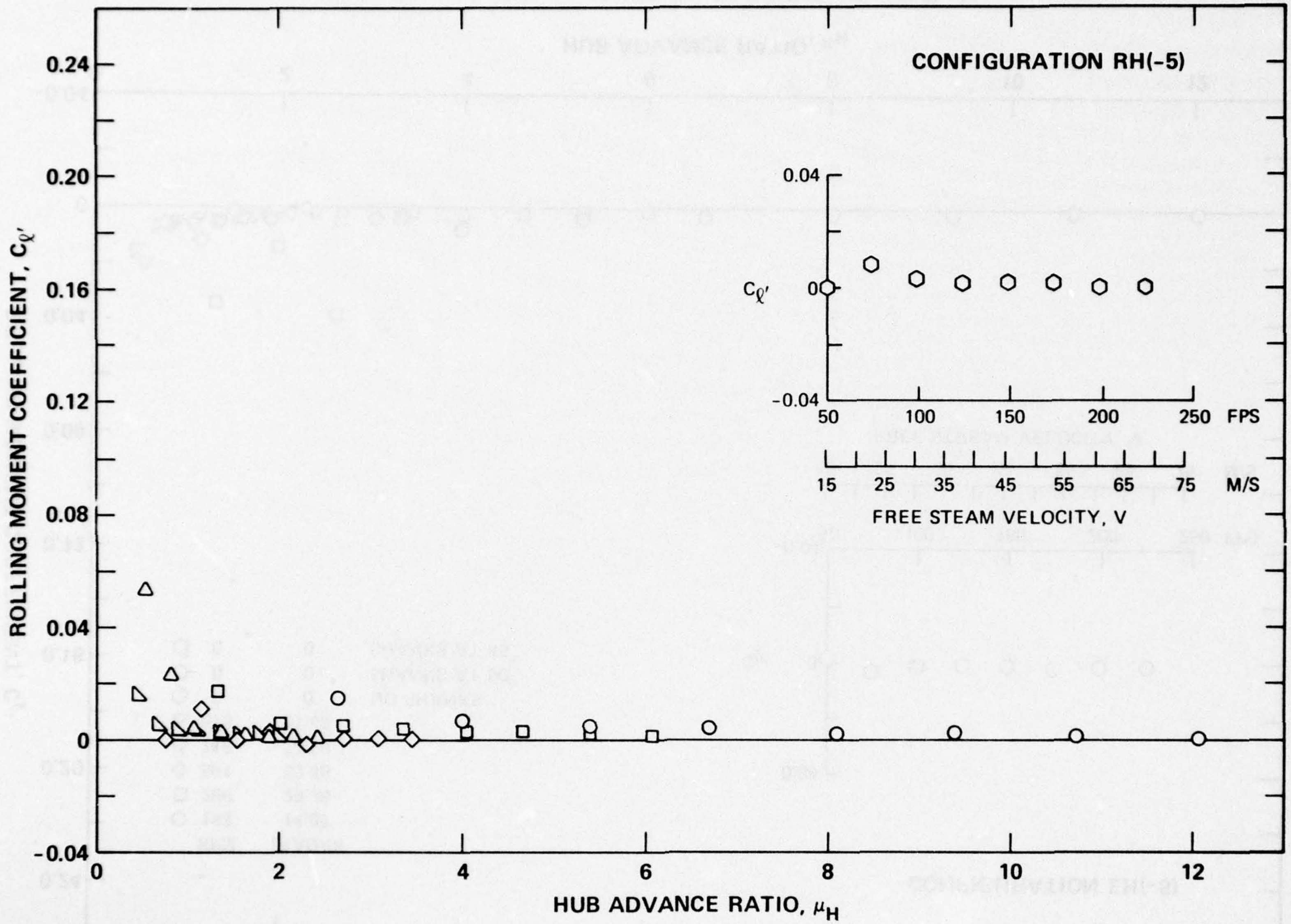

Figure 7 – (continued)

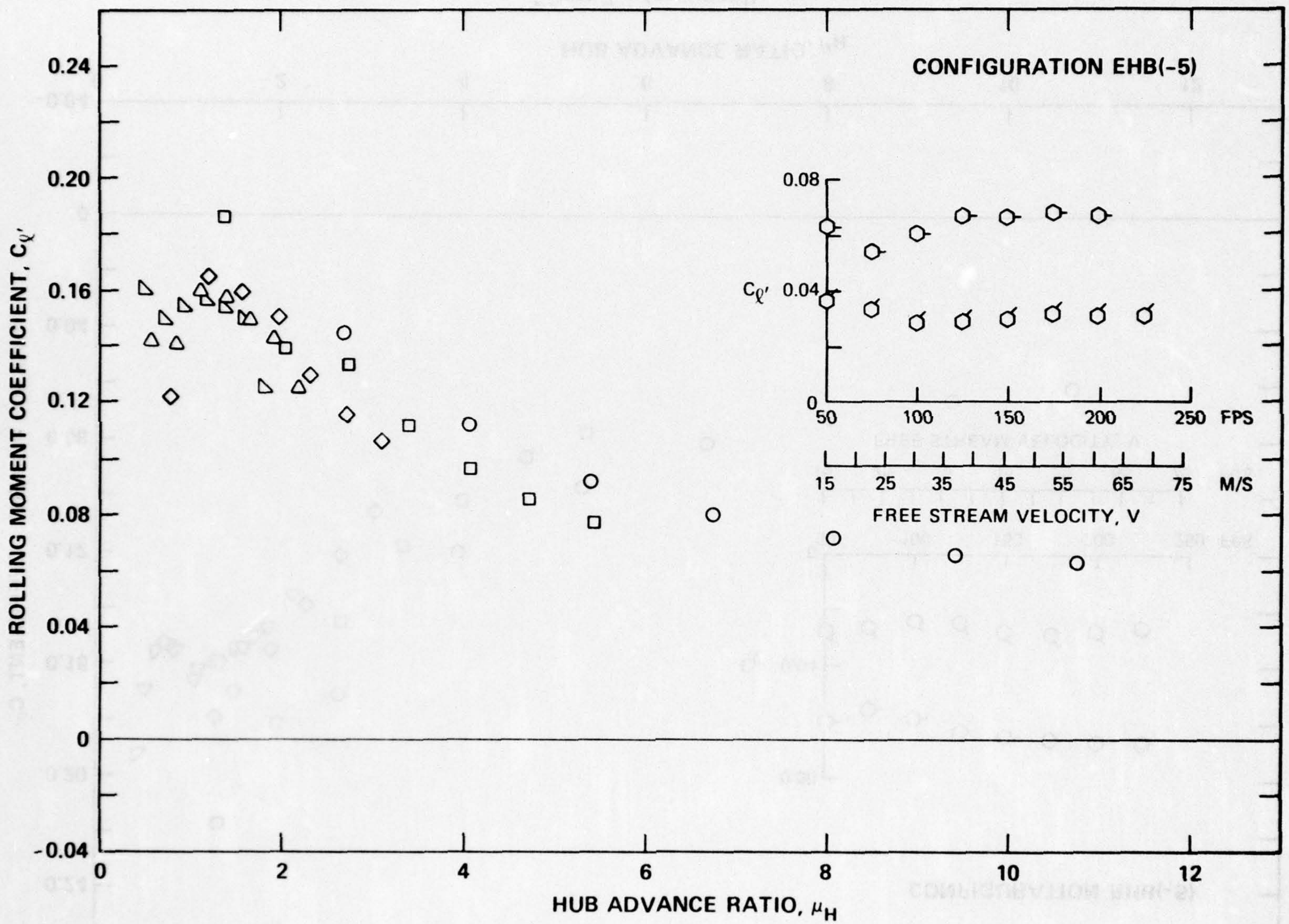

Figure 7 – (continued)

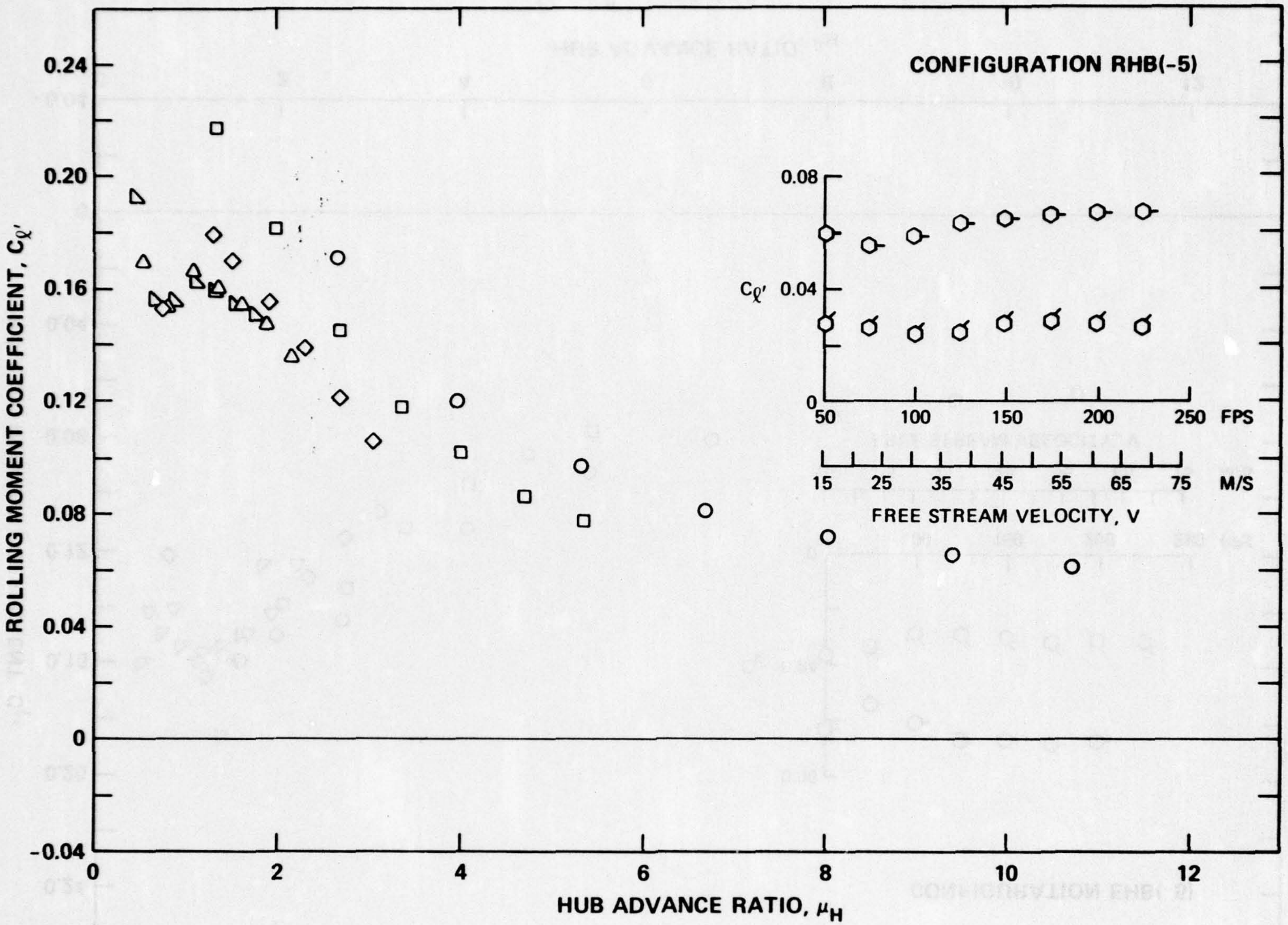

Figure 7 – (continued)

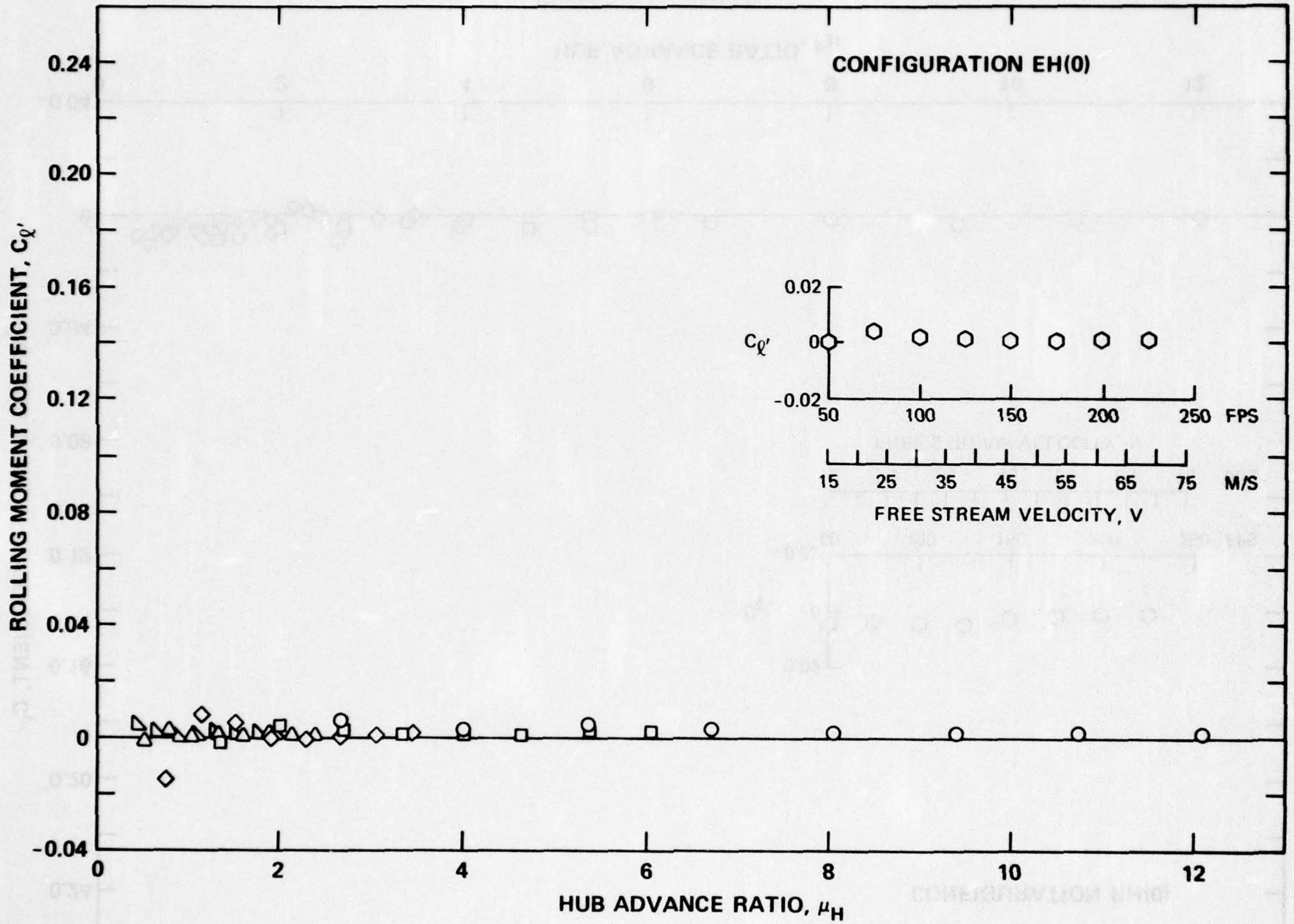

Figure 7 – (continued)

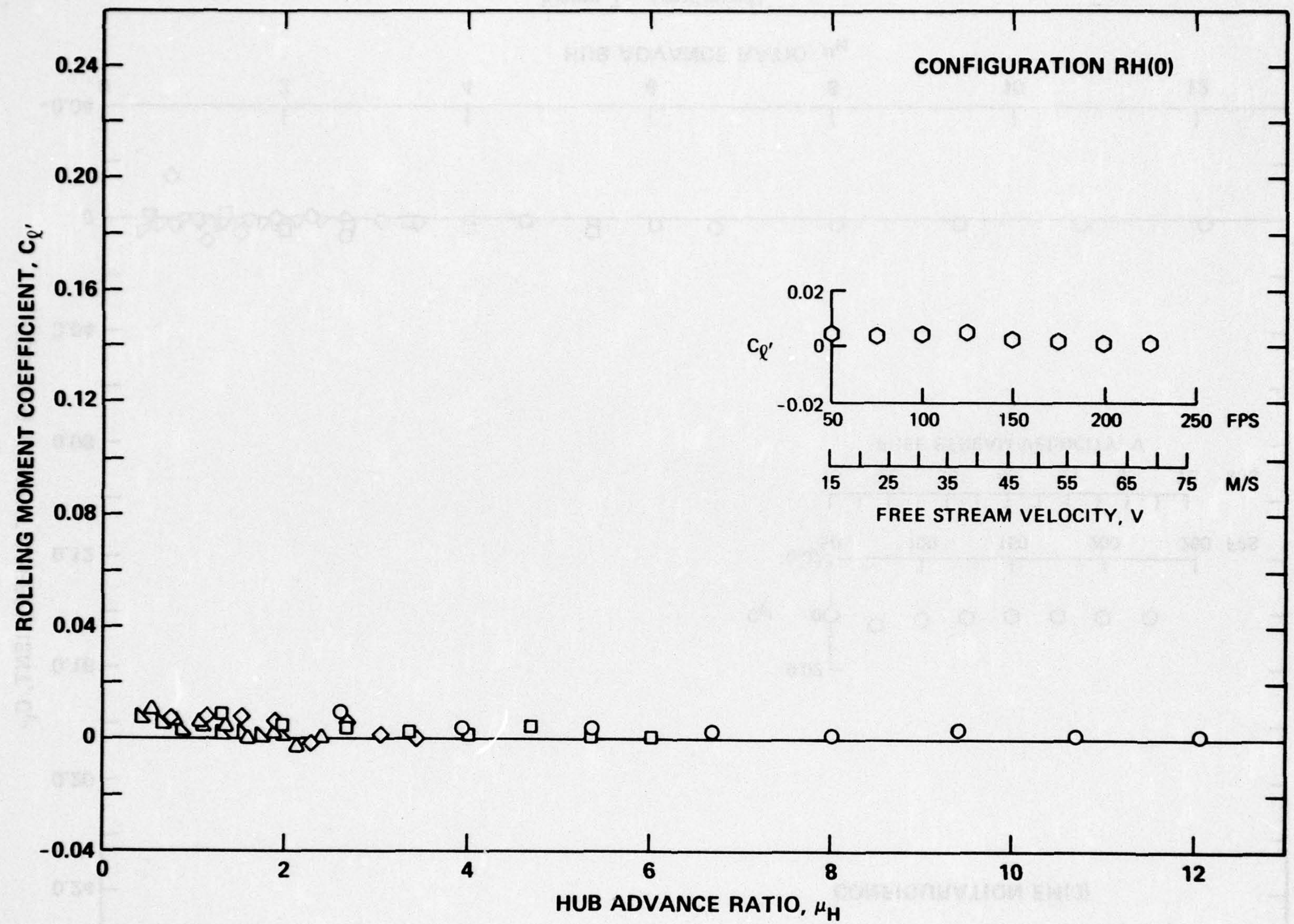

Figure 7 – (continued)

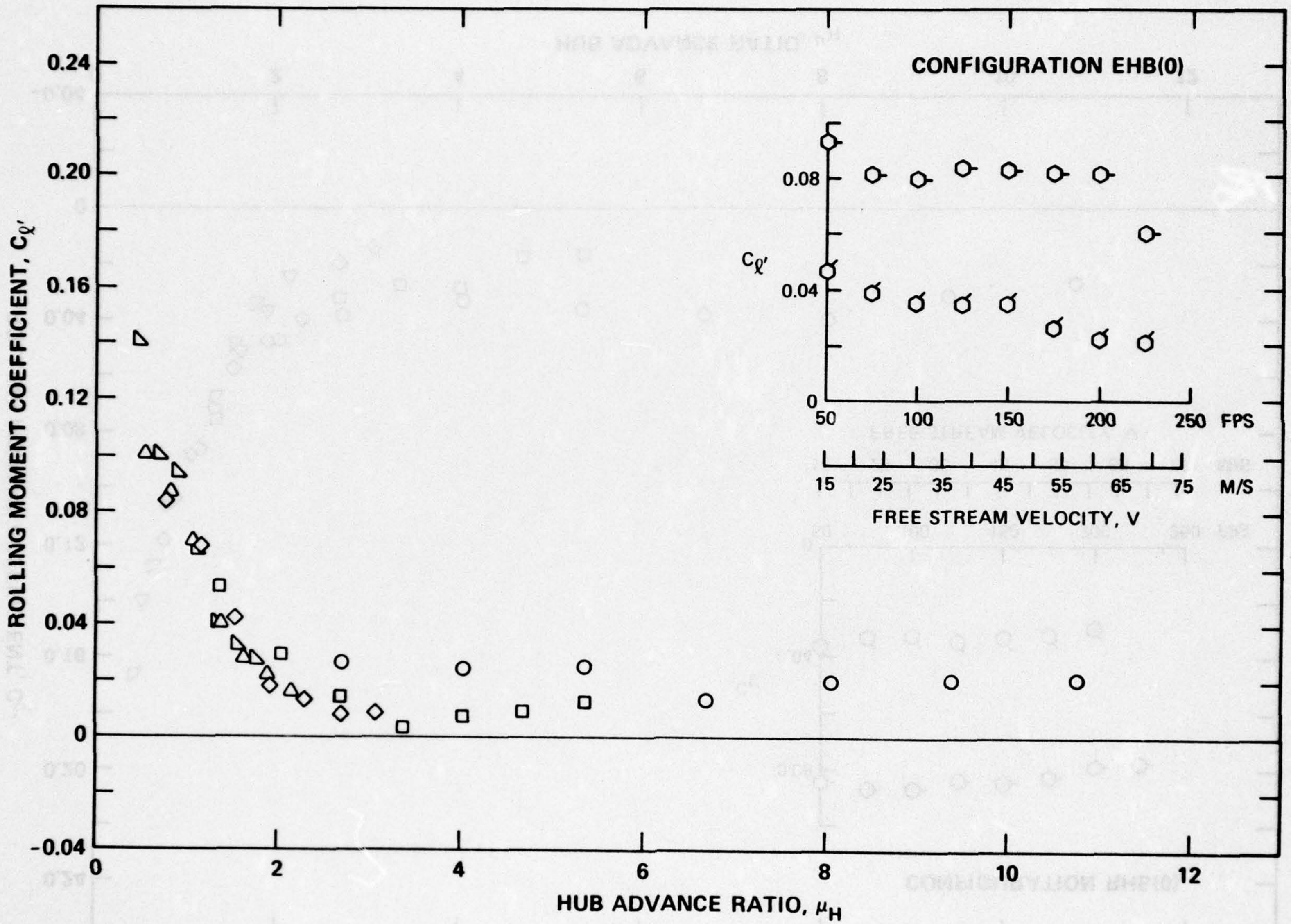

Figure 7 – (continued)

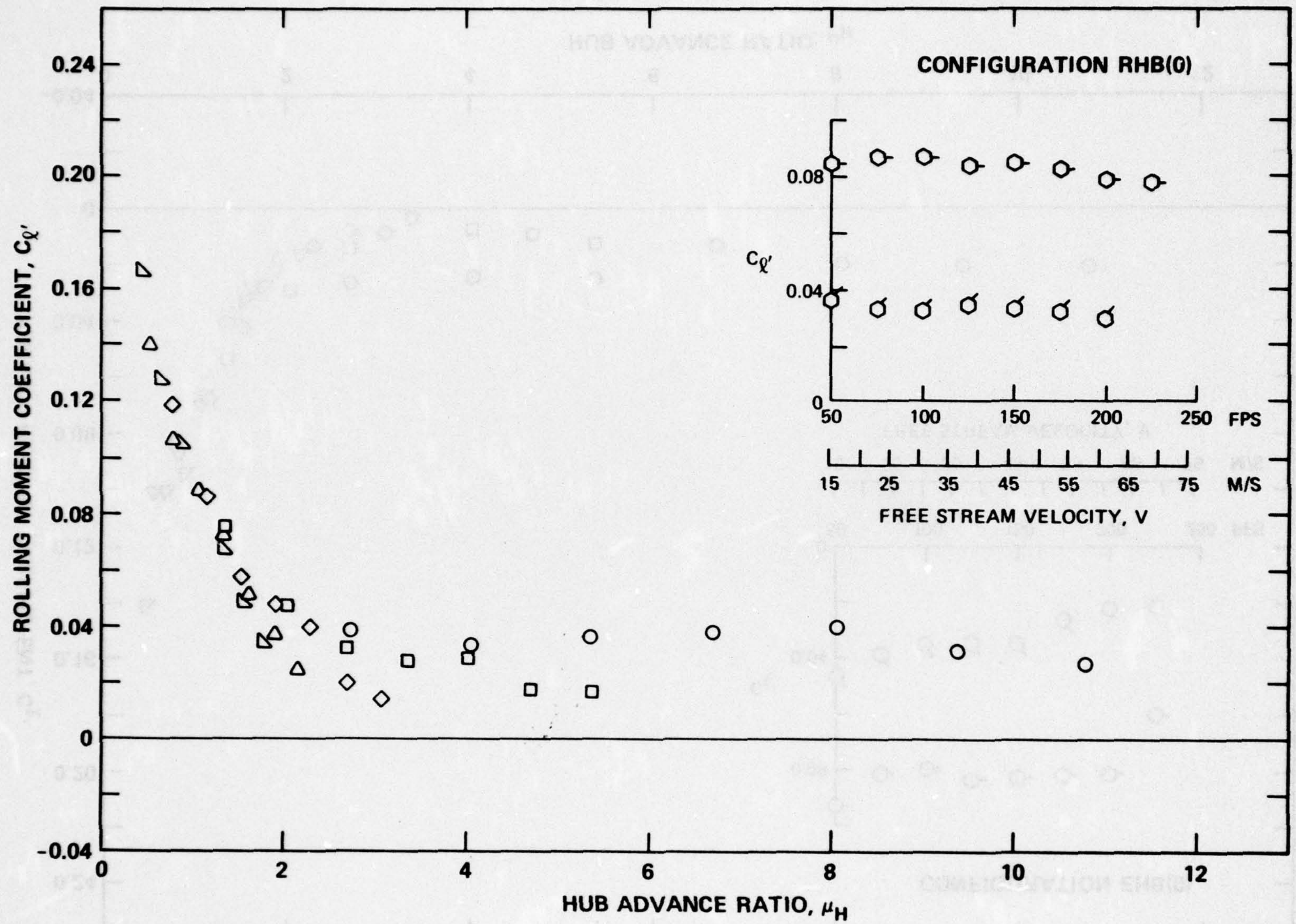

Figure 7 – (concluded)

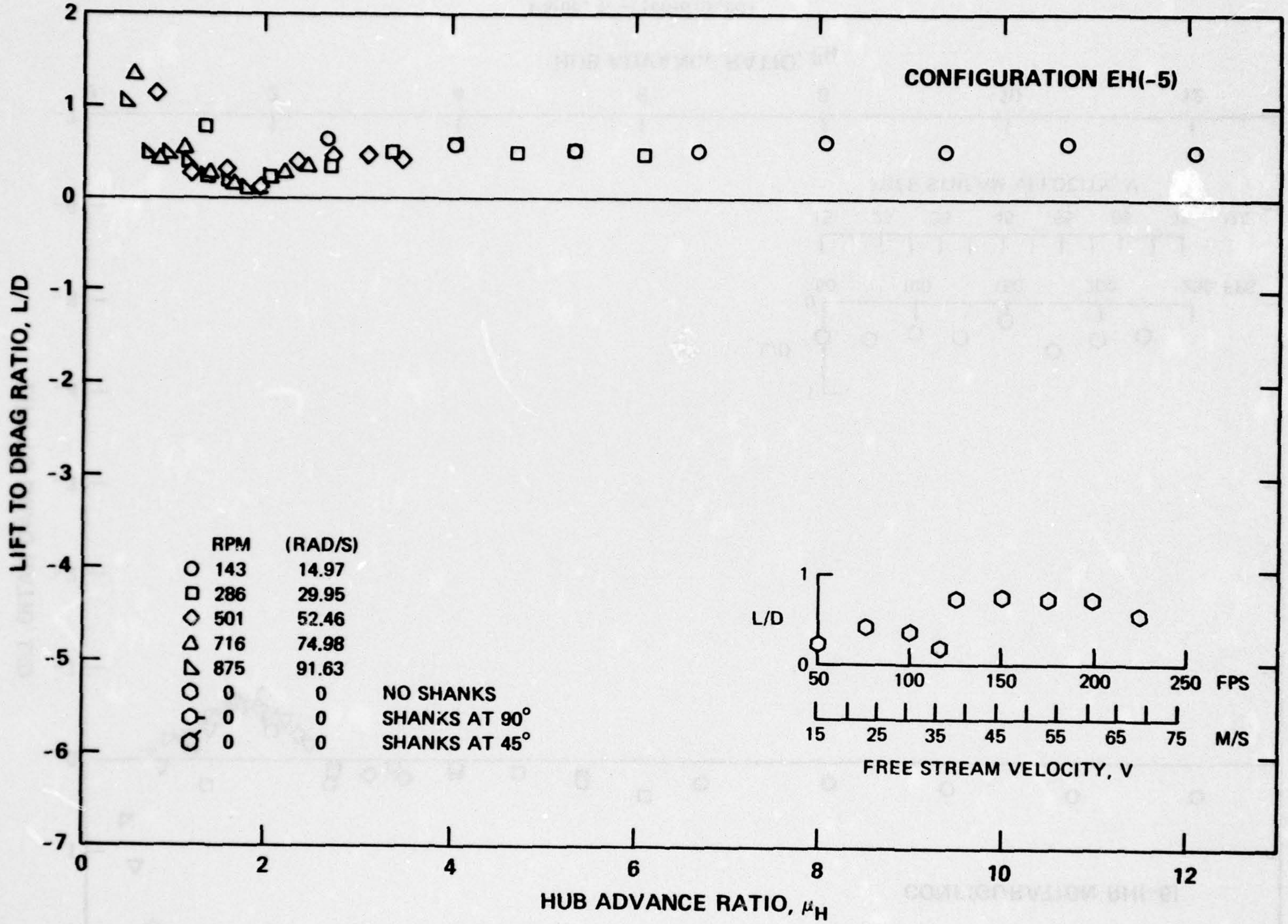

Figure 8 – Lift to Drag Ratio Versus Hub Advance Ratio

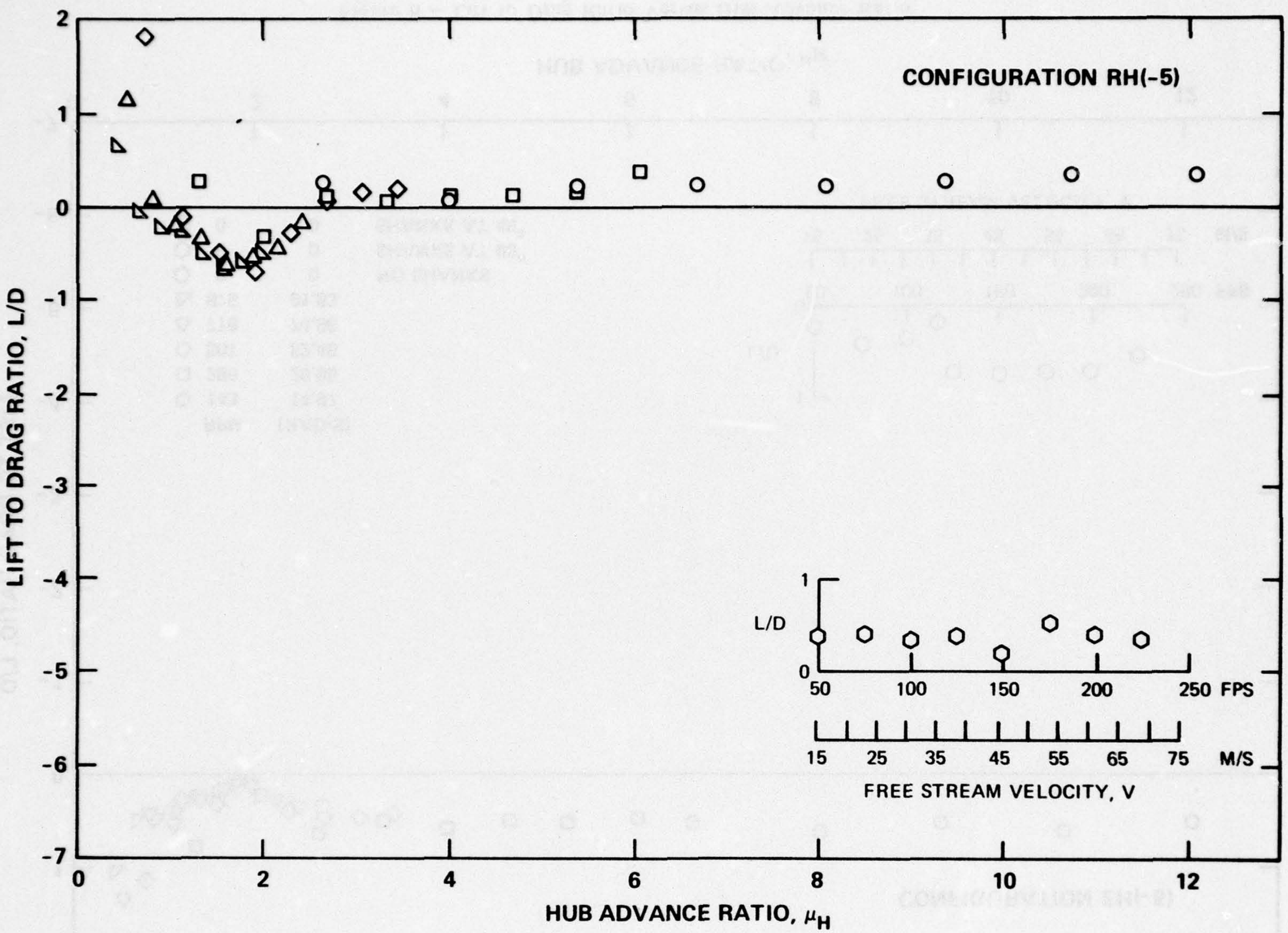

Figure 8 – (continued)

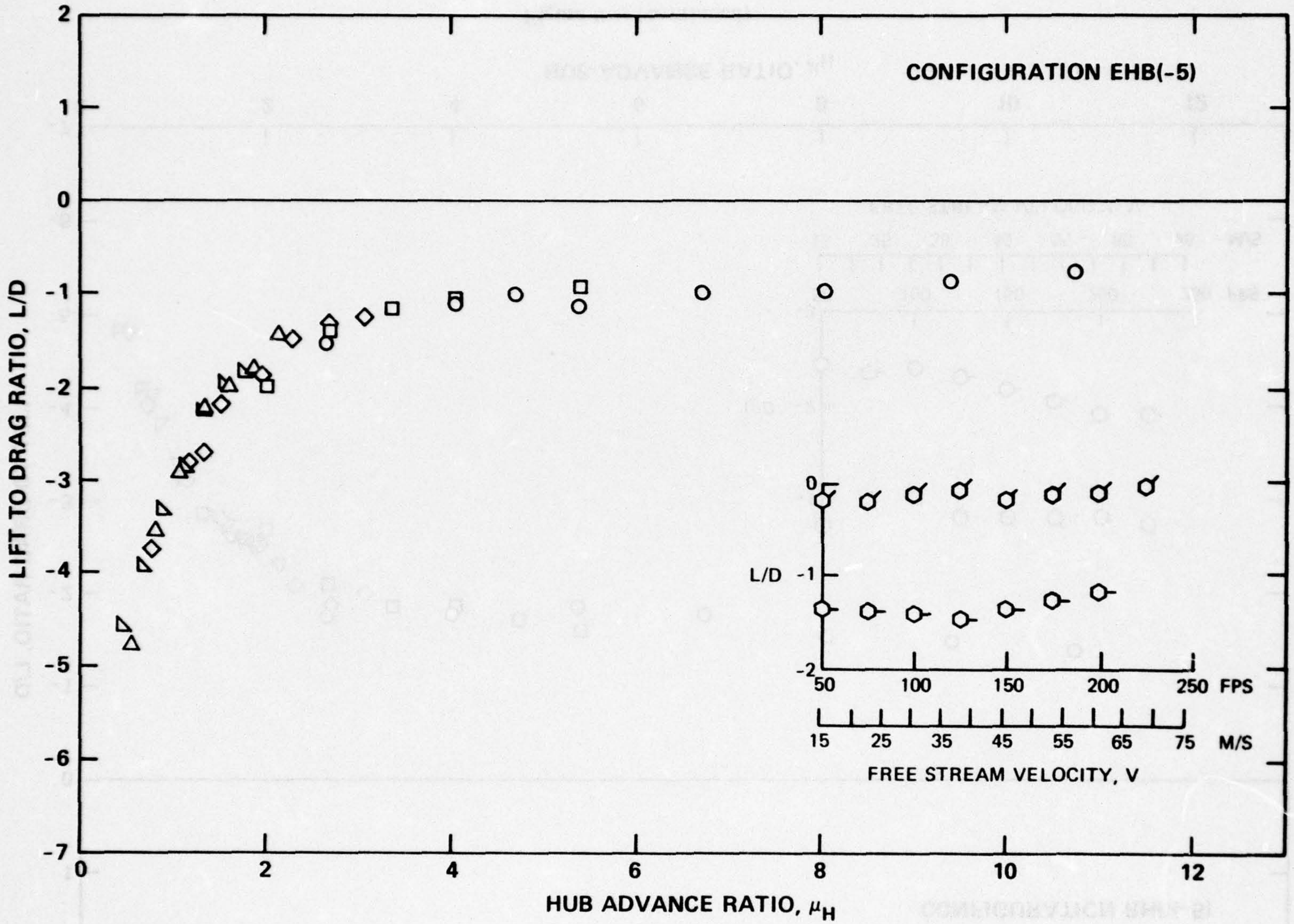

Figure 8 – (continued)

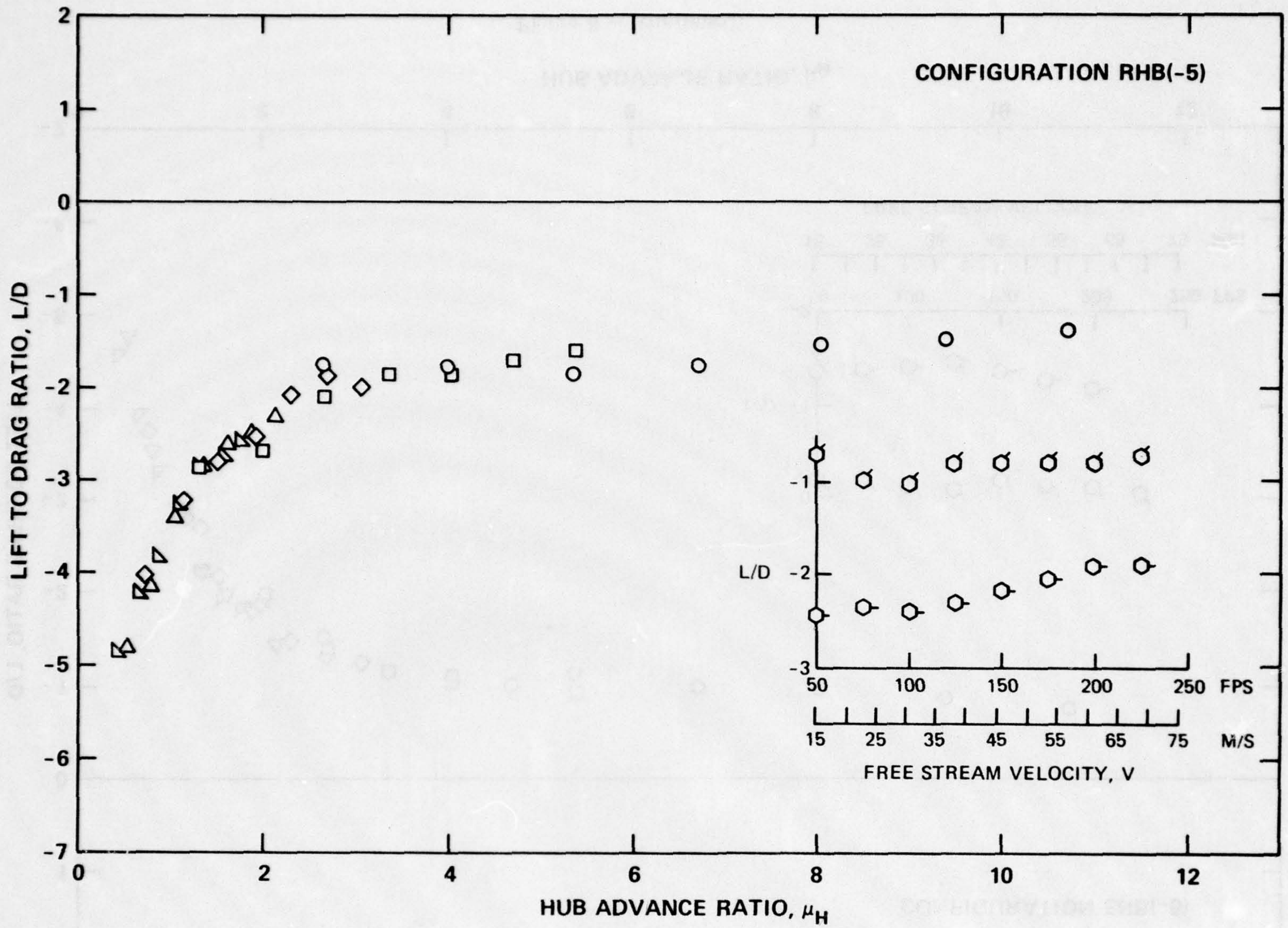

Figure 8 – (continued)

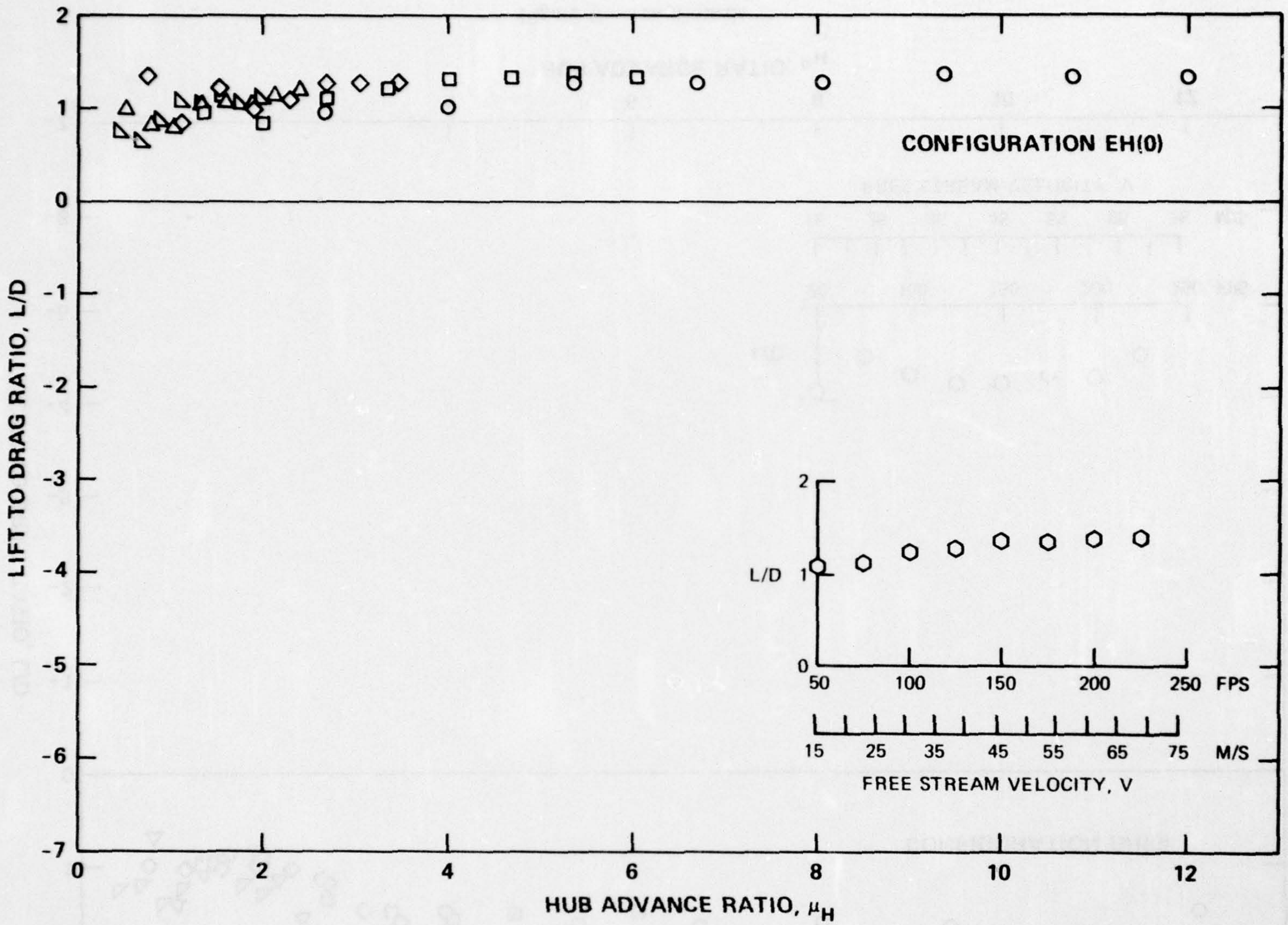

Figure 8 – (continued)

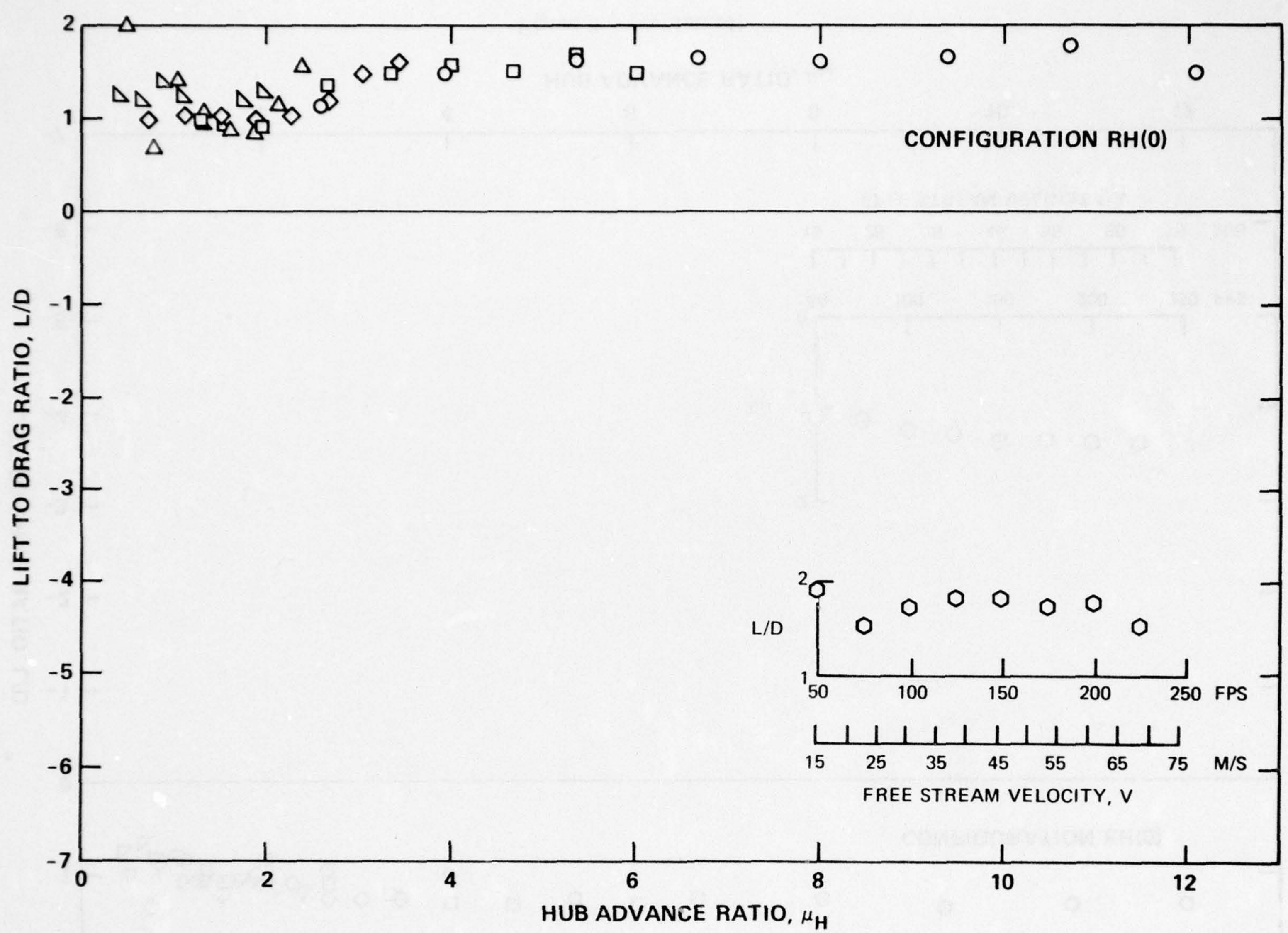

Figure 8 – (continued)

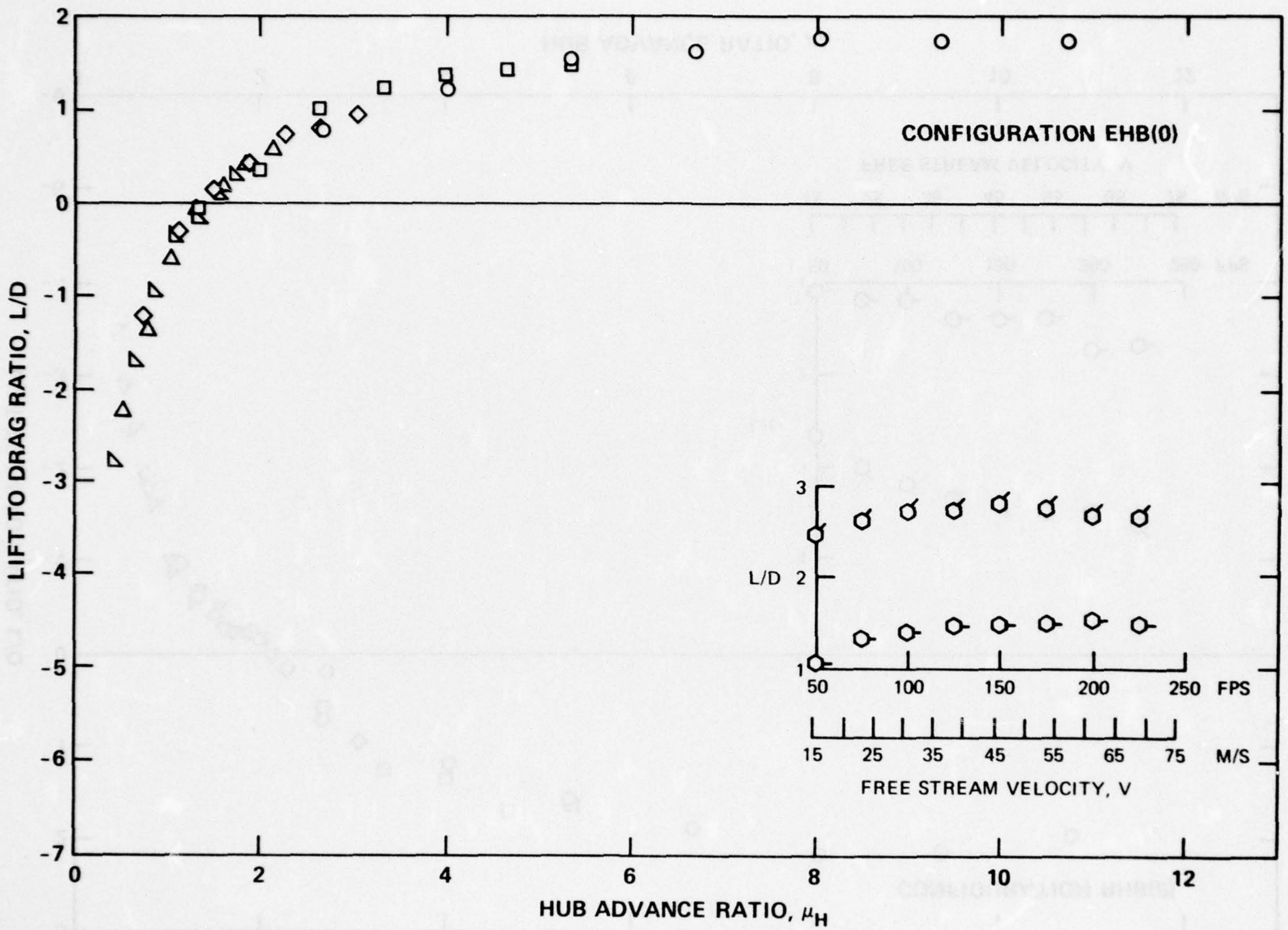

Figure 8 – (continued)

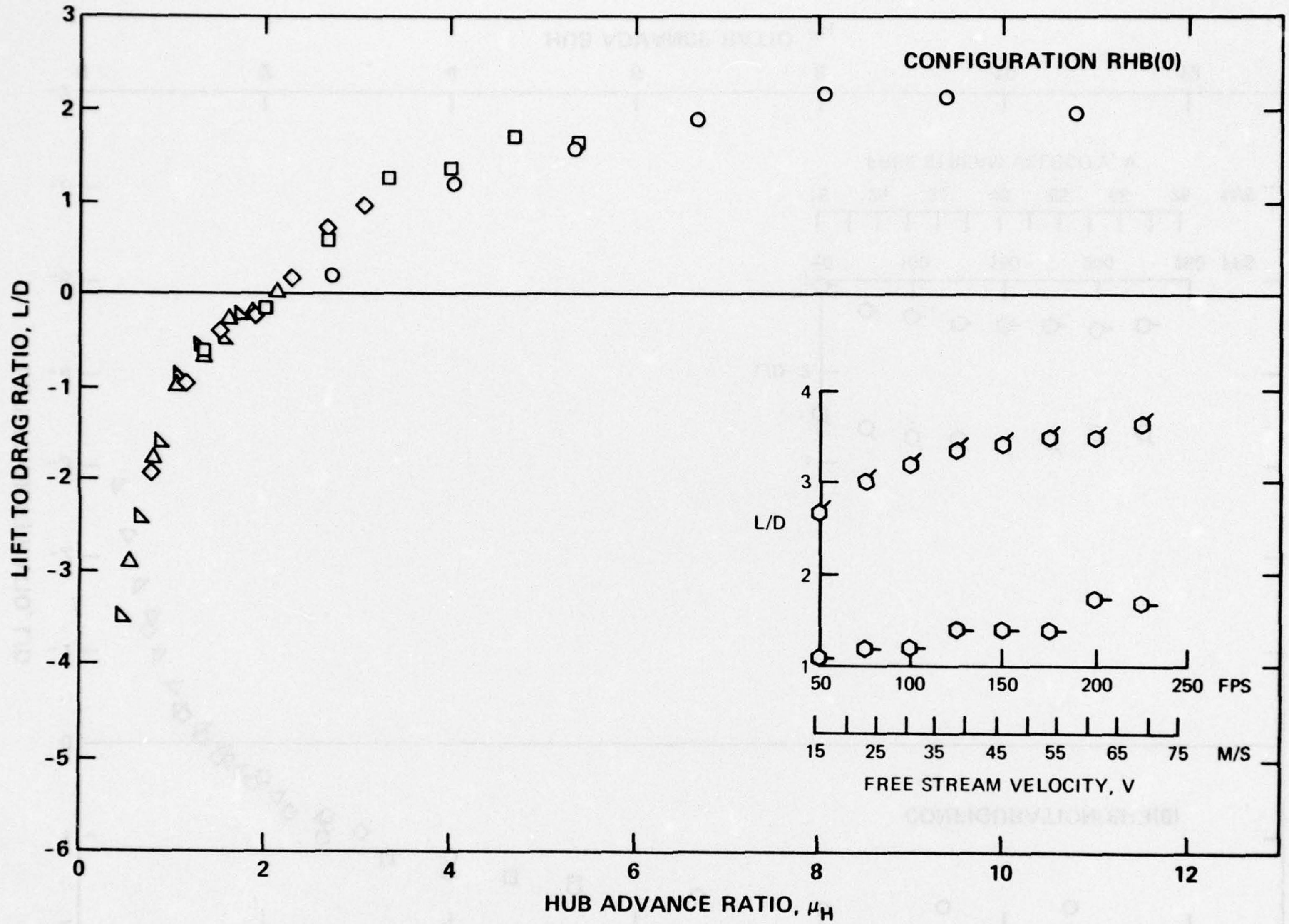

Figure 8 – (concluded)